PACKET SCHEDULING IN SATELLITE LTE NETWORKS EMPLOYING MIMO TECHNOLOGY

By

Gbolahan Rilwan Aiyetoro

A thesis Submitted in Fulfilment of the Academic Requirements for the Degree of Doctor of Philosophy (PhD) in Electronic Engineering

Discipline of Electrical, Electronic and Computer Engineering

School of Engineering

April 2014

Supervised by Professor Fambirai Takawira

Co-supervised by Dr. Tom Walingo

DISSERTATION TITLE

Packet Scheduling in Satellite LTE Networks employing MIMO technology

SUBMITTED BY

Gbolahan Rilwan Aiyetoro

IN FULFILLMENT OF THE DEGREE

Doctor of Philosophy in Electronic Engineering from University of KwaZulu-Natal

(Howard College Campus)

DATE OF SUBMISSION

APRIL 2014

SUPERVISED BY

Professor Fambirai Takawira

Dr. Tom Walingo

As the candidate's supervisor, I have approved this dissertation for submission.

Signed: _____

Name: _____ Date: _____

DECLARATION

I, Gbolahan Rilwan Aiyetoro, declare that:

(i) The research reported in this thesis, except where otherwise indicated, is my original work.

(ii) This thesis has not been submitted for any degree or examination at any other university.

(iii) This thesis does not contain other persons' data, pictures, graphs or other information, unless specifically acknowledged as being sourced from other persons.

(iv) This thesis does not contain other persons' writing, unless specifically acknowledged as being sourced from other researchers. Where other written sources have been quoted, then:

a) their words have been re-written but the general information attributed to them has been referenced;

b) where their exact words have been used, their writing has been placed inside quotation marks, and referenced.

(v) Where I have reproduced a publication of which I am an author, co-author or editor, I have indicated in detail which part of the publication was actually written by myself alone and have fully referenced such publications.

(vi) This thesis does not contain text, graphics or tables copied and pasted from the Internet, unless specifically acknowledged, and the source being detailed in the thesis and in the References sections.

Signed:

Gbolahan Aiyetoro

ACKNOWLEDGEMENTS

Firstly, I give thanks to God Almighty for granting me the ability, wisdom and strength to commence and conclude this thesis. My deepest gratitude goes to Professor Fambirai Takawira for giving me the opportunity to do my thesis under his supervision as well as his support and guidance. His valuable supervision and financial support is highly appreciated. I would also like to thank my co-supervisor, Dr. Tom Walingo for his support and supervision. I am also grateful to Professor Giovanni Giambene of the University of Siena, Italy, for his continuous research support during the course of this study.

A special thanks to Guissepe Piro, Łukasz Rajewski and Ibrahim Lawal who all assisted me in the development of simulation codes. The financial support of the Centre for Radio Access and Rural Technologies (CRART) and Centre for Engineering Postgraduate Studies (CEPS) is much appreciated.

I also wish to express my unreserved appreciation to my darling wife, Ganiyah Olushola, and lovely son, Zayd, for their support and understanding. My deep gratitude goes to my parents Mr. AbdulMojeed and Mrs. Iyabo Aiyetoro, my sisters (Biola and Bimbo), Dr. (Mrs) Sulaimon and her family, and my in-laws for their unconditional support, words of encouragement and understanding during the course of my PhD programme.

I must not forget my colleagues, who include, but are not limited to Jules Merlin Mouatcho Moualeu, Remmy Musumpuka and John Msumba. You all made my work easier and enjoyable.

Many thanks to Nurudeen Ajayi, Olabode Ojugbele, AbdurRahman Mogbonjubola, Nasirudeen Ajayi, Dr. Abisola, Dr. Tahmid Quazi, Sulaiman Muse, AbdurRasheed Adebayo and their respective families for their brotherly support, words of encouragement and making Durban a home away from home for me.

I thank my friends, brethren and colleagues for their support, and encouragement. To all who have in one way or the other contributed to the success of this thesis, I say thank you!

ABSTRACT

Rapid growth in the number of mobile users and ongoing demand for different types of telecommunication services from mobile networks, have driven the need for new technologies that provide high data rates and satisfy their respective Quality of Service (QoS) requirements, irrespective of their location. The satellite component will play a vital role in these new technologies, since the terrestrial component is not able to provide global coverage due to economic and technical limitations. This has led to the emergence of Satellite Long Term Evolution (LTE) networks which employ Multiple-In Multiple-Out (MIMO) technology.

In order to achieve the set QoS targets, required data rates and fairness among various users with different traffic demands in the satellite LTE network, it is crucial to design an effective scheduling and a sub-channel allocation scheme that will provide an optimal balance of all these requirements. It is against this background that this study investigates packet scheduling in satellite LTE networks employing MIMO technology.

One of the main foci of this study is to propose new cross-layer based packet scheduling schemes, tagged Queue Aware Fair (QAF) and Channel Based Queue Sensitive (CBQS) scheduling schemes. The proposed schemes are designed to improve both fairness and network throughput without compromising users' QoS demands, as they provide a good trade-off between throughput, QoS demands and fairness. They also improve the performance of the network in comparison with other scheduling schemes. The comparison is determined through simulations. Due to the fact that recent schedulers provide a trade-off among major performance indices, a new performance index to evaluate the overall performance of each scheduler is derived. This index is tagged the Scheduling Performance Metric (SPM).

The study also investigates the impact of the long propagation delay and different effective isotropic radiated powers on the performance of the satellite LTE network. The results show that both have a significant impact on network performance.

In order to actualize an optimal scheduling scheme for the satellite LTE network, the scheduling problem is formulated as an optimization function and an optimal solution is obtained using Karush-Kuhn-Tucker multipliers. The obtained Near Optimal Scheduling Scheme (NOSS), whose aim is to maximize the network throughput without compromising users' QoS demands and fairness, provides better throughput and spectral efficiency performance than other

schedulers. The comparison is determined through simulations. Based on the new SPM, the proposed NOSS1 and NOSS2 outperform other schedulers. A stability analysis is also presented to determine whether or not the proposed scheduler will provide a stable network. A fluid limit technique is used for the stability analysis.

Finally, a sub-channel allocation scheme is proposed, with the aim of providing a better sub-channel or Physical Resource Block (PRB) allocation method, tagged the Utility Auction Based (UAB) subchannel allocation scheme that will improve the system performance of the satellite LTE network. The results show that the proposed method performs better than the other scheme. The comparison is obtained through simulations.

TABLE OF CONTENTS

LIST OF FIGURES

LIST OF TABLES

LIST OF ACRONYMS

2G	Second Generation Communications Systems
3G	Third Generation Communications Systems
3GPP	Third Generation Partnership Project
4G	Fourth Generation Communications Systems
AM	Acknowledged Mode
AMC	Adaptive Modulation and Coding
ARP	Allocation and Retention Policy
ARQ	Automatic Repeat Request
BER	Bit Error Rate
BGAN	Broadband Global Area Network
BLER	Block Error Rate
BR	Best Rate
BS	Base Station
CBQS	Channel Based Queue Sensitive
CDMA	Code Division Multiple Access
CP	Co- Polar
CQI	Channel Quality Indicator
CSI	Channel State Information
DRR	Deficit Round Robin
DVB	Digital Video Broadcasting
DVB-RCS	Digital Video Broadcasting Return Channel via Satellite
DVB-S	Digital Video Broadcasting via Satellite

DVB-SH	Digital Video Broadcasting via Satellite Handheld
EDGE	Enhanced Data GSM Environment
EESM	Effective Exponential SINR Mapping
EIRP	Effective Isotropic Radiated Power
eNodeB	Evolved Node B
EPC	Evolved Packet Core
ESA	European Space Agency
E-USRA	Evolved UMTS Satellite Radio Access
EXP-PF	Exponential Proportional Fair
FDD	Frequency Division Duplex
FDMA	Frequency Division Multiple Access
FIFO	First In First Out
FSL	Free Space Loss
GBR	Guaranteed Bit Rate
GEO	Geosynchronous Orbit
GGSN	Gateway GPRS Support Node
GPRS	General Packet Radio Service
GSM	Global Systems for Mobile Communications
GW	Gateway
HARQ	Hybrid Automatic Repeat Request
HEO	Highly Elliptical Orbit
HOL	Head of Line
HRR	Hierarchical Round Robin
HSDPA	High Speed Downlink Packet Access

HSPA	High Speed Packet Access
HSUPA	High Speed Uplink Packet Access
IEEE	Institute of Electrical and Electronics Engineers
IET	Institution of Engineering and Technology
ILP	Integer Linear Programming
IMT	International Mobile Telecommunications
IMT-2000	International Mobile Telecommunications 2000
IP	Internet Protocol
ITU	International Telecommunication Union
ITU-R	International Telecommunication Union Radio Communication Sector
JFI	Jain Fairness Index
KKT	Karush Kuhn Tucker
LAN	Local Area Network
LEO	Low Earth Orbit
LHCP	Left Hand Circularly Polarized
LMS	Land Mobile Satellite
LMSS	Land Mobile Satellite Systems
LOS	Line of Sight
LTE	Long Term Evolution
MAC	Medium Access Control
MCS	Modulation and Coding Scheme
MDD	Maximum Deviation Delete
MDTT	Maximum Difference Top Two
MEO	Medium Earth Orbit

MF-TDMA	Multiple Frequency Time Division Multiple Access
MIMO	Multiple Input Multiple Output
MIMO LMS	MIMO Land Mobile Satellite
MLD	Maximum Loss Delete
M-LWDF	Modified Largest Weighted Delay First
MSS	Mobile Satellite Systems
MU MIMO	Multi-User MIMO
NGN	Next Generation Networks
NLOS	Non Line of Sight
NRT	Non Real Time
NS-3	Network Simulator 3
OFDM	Orthogonal Frequency Division Multiplexing
OFDMA	Orthogonal Frequency Division Multiplexing Access
PBCH	Physical Broadcast Channel
PDF	Probability Density Function
PER	Packet Error Rate
PF	Proportional Fair
PI	Priority Index
PMI	Precoding Matrix Indicator
PRB	Physical Resource Block
QAF	Queue Aware Fair
QCI	QoS Class Identifier
QoS	Quality of Service
QSI	Queue State Information

RAN	Radio Access Network
RHCP	Right Hand Circularly Polarized
RI	Rank Indicator
RLC	Radio Link Control
RNC	Radio Network Controller
RR	Round Robin
RRC	Radio Resource Control
RRM	Radio Resource Management
RT	Real Time
RTP	Round Trip Propagation
RTPD	Round Trip Propagation Delay
SC-FDMA	Single Carrier Frequency Division Multiple Access
SGSN	Serving GPRS Support Node
S-HSDPA	Satellite High Speed Downlink Packet Access
SINR	Signal to Noise plus Interference Ratio
S-LTE	Satellite Long Term Evolution
S-MBMS	Satellite Multicast and Broadcast Multimedia Systems
SNR	Signal to Noise Ratio
S-PCS	Satellite Personal Communications Services
S-UMTS	Satellite Universal Mobile Telecommunications Systems
TBS	Transport Block Size
TDD	Time Division Duplex
TDMA	Time Division Multiple Access
TTI	Transmission Time Interval

T-UMTS	Terrestrial Universal Mobile Telecommunications Systems
UAB	Utility Auction Based
UE	User Equipment
UMTS	Universal Mobile Telecommunications Systems
USRAN	UMTS Satellite Radio Access Network
UTRAN	UMTS Terrestrial Radio Access Network
VOIP	Voice over Internet Protocol
WCDMA	Wideband Code Division Multiple Access
WIMAX	Worldwide Interoperability of Microwave Access
XP	Cross Polar
XPD	Cross Polar Ratio

LIST OF SYMBOLS

α	Smoothing parameter
a_k	QoS differentiator for user k
δ^{υ}	Average drift vector
A_k	Arrival rate in user k
C_{large}	A 4 x 4 correlation matrix
δ_k	Maximum allowed probability of exceeding the deadline
G_R	Gain of receiving antenna
G_T	Gain of transmitting antenna
H_{small}	Small scale fading (multipath) matrix
H_{large}	Large scale fading (shadowing) matrix
I	Inter-spot-beam interference
L_{Fs}	Free Space Loss
L_p	Polarization loss
L_{Total}	Total Loss
n	Number of Transmission Time Intervals (TTIs)
N_f	Sampling factor
P_{ij}	Transition probability from state i to state j
$S_{low\|c}$	Correlated low shadowing
$S_{high\|c}$	Correlated high shadowing
r_c	Coherence distance
v_m	Mobile speed

$\emptyset_i$	Angle of arrival
θ_i	Random phase
P_r	Received power
$P_{k,c}$	Probability that a user *k* is in channel state *c*
R_{cp}	Co-polar correlation matrix
R_{xp}	Cross-polar correlation matrix
$R_{k,j}$	Instantaneous data rate of user *k* over subchannel *j*
$\mu_{k,c}$	Departure probability of channel state c
$S_{k,c}$	Total number of users *k* that have completed transmission in channel *c*
W_k	Waiting time or Delay of HoL Packet for user *k*
T_k	Average data rate of user *k*
$T_{k,deadline}$	Delay Deadline for the UE traffic flow *k*
T_k^L	Time spent to serve user *k* using scheduling policy *L*.
$T_{k,c}^{L,r}$	Time spent on serving user *k* at channel *c* under a scheduling policy *L*
$L_{k,j}$	Utility function that depends on the scheduling algorithm
$U_{k,j}$	Variable that indicates whether user *k* is assigned to subchannel *j*
V_k	Variance of the service time of user *k*

Chapter 1

INTRODUCTION

1.1 Evolution of Satellite Mobile Communication Networks

Satellite communication systems have become a vital component of mobile communications. Although mobile satellite systems have been used for navigational purposes, systems tracking, and safety and emergency communications [1], recent developments have made it possible to use satellite systems to provide telecommunication services such as voice calls, video streaming and so on, using portable mobile phones either as standalone satellite receivers or operating in dual modes, for both terrestrial and satellite networks. This was first achieved with the introduction of Satellite Personal Communication Services (S-PCS) through the use of non-geostationary satellites like LEO and MEO satellite systems [1]. It is worth noting that mobile smart phone devices are a recent development, with capabilities of connecting to 2G and 3G cellular networks and S-band Satellite networks.

The new developments in GEO satellite systems have made them more suitable to provide portable mobile communications facilities [2]. The need to extend telecommunication services such as voice calls, video streaming or downloads, web browsing and file downloads provided by cellular networks to remote areas, sparsely populated areas and aeroplane or ships has made satellite communications a key element of next generation mobile networks.

1.1.1 Satellite Universal Mobile Telecommunications System (S-UMTS)

Satellite Universal Mobile Telecommunications systems complement their terrestrial counterparts. Due to their improved global coverage, satellite systems offer seamless global roaming and transparent handovers between the terrestrial and satellite networks. The UMTS therefore provides mobile users with telecommunication services anytime, anywhere. The S-UMTS operates in two frequency bands which fall between 1.980 and 2.010 GHz and between

2.17 and 2.20 GHz. The three circular orbit satellite systems, namely, the LEO, MEO and GEO systems, can be used to implement S-UMTS. The S-UMTS supports both broadband applications and multimedia services [3]. The S-UMTS Family G specification set aims to ensure that the satellite's interface will be fully compatible with Terrestrial UMTS (T-UMTS)-based systems, even though some modifications will be made due to the differences between the terrestrial and the satellite channels [4]. The satellite cell is one of five basic cell types, as agreed by the IMT-2000, to provide complete coverage to support all possible UMTS transmission environments. One of the existing satellite networks, the Broadband Global Access Network (BGAN) provided by INMARSAT can also provide UMTS services.

1.1.2 Satellite High Speed Downlink Packet Access (S-HSDPA)

The Satellite High Speed Downlink Packet Access (S-HSDPA) is an appealing S-UMTS service for point-to-point connections due to the satellite's inherent high data rate capacity. It is an evolution of S-UMTS based on GEO Satellite in order to support higher data rate services such as multimedia services to mobile users [5]. The higher data rate is achieved through Adaptive Modulation Coding (AMC) that offers a scheduling scheme at Transmission Time Interval (TTI) of 2ms, an extensive multi-code operation and a fast and spectral efficient retransmission strategy, known as Fast Physical Layer Hybrid ARQ (F-L1 HARQ). The adaptation of the HSDPA to the satellite air interface is being carried out by the European Commission's FP6 project, MAESTRO [6]. In S-HSDPA, the radio resource management functions are performed at the Node B located at the earth station that is directly connected to the Radio Network Controller (RNC) which serves as gateway to the same core network used by the terrestrial counterpart [7].

1.1.3 Satellite Long Term Evolution (S-LTE)

The need for mobile networks to improve system capacity and comply with QoS requirements formed the basis for ITU-R WP 8F to define evolution towards future Fourth Generation Mobile (4G) which is also known as International Mobile Telecommunications (IMT)-Advanced [8]. This led to the emergence of Long Term Evolution (LTE) and Worldwide Interoperability for Microwave Access (WiMAX) 802.16x. Although these two technologies do not completely fulfil the requirements, they are the first steps towards the given 4G definitions [9].

Future satellite air interfaces are being proposed with a high degree of commonality with the 4G terrestrial air interface. Hence, both 3GPP LTE and WiMAX air interfaces have been proposed for the satellite environment, especially for unicast communications. Key technology enablers are being designed that will enable the LTE air interface to be used in the satellite channel [10],[11], despite peculiarities like long Round Trip Propagation Delay (RTPD), on-board amplifier and specific channel model experienced in satellite systems. The whole system will have both terrestrial and satellite RAN connecting to the same core network and an S-band GEO satellite system has been recommended for this purpose (land mobile users) [11].

The Satellite LTE technology, which is of interest to this study, is the next step in the evolution of 2G and 3G systems. It is made up of radio access and packet core networks. The radio access network of LTE is referred to as Evolved UMTS Satellite Radio Access (E-USRA) and the core network is denoted as Evolved Packet Core (EPC). LTE uses a new multiple access technology, Orthogonal Frequency Division Multiple Access (OFDMA), for downlink transmission [10] and Single Carrier Frequency Division Multiple Access (SC-FDMA) for uplink, to serve as return channel [12]. It also uses AMC and Multiple-in Multiple-out (MIMO) technology to provide higher data rates than previous technologies.

1.2 Application of MIMO to Satellite Networks

Major breakthrough MIMO technology used in terrestrial networks has stimulated the need for satellite networks to move in the same direction. The initial challenge is to determine the best MIMO technique for the satellite network, since terrestrial networks' characteristics such as channel impairments, propagation delay, service coverage area and the geometry of the link differ from those of the satellite network. Furthermore, the varying nature of satellite networks has challenged research on the application of MIMO technology in the satellite network. Operating frequency bands, multiplexing schemes and whether a fixed or mobile satellite system is required have made such research more complicated.

The other major challenge in the application of MIMO to satellite systems is the spacing between the MIMO antennas. In order to take advantage of the spatial multiplexing and diversity gains offered by MIMO technology the antenna spacing should be large and the scattering distribution around the transmitter and the receiver should be dense [13]. Due to the fact that there is little space for satellites positioned in the geostationary orbit, the use of more than two satellites has become expensive; this limits the number of satellites that can be used [14]. This stimulated research on the optimal positioning of MIMO satellite antennas to achieve maximum capacity [14],[15]. The dual polarization principle has been found to be a useful and

economical way of implementing MIMO technology in a satellite scenario. This is achieved by using only one physical dual-polarized transmitting and receiving antenna.

The channel capacity of MIMO satellite systems can be distinguished in two categories; when the satellite uses regenerative payload and when it uses transparent payload [16]. For regenerative payload, the downlink and uplink are treated as separate end to end communication links and the smaller capacity of the two links is used as the MIMO satellite system's data rate. As stated in [16], the MIMO channel capacity for satellite that uses a regenerative payload can be stated as;

$$C = \log_2[det(I_M + \rho . HH^H)] \tag{1.1}$$

Where $\{.\}^H$ is the complex conjugate transpose, H is the channel matrix and ρ is the linear ratio of the transmit power at each transmit antenna to the noise at each of the receiving antenna. The ρ for the uplink and downlink can be respectively computed as follows;

$$\rho_u = 10^{(SNR_u + L_u)/10} \tag{1.2}$$

$$\rho_D = 10^{(SNR_D + L_D)/10} \tag{1.3}$$

Where SNR_u ,SNR_D, L_u and L_D are the SNR and the path loss for the uplink and downlink respectively.

For the transparent payload, the satellite is also made up of both uplink and downlink channels. The setup is said to have T transmit antenna of the uplink ground station, M receive antenna and M transmit antenna at the satellite, and R receive antenna at the downlink ground terminal. As stated in [16], the channel capacity can be stated as;

$$C = \log_2[det(I_M + \rho_u . H_u H_u^H - \rho_u . H_u H_u^H S^{-1})] \tag{1.4}$$

Where S is given as;

$$S = I_M + {\sigma_u^2}/{\sigma_d^2} . F^H H_D H_D^H F \tag{1.5}$$

Where F is the transfer matrix of the satellite payload (relay), σ_u^2 and σ_d^2 is the noise power at the receiver for the uplink and downlink respectively.

As identified in [17], the potential application of MIMO technology to a satellite network can be broadly divided into fixed and mobile satellite as pictorially presented in Fig. 1-1 There are currently several ongoing projects on the application of MIMO technology in a satellite network, two of which are driven by the European Space Agency (ESA). One of the projects is

the MIMO HW demonstrator which is evaluating the applicability of the MIMO technique to satellite networks with a primary focus on Digital Video Broadcasting Satellite Handheld (DVB-SH) and the other is MIMOSA, which focuses on the development of an MIMO propagation channel model for mobile satellite networks [18],[19].

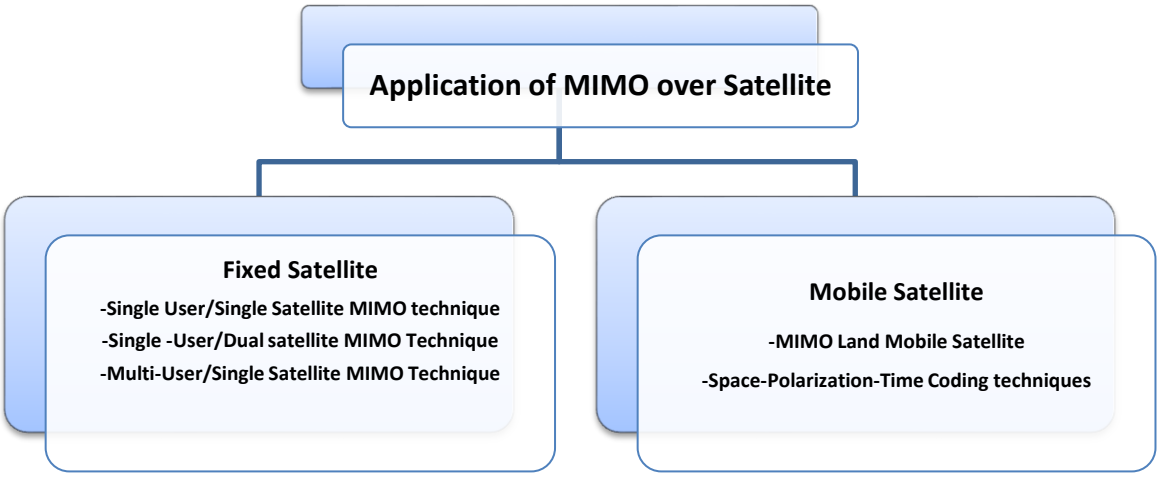

Figure 1-1 MIMO over Satellite Network

The diversity techniques used in MIMO Land Mobile Satellite (MIMO LMS) of interest to this work are satellite diversity and polarization diversity. The satellite diversity, which is considered in [20],[21], is implemented using multiple satellites which are adequately spaced to provide independent fading channels, in order to communicate with a user terminal with single or multiple antennas. This technique has been proposed to produce a MIMO channel matrix for satellites operating low frequency bands (L and S band) [22]. While satellite diversity provides a practical solution, the major issues are the cost of implementation and the asynchronous nature of the data streams received at the user terminal due to the difference in delay as a result of the wide separation between the two antennas. Various solutions have been proposed in the literature to address the latter.

On the other hand, polarization diversity works on the principle of the sensitivity of polarization to refraction and diffraction processes. This diversity technique, which is used in [23]-[26], employs a single, dual-polarized orthogonal satellite to communicate to a user terminal with a dual-polarized orthogonal antenna. It is a practical solution for land mobile satellites which operate at S band. Its main advantage over satellite diversity is the fact that implementation does not involve any additional costs, since there is no need for an extra satellite. Another advantage is that it avoids the asynchronous nature of data streams experienced in the satellite diversity scenario. However, polarization diversity is not suitable at high frequency bands due to the highly correlated rainfall medium experienced in these bands [27]. Polarized diversity has been adopted for this study for the stated reasons and because it is being used at S band (low

frequency band). It is worth noting that the capacity of polarization diversity can only increase by 2, while that of satellite diversity can be increased by *k* numbers of satellite [27].

1.3 Challenges confronting Satellite Mobile Communication Networks

Mobile satellite systems are key solutions that offer global coverage and seamless global roaming with the capability to provide broadband and multimedia services at an acceptable QoS. However, in order to realise this potential, there is need to address the technical challenges confronting satellite systems. Some of these challenges are presented below.

1.3.1 Long Propagation Delay

The delay experienced along the link in satellite communications varies depending on the satellite orbit, the user's position on the earth and the satellite type. GEO satellite is situated at high altitude and therefore has higher propagation delay than LEO and MEO. This causes many problems for link adaptation, radio resource management and transmission of delay sensitive applications like video and voice [4].

1.3.2 Atmospheric Effects

Atmospheric effects include atmospheric gasses, rain attenuation, scintillation, fog and clouds. Rain attenuation is the main effect and can be neglected for frequency below 10 GHz. Scintillation affects communication at frequencies below 10 GHz and at an elevation angle of above 10°, while fog and clouds are significant at frequencies above 30 GHz [4].

1.3.3 Channel Losses

The atmospheric effects experienced in satellite communications render the Bit Error Rate (BER) very high. This causes the satellite link to experience rapid degradation, which can lead to erroneous bits during transmission [4].

1.3.4 Satellite Lifetime

Due to the ageing of the components used to build satellites, as well as the effect of radiation and other factors, satellites' lifespan is very limited, although it varies depending on the type of satellite. GEO satellites have a lifetime of 10-15 years, while MEO satellites function well for 10-12 years and LEO satellites are useful for 5-8 years [4].

1.4 Motivation for Research

The satellite component of 4G systems will play a vital role in ensuring the seamless provision of mobile services to users, irrespective of their location, which is one of the set requirements, since the terrestrial component is not be able to provide global coverage due to economic and technical limitations [28]. Due to the uniqueness of the satellite air interface, the design and implementation of satellite LTE networks becomes more challenging.

The nature of the satellite channel and the long propagation delay are major challenges in achieving high system performance in satellite LTE networks. The long propagation delay causes misalignment between the Channel Quality Indicator (CQI) reported at the eNodeB (base station) and the actual CQI experienced by the User Equipment (UE). Link adaptation needs to be addressed since the packet scheduling and resource allocation schemes rely on link adaptation in satellite LTE networks. The aim of this study is to investigate the impact of the satellite channel model and RTPD, by comparing it with its terrestrial counterparts and investigating the effect of RTPD on channel reporting on a satellite LTE network's performance.

In order to achieve the ambitious 4G targets in terms of QoS, data rates and fairness, an effective scheduling scheme is required to provide an optimal balance of all these requirements. Since the LTE specifications do not compel the use of a particular scheduler, the literature has proposed several schedulers for the terrestrial LTE network with the aim of improving network performance and satisfying users' QoS requirements. However, there is a paucity of research on the satellite LTE network. This study therefore proposes a novel, cross-layer approach based packet scheduling and optimal packet scheduling schemes that will improve the satellite LTE network's performance without compromising users' QoS demands and fairness among users. A performance comparison of the proposed schemes with the schemes identified in the literature is conducted for a satellite LTE air interface through simulations.

Since there are several available subchannels, depending on the bandwidth size of the network, the ability to design a subchannel allocation scheme that will effectively map the scheduled users to the available sub-channels in order to improve network performance is a key issue in a satellite LTE network and Orthogonal Frequency Division Multiple Access (OFDMA)-based network as a whole. This study also proposes a new subchannel allocation scheme for a satellite LTE network that will effectively map the scheduled user(s) to the available sub-channels, in order to improve network performance. A performance comparison of the proposed schemes with those identified in the literature is conducted for a satellite LTE air interface.

1.5 Structure of the Thesis

This thesis is divided into seven chapters. Chapter 1 provided an overview of various satellite systems, and an overview of satellite mobile communication systems and the application of MIMO to satellite networks. It also outlined the motivation for this study; the structure of the thesis, the original contributions made by this work and publications produced from this research study.

Chapter 2 presents a description of the satellite LTE air interface and the system model of the satellite LTE network. It also describes the MIMO channel model considered for the satellite LTE network in detail. The link budget analysis and CQI computation is presented, as well as an overview of the Medium Access Control (MAC) Layer and the traffic models considered.

Chapter 3 considers the packet scheduling problem in a satellite LTE and examines the scheduling schemes identified in the literature as well as the proposed cross-layer based scheduling schemes. The simulation set-up and results obtained from the comparison of the proposed cross-layer based schedulers and the two throughput optimal scheduling schemes are presented. Throughput, delay, fairness and spectral efficiency are the considered performance metrics. A new overall performance scheduling index tagged Scheduling Performance Metric (SPM) is derived and used to evaluate the overall performance of each scheduler. LTE-Sim, which is a standalone version of the LTE module in Network Simulator 3 (NS-3), is used as the simulation software. The results and conclusions are discussed.

Chapter 4 commences with an overview of link adaptation in a satellite LTE network. The proposed scheduler used for this investigation is presented. The simulation set-up and results obtained from the investigation on the impact of RTPD, experienced in CQI reporting on network performance in satellite LTE networks are presented, as well as the simulation results from the investigation of the impact of RTPD on satellite LTE, compared with terrestrial LTE networks. LTE-Sim, which is a standalone version of the LTE module in Network Simulator 3 (NS-3), is used as the simulation software. The results and conclusions are discussed.

Chapter 5 begins by discussing the optimization problem formulation of the scheduling problem. A detailed near-optimal solution of the optimization problem is presented using Karush Kuhn Tucker (KKT) multipliers. The simulation set-up and results obtained from the comparison of the proposed schedulers with the two throughput optimal scheduling schemes are presented. Throughput, delay, fairness, spectral efficiency and the proposed index, SPM, are the considered performance metrics. LTE-Sim, which is a standalone version of the LTE

module in Network Simulator 3 (NS-3), is used as the simulation software. The results and conclusions are discussed.

Chapter 6 reviews the literature on the stability analysis of schedulers and describes the adopted model for the stability analysis. The scheduling policy, which is the proposed near-optimal scheduling scheme to be analysed or tested is presented. The fluid limit technique adopted, which consists of both weak fluid and hard fluid limits, is also presented. The stability tests as well as the conclusions are discussed.

In Chapter 7, a sub-channel allocation problem is presented. Existing subchannel allocation schemes in the literature and proposed subchannel allocation scheme are presented. The simulation set-up and results obtained from the comparison of the proposed subchannel allocation scheme with other subchannel allocation schemes are presented. Throughput, spectral efficiency and fairness are the considered performance metrics. LTE-Sim, which is a standalone version of the LTE module in Network Simulator 3 (NS-3), is used as the simulation software. The results and conclusions are discussed.

Finally, Chapter 8 presents the study's final conclusions and makes suggestions for further research.

1.6 Original Contributions in this Research

The original contributions of this research study are:

- Investigation of the impact of RTPD in CQI reporting on the performance of satellite LTE networks.
- Design of a novel, cross-layer approach-based packet scheduling scheme to provide a good trade-off between network throughput, degree of fairness and an acceptable QoS in a satellite LTE network.
- Design of a novel, near-optimal packet scheduling scheme to provide optimal throughput and a good trade-off between network throughput, degree of fairness and an acceptable QoS in a satellite LTE network.
- Stability analysis of the proposed near-optimal packet scheduling scheme in order to confirm its stability.

1.7 Published/Submitted Work

The work presented in this thesis has either been presented by the author as a peer-reviewed paper at conferences or submitted/accepted as journal publications. The publications are as follows;

1. Gbolahan Aiyetoro, Giovanni Giambene and Fambirai Takawira, "Performance Analysis of M-LWDF and EXP-PF schedulers for real time traffic for satellite LTE networks", Proceedings of South Africa Telecommunications Networks and Applications Conference (SATNAC), George, September 2012.

2. Gbolahan Aiyetoro, Giovanni Giambene and Fambirai Takawira, "A New Packet Scheduling Scheme in Satellite LTE networks", Proceedings of IEEE AFRICON Conference, Mauritius, September 2013.

3. Gbolahan Aiyetoro, Giovanni Giambene and Fambirai Takawira, "Impact of Long Propagation Delay in Satellite LTE Networks", Advance Science Letters, Vol. 20, No. 2, February 2014 , pp. 397-401.

4. Gbolahan Aiyetoro and Fambirai Takawira, "Cross-layer based Packet Scheduling for Multimedia traffic in Satellite Long Term Evolution (LTE) Networks", Sixth IFIP International Conference on New Technologies, Mobility & Security (NTMS 2014).

5. Gbolahan Aiyetoro, Giovanni Giambene and Fambirai Takawira, "Packet Scheduling in MIMO satellite Long Term Evolution (LTE) Networks". Submitted to IET Networks.

6. Gbolahan Aiyetoro, Fambirai Takawira and Tom Walingo, "Near-Optimal Packet Scheduling in satellite Long Term Evolution (LTE) Networks". Submitted to IET Networks.

Chapter 2

SATELLITE LTE SYSTEM MODEL

2.1 Introduction

This chapter introduces the emerging satellite LTE air interface and the adopted MIMO technology. The satellite LTE architecture is described and the concepts of resource allocation in a satellite LTE network and Medium Access Control (MAC) layer are presented. Finally, the system model considered for the downlink scenario of a satellite LTE network throughout this study, which includes the network model, channel model and traffic model, is also presented.

2.2 Satellite LTE Air Interface

It is envisaged that, like its terrestrial counterpart, satellite LTE radio access technology will use OFDMA for downlink transmission.. As stated in [10], OFDMA can be adopted for satellite systems due to the fact that it easily exploits frequency selectivity and allows flexible bandwidth operation with low-complexity receivers. It supports both Frequency Division Duplexing (FDD) and Time Division Duplexing (TDD) and allows for a wide range of different bandwidths (1.5, 3, 5, 10, 15 and 20 MHz) [29]. It also supports downlink MIMO schemes, including transmit diversity, spatial multiplexing and beamforming [30]. Spatial multiplexing, which includes single user and MU MIMO, is of interest to this study. For the downlink of 3GPP LTE, the 2 x 2 MIMO is assumed to be the baseline configuration [31]. The transmission modes are: single antenna, transmit diversity, open-loop spatial multiplexing, closed-loop spatial multiplexing, MU MIMO, closed-loop single layer precoding and single antenna (beamforming). Four of these seven transmission modes as specified for LTE are related to MIMO transmissions. Two new transmission modes have recently been added [32]. These nine transmission modes are presented in Table 2-1.

Table 2-1: Transmission modes in LTE [32]

Transmission mode	**Transmission scheme of Physical Downlink Shared Channel (PDSCH)**
1	Single-antenna port, port 0
2	Transmit diversity
3	Transmit diversity if the associated rank indicator is 1, otherwise, large delay CDD
4	Closed-loop spatial multiplexing
5	Multi-user MIMO
6	Closed-loop spatial multiplexing with a single transmission layer
7	If the number of Physical Broadcast Channel (PBCH) antenna ports is one, Single-antenna port, port 0; otherwise, Transmit diversity
8	If the UE is configured without Precoding Matrix Indicator/Rank Indication (PMI/RI) reporting: if the number of PBCH antenna ports is one, single-antenna port, port 0; otherwise, transmit diversity If the UE is configured with PMI/RI reporting: closed-loop spatial multiplexing
9	If the UE is configured without PMI/RI reporting: if the number of PBCH antenna ports is one, single-antenna port, port 0; otherwise, transmit diversity If the UE is configured with PMI/RI reporting: if the number of Channel State Information-Reference Signal (CSI-RS) ports is one, single-antenna port, port

2.2.1 Architecture of Satellite LTE Air Interface

For the purpose of this study, the evolved Node B (eNodeB), which acts as the base station, is located on the earth station and is equipped with two transmit antennas. The User Equipment (UE) also two antennas according to the 2 x 2 MIMO configuration. A transparent GEO Satellite has been considered in this study. Dual-polarized antennas, consisting of Right Hand

Circular Polarized (RHCP) and Left Hand Circular Polarized (LHCP) antennas [17], have been considered for both the GEO satellite and UEs. As shown in Fig. 2-1, the satellite eNodeB uses two satellite dishes (which serve as the two transmitting antennas) to transmit to mobile users via the dual-polarized antennas of the GEO satellite [14]. Transmission mode #5 for MU MIMO has been considered here, since the main focus of this study is to evaluate the performance of schedulers and subchannel allocation schemes in a multi-user scenario with MIMO technology. This allows simultaneous transmissions from the two polarized antennas of the GEO satellite to different UEs. This transmission mode is closed-loop; hence, there is a UE feedback for link adaptation purposes, which is vital in determining the transmission rate.

The Channel Quality Indicator (CQI) is sent by the UE to the eNodeB. The reported CQI via feedback signaling is used for transmission (i.e., modulation and coding selection) and scheduling purposes at the eNodeB on the earth station [11]. A RTPD of approximately 540 ms is experienced in this scenario. This causes misalignment between the reported UE's CQI at the eNodeB and the instantaneous CQI level, actually experienced by the UE. This problem will either lead to the underutilization of resources, if a lower CQI is used, or packet losses if a higher CQI is used. This misalignment in link adaptation due to RTPD represents a serious challenge in the satellite scenario.

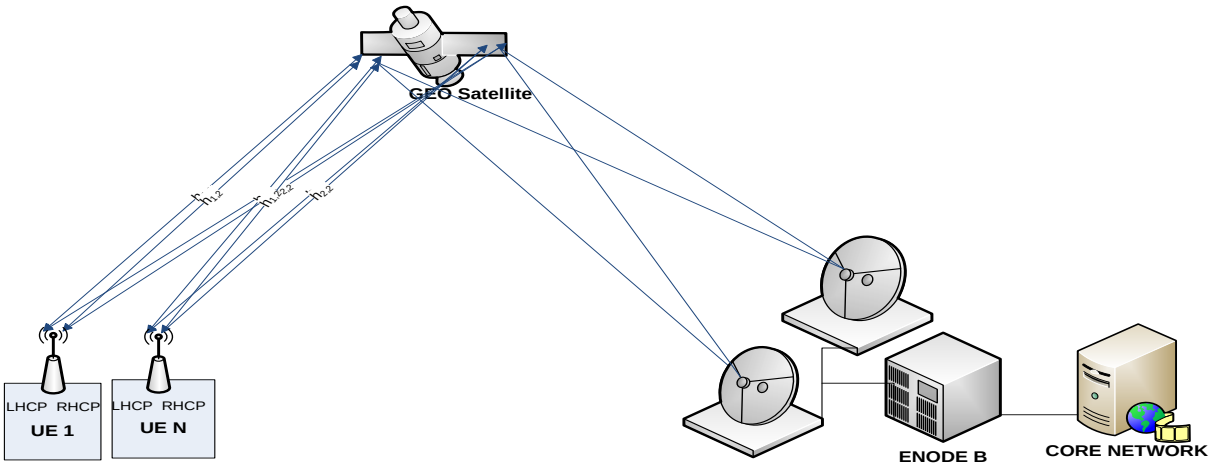

Figure 2-1: The system architecture of a dual-polarized MIMO satellite LTE network

2.2.2 Resource Allocation

At the MAC layer of the eNodeB, the packet scheduler works with the Link Adaptation (LA) module and Hybrid Automatic Repeat reQuest (HARQ) to schedule the various users on the transmission resources at every Transmission Time Interval (TTI), which is 1 ms, as specified in the LTE standard. The scheduler for unicast transmissions dynamically allocates resources in time/frequency domain. The basic time-frequency resource to be allocated is the Physical

Resource Block (PRB). The packet scheduler regularly interacts with the link adaptation module in order to determine the supported transmission rate for each user. Scheduling decisions depend on the algorithm adopted and the selected UEs in a TTI are then mapped to the corresponding PRBs.

Physical layer resources are organized in PRBs. Each PRB consists of 12 consecutive subcarriers (180 kHz of the whole bandwidth) for a duration of 0.5 ms (time slot) [33], which contains 6 or 7 symbols depending on the type of cyclic prefix used. Subcarrier spacing is of 15 kHz. Assuming a normal cyclic prefix of 7 symbols is used, a PRB is composed of 84 symbols. It is important to note, that the resource allocation is made on a sub-frame basis (i.e., TTI equal to 1 ms), that is, PRBs are allocated in pairs (called Scheduling Block) on a TTI (= 1 ms) basis.

As shown in Fig. 2-2, the LTE frame is made up of 10 sub-frames; hence, each LTE frame lasts 10 ms or 20 slots. The smallest unit within the PRB is the Resource Element (RE). An RE can be 2, 4 or 6 bits, depending on the modulation used, that is QPSK, 16QAM or 64 QAM, respectively. The modulation type that will be used depends on the reported CQI value sent by the UE to the eNodeB.

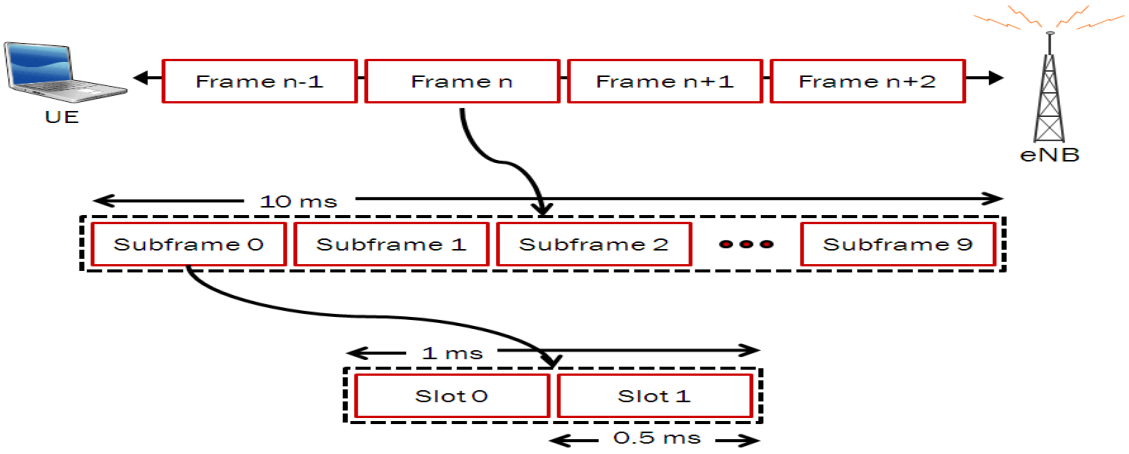

Figure 2-2: The LTE frame structure [34]

The number of PRBs available in a scheduling interval depends on the size of bandwidth used and the number of antennas deployed. The number of PRBs for a single antenna ranges from 12 to 200, depending on the bandwidth size, which ranges from 1.4 to 20 MHz [35]. An example of the resource allocation format is shown in Fig. 2-3 for a 2 x 2 MU MIMO satellite LTE scenario, which allows 2 streams to different UEs. PRBs are allocated in pairs to the selected UE at every TTI for the two available antenna ports. The pair of PRBs allocated to the same UE use the same transmission rate (CQI).

Antennas		TTI 1	TTI 2	…..	TTI T
Antenna port 0	Subchannel 1	User A	User D	….	User A
	…….	….	…..	….	….
	Subchannel S	User C	User A	….	User B
Antenna port 1	Subchannel 1	User F	User E	….	User B
	……	….	….	….	….
	Subchannel S	User C	User F	….	User C

Figure 2-3: An example of a resource allocation scheme in 2 x 2 MU MIMO satellite LTE network

The adoption of AMC in satellite LTE networks causes the transmission rate of each subchannel to vary depending on the reported CQI of that particular subchannel. The CQI values varies from 1 to 15, with each CQI having its own corresponding spectral efficiency based on its associated Modulation and Coding Scheme (MCS). The 4 bit CQI table is presented in Table 2-2 below.

Table 2-2: 4-bit CQI table [32]

CQI	Modulation	code rate x 1024	Efficiency
0	Out of Range	Out of Range	Out of Range
1	QPSK	78	0.1523
2	QPSK	120	0.2344
3	QPSK	193	0.377
4	QPSK	308	0.6016
5	QPSK	449	0.877
6	QPSK	602	1.1758
7	16QAM	378	1.4766
8	16QAM	490	1.9141
9	16QAM	616	2.4063
10	64QAM	466	2.7305
11	64QAM	567	3.3223
12	64QAM	666	3.9023
13	64QAM	772	4.5234
14	64QAM	873	5.1152
15	64QAM	948	5.5547

2.2.3 Medium Access Control (MAC) Layer

At the MAC layer of the eNodeB, each UE has its own queue. The MAC layer handles the scheduling [36] in satellite LTE networks. Every TTI, the scheduler selects a set of UE(s) from all the available queues that is then mapped to pairs of PRBs of a suitable antenna port, depending on the scheduling algorithm. The link adaptation and scheduling modules at the MAC layer require the CQI feedbacks [37] to schedule and allocate PRBs to users. At certain reporting intervals, the UEs send the information on the channel state, in the form of CQI value, to the eNodeB via the satellite. This CQI is available to the MAC-layer scheduler in order to make channel-aware scheduling decisions. Queue State Information (QSI), such as Head of Line (HoL) packet waiting time and the instantaneous queue length, are also available to the scheduler every TTI to make scheduling decisions. The MAC of LTE receives cross-layer information from both lower layers (channel state information, CQI) and higher layers (e.g., traffic class used by the application).

Table 2-3: Standardized QCI characteristics for LTE [38]

QCI	Resource Type	Priority	Packet Delay Budget	Packet Error Loss Rate	Example Services
1	GBR	2	100 ms	10^{-2}	Conversational Voice
2		4	150 ms	10^{-3}	Conversational Video (Live Streaming)
3		3	50 ms	10^{-3}	Real Time Gaming
4		5	300 ms	10^{-6}	Non-Conversational Video (Buffered Streaming)
52	Non-GBR	1	100 ms	10^{-6}	IMS Signalling
6		6	300 ms	10^{-6}	Video (Buffered Streaming) TCP-based (e.g., www, e-mail, chat, ftp, p2p file sharing, progressive video, etc.)
7		7	100 ms	10^{-3}	Voice, Video (Live Streaming) Interactive Gaming
8		8	300 ms	10^{-6}	Video (Buffered Streaming), TCP-based (e.g., www, e-mail, chat, ftp, p2p file sharing, progressive video, etc.)
9		9			

The LTE standard supports QoS; hence, the network ensures that the bearer characteristics are defined and controlled during the whole session between the UE and eNodeB-gateway (GW). The QoS Class Identifier (QCI) and the Allocation and Retention Policy (ARP) are the indices used to characterize the QoS level of each bearer [38]. There are 9 possible QCI levels [39] and two broad classes, namely, Guaranteed Bit Rate (GBR) and Non-GBR, as specified in [40] that

a bearer can be associated with. The QCI associated with each bearer is characterized by a priority and a constraint in relation to the packet delay and the packet loss rate, as shown in Table 2-3. These characteristics determine how the packet scheduler at the MAC layer handles the packets sent over the bearer and the Radio Link Control (RLC) transmission mode used. The eNodeB is responsible for ensuring QoS for all bearers.

2.3 System Model for Satellite LTE Network (Downlink Case)

The details of the system model used to investigate the impact of link adaptation and to study the network performance of the proposed schedulers is presented below. This system model is also used to study the network performance of sub-channel allocation schemes in a satellite LTE network.

2.3.1 Network Model

The model for downlink transmissions of a satellite LTE network is shown in Fig. 2-4. Both the eNodeB and the UE have two antennas. Each UE has a queue at the MAC layer of the eNodeB. The User scheduler module computes the metrics for all the available sets of queues, based on the considered scheduling algorithm, on a subchannel basis as shown in Fig. 2-4. The scheduler at the MAC layer makes decisions based on CQI values, QoS constraints, information from the application layer, and Queue State Information (QSI) such as delay and packet length. The resource block mapping module maps the selected UEs to the available PRBs or subchannels. Then, the packets in the selected users' queues are transmitted to the UE according to the resources allocated. The details of the channel and traffic models for this network model are presented in the following sections.

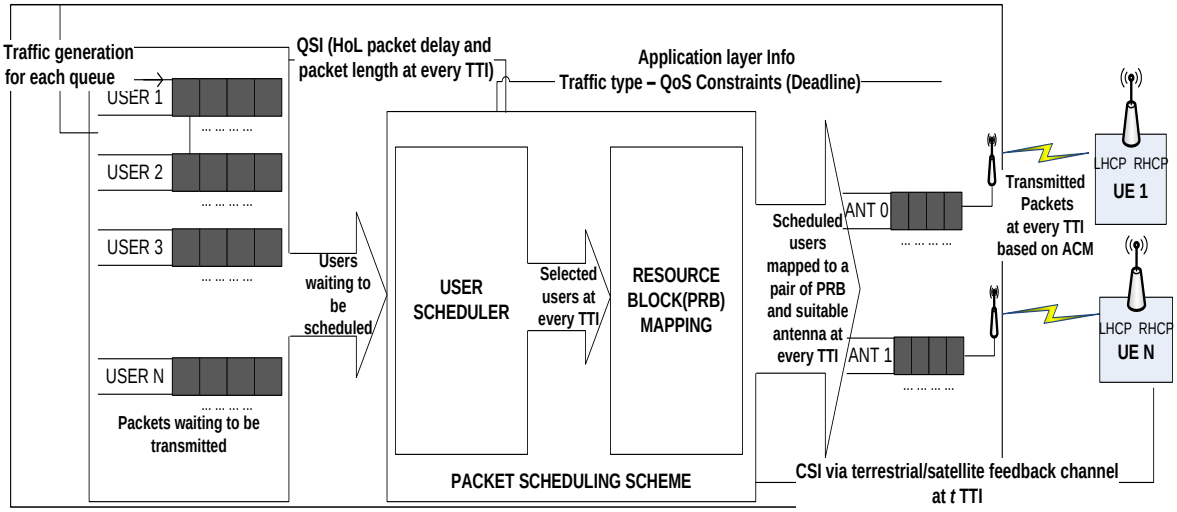

Figure 2-4: The system model for MU MIMO Satellite LTE network (downlink case)

2.3.2 Channel Model

The channel model considered here is an empirical-stochastic model for LMS-MIMO [41]. This model has been validated and compared with other existing models [42]. The stochastic properties of this model are derived from an S-band tree-lined road measurement campaign (suburban area), using dual circular polarizations at low elevations [41]. A 4-state Markov model, presented in Fig. 2-5 later in this section, is used to determine the current channel state, using the probability transition matrix presented in (2.2); the corresponding parameters for the current channel state are then used to compute large scale fading (shadowing) matrix H_{large} and small scale fading (multipath) matrix H_{small}, which are summed together to produce the channel matrix, H, below:

$$H = \begin{pmatrix} h_{RR} & h_{LR} \\ h_{RL} & h_{LL} \end{pmatrix} \tag{2.1}$$

A Markov chain is used to select between the possible regions of high and low shadowing values, for both co-polar and cross-polar channels, to model the mobile user's movement across the buildings. The four possible Markov states are presented in Fig. 2-5 below. These states are due to the high or low state of both the co-polar (CP) and cross-polar (XP) channels, according to a 2x2 MIMO configuration. Transitions between the states occur at every TTI.

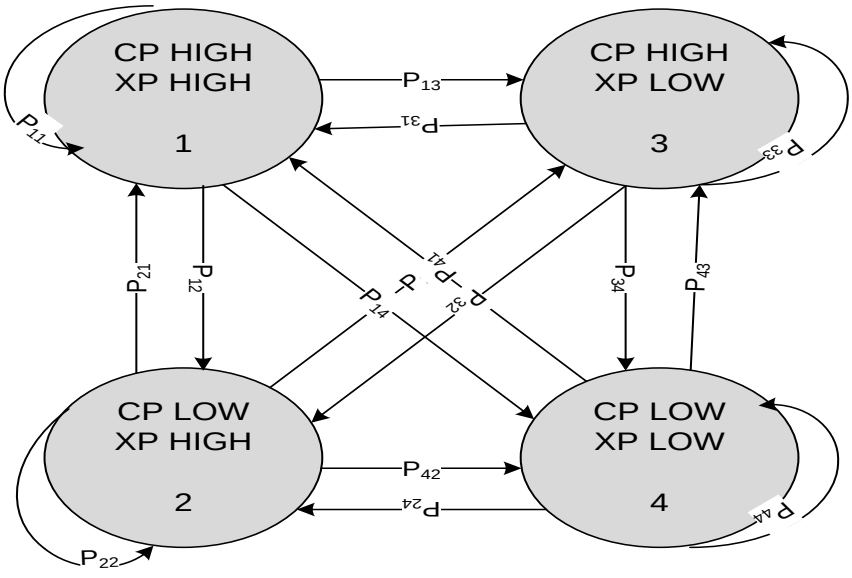

Figure 2.5: Four-state Markov model of an LMS-MIMO channel

The 4 x 4 transition matrix *P* below is used to predict the next possible state and is derived from the measurements carried out as stated in [43]. States are numbered as follows: State 1 is CP Low XP Low, State 2 is CP Low XP High, State 3 is CP High XP Low and State 4 is CP High

XP High. Hence, P_{ij} is the transition probability from state i to state j, where $i, j \in \{1, 2, 3, 4\}$. The P_{ij} values of the probability matrix below are derived from the measurements obtained in [41]. For instance, the top right corner value of 0.1037 is the probability of transition from "CP High, XP High" to "CP Low XP Low".

$$P = \begin{bmatrix} 0.6032 & 0.1579 & 0.0561 & 0.1037 \\ 0.2887 & 0.2474 & 0.0447 & 0.4192 \\ 0.1682 & 0.0966 & 0.1745 & 0.5607 \\ 0.0098 & 0.0199 & 0.0150 & 0.9554 \end{bmatrix} \quad (2.2)$$

2.3.2.1 Shadowing model (large-scale fading)

Depending on the state from the transition matrix above, a high and low shadowing channel sequence vector is generated as follows.

Vector S_{high} or S_{low} is generated by using zero-mean and unity standard deviation Gaussian random noise signals. The correlated shadowing for low and high shadowing are obtained by applying a 4 x 4 correlation matrix C_{large} [41]. This will ensure interdependency among the four MIMO channels.

$$S_{high|c}(n) = C_{large}^{\frac{1}{2}} S_{high}(n)$$

$$S_{low|c}(n) = C_{large}^{\frac{1}{2}} S_{low}(n) \quad (2.3)$$

The superscript ½ denotes the Cholesky factorization [41]. $S_{low|c}$ and $S_{high|c}$ are correlated low and high shadowing respectively. The C_{large} used for this channel model is obtained from the measurements carried out in [41]. Second order statistics are obtained using the following process [41]:

$$S_{high|cf}(n) = S_{high|c}(n) + e^{-\frac{v_m \Delta t}{r_c}} S_{high|cf}(n-1)$$

$$S_{low|cf}(n) = S_{low|c}(n) + e^{-\frac{v_m \Delta t}{r_c}} S_{low|cf}(n-1) \quad (2.4)$$

where r_c is the coherence distance for a given mobile speed v_m with sample time Δt. The obtained correlated shadowing is then normalized using standard deviations of σ_{high} and σ_{low} and means of μ_{high} and μ_{low} that are represented by vectors. The normalized shadowing is obtained as follows [41];

$$S_{high|cfn}(n) = \left(S_{high|cf}(n)^{\circ}\, \sigma_{high}{}^{\circ}\sqrt{1 - e^{-\frac{2v_m \Delta t}{r_c}}} \right) + \mu_{high}$$

$$S_{low|cfn}(n) = \left(S_{low|cf}(n)^{\circ}\sigma_{low}{}^{\circ}\sqrt{1 - e^{-\frac{2v_m \Delta t}{r_c}}} \right) + \mu_{low} \qquad (2.5)$$

where ° is element-wise multiplication. This means that each component or element of each vector is multiplied by each other. The values obtained from (2.4) and (2.5) form the component of the large scale fading channel matrix, H_{large} depending on the channel state. The empirical values for standard deviations σ_{high} and σ_{low} and mean values μ_{high} and μ_{low} for co-polar and cross-polar channels measured in dB are detailed in [41]. The values used are presented in Table 2-2 below.

Table 2-2: Shadowing model mean and standard deviation in (dB)

Polarization	High Shadowing		Low Shadowing	
	μ_{high}	σ_{high}	μ_{low}	σ_{low}
Co-polar	-20.5	6.5	-1.5	4.0
Cross-polar	-21.5	6.0	-4.5	3.0

2.3.2.2 Multipath Fading model (small-scale fading)

The small scale fading is modelled using a Ricean distribution. The Ricean fading for each of the MIMO branches are generated using Ricean factors. Small scale fading elements $h_{small,xx}$ for each sample *n*, are obtained as follows [41]:

$$h_{smallxx}(n) = \frac{\sqrt{k_{xx}} e^{j\frac{n2\pi f_m}{N_f}} + \sum_{i=1}^{N_S} M_{norm} e^{j\left(\frac{2\pi n \sin\emptyset_i}{N_f} + \theta_i\right)}}{\sqrt{k_{xx}+1}} \qquad (2.6)$$

Where, N_f, is the sampling factor equal to the sampling frequency divided by the maximum Doppler shift, f_m, due to mobile movement. M_{norm} is used to normalize the scattered part of the small scale fading, $\emptyset_i$ is the angle of arrival [44], θ_i is the random phase and k_{xx} is the *K* factor. The four $h_{smallxx}$ elements make up the 2 x 2 matrix H_{small}. The correlated small scale fading for the case of Non-Line of Sight (NLOS) is obtained using the Kronecker model and can be stated as follows;

$$vec(\, H_{small|c}) = R_{small|c}^{\frac{1}{2}} vec(\, H_{small|NLOS}) \qquad (2.7)$$

Where, *vec* is the vector function which is actualized by converting the matrix H_{small} to a vector. The values of the Correlation matrix $R_{small|c}$ are obtained from the measurements carried out in [41]. In the case of LOS, the co-polar and cross-polar correlation matrix R_{cp} and R_{xp} stated below are used to obtain the correlated small scale fading.

$$R_{CP} = \begin{pmatrix} 1 & r_{CP}^{*} \\ r_{CP} & 1 \end{pmatrix} \qquad R_{XP} = \begin{pmatrix} 1 & r_{XP}^{*} \\ r_{XP} & 1 \end{pmatrix} \qquad (2.8)$$

The 1 x 2 channel vectors of the co-polar and cross-polar components obtained from (6) are correlated respectively as follows;

$$h_{CP|small|C}(n) = R_{CP}^{\frac{1}{2}} h_{CP|small}(n)$$

$$h_{XP|small|C}(n) = R_{XP}^{\frac{1}{2}} h_{XP|small}(n) \qquad (2.9)$$

The four elements obtained are inserted in a 2 x 2 matrix of small scale fading, H_{small}. The cross-polar components are re-normalized by dividing the values by the square root of the cross-polar ratio XPD. The values used for the computation are derived from the measurements available in [41] and are presented in Table 2-3 below.

Table 2-3: Parameters for small scale fading

Parameters	XPD (dB)	r_{CP}	r_{XP}	k_{cp}	k_{xp}
	8.1	0.92	0.61	6.01	2.04

2.3.2.3 Total path loss

The transition matrix above determines the channel state, after which the large scale fading and small scale fading expressed above are determined. The large-scale fading, *S*, and small-scale fading, *M,* are the maximum fading values from the corresponding matrices of H_{large} and H_{small} respectively. These two fadings, *S* and *M,* are considered together with the path loss and polarization loss, as part of the total loss experienced in the channel. The power received is then obtained after subtracting the total loss from the sum of the Effective Isotropic Radiated Power (EIRP) and the gain of the receiver. The Signal-to-Noise Ratio (SNR) is obtained by dividing the received power by the noise power. The EIRP value of 63 dBW, Polarization loss of 3.5 dB

and a noise of 208.1dB, for each subchannel, is used to compute the SNR. Moreover, there is inter-spot-beam interference as a result of power received from eNodeBs sharing the same frequency. The conventional frequency reuse factor of 7 has been considered for the spotbeam GEO satellite [45]. The free space path loss (in dB) at 2 GHz is computed as follows:

$$L_{Fs} = 190.35 + 20\log\left(\frac{38500+D}{35788}\right) \quad (2.10)$$

Where *D* is the distance in km between the mobile user and the GEO satellite (the dependence on *D* is, however, negligible). L_{Total} is sum of L_{Fs} obtained in (2.10), large-scale fading, *S*, obtained in (2.5), small-scale fading, *M*, obtained in (2.9) and the polarization loss, L_p and is presented as follows:

$$L_{Total} = L_{Fs} + S + M + L_p\ (dB) \quad (2.11)$$

The SINR is due to the combination of uplink and downlink contributions to the downstream path via satellite from gateway to UE: 1/SINR= $1/SINR_{downlink}$ + $1/SINR_{uplink}$. However, for the sake of simplicity, we refer here only to the most critical link in the path, that is the satellite downlink and we use that $SINR_{downlink}$ as the SINR of the whole downstream path. The SINR which is obtained on a subchannel basis for each antenna can be expressed as follows;

$$SINR(dB) = EIRP + G_R - L_{Total} - N - I\ (dB) \quad (2.12)$$

Where *I* denotes the inter-spot-beam interference, due to the power received from the beams sharing the same frequency (frequency re-use) [46], It can be obtained as follows (46);

$$I = \sum_{i=1}^{NB} (P_r - L_{FS} - F) \quad (2.13)$$

Where P_r is the received power for each subchannel, *F* is the channel fading, *NB* is the number of other spotbeams sharing the same frequency with considered spotbeam and L_{FS} is the free space path loss as computed above.

2.3.2.4 CQI mapping

Previous studies have considered the mapping from SINR and CQI on the basis of SINR thresholds and the channel conditions. For the AWGN case, reference [47] provides a mapping for a Block Error Rate (BLER) of 10^{-1} for terrestrial cellular systems. This low BLER target value is considered here as retransmissions are possible and entail a negligible propagation delay. Unfortunately, this is not the case for the satellite scenario, where a lower target BLER

value of 10^{-3} has been considered to reduce the number of retransmissions due to the huge RTPD that they entail; accordingly, we determine the mapping from SINR to CQI.

It should be noted that the effective exponential SINR mapping (EESM), which has been shown to be an accurate estimation of AWGN equivalent SINR, has been considered for the purpose of CQI mapping and feedback in this study. The EESM enables the mapping of a set of instantaneous subchannel SINR into one effective SINR [48],[49] as considered in [50] for mobile satellite networks. The effective SINR can be expressed as follows;

$$SINR_{eff} = -\log\left(\frac{1}{N}\sum_{i=1}^{N} e^{-SINR_i}\right) \qquad (2.14)$$

Where $SINR_i$ is the SINR for the $i\ th$ subchannel and N is the number of subchannels. Then, using the effective SINR and adapting the mapping in [47] to the satellite scenario conditions by using a very low BLER as considered in [51] for satellite LTE, we have:

$$\begin{gathered} if\ SINR_{eff} < -3.8; \quad CQI = 1 \\ if\ -3.8 \le SINR_{eff} \le 22.6; \quad CQI = (0.55 * SINR) + 3.45 \\ if\ SINR_{eff} > 22.6; \quad CQI = 15 \end{gathered} \qquad (2.15)$$

The CQI obtained by the UE (on the basis of a SINR measurement and the above mapping) is reported to the eNodeB via satellite at certain reporting intervals. The resulting distribution for the channel model presented above, which is represented in the form of CQI as obtained in (2.15), is shown for EIRP of 53 dB and 63 dB in Fig. 2-6 and Fig. 2-7, respectively. These CQI distributions are for a particular UE.

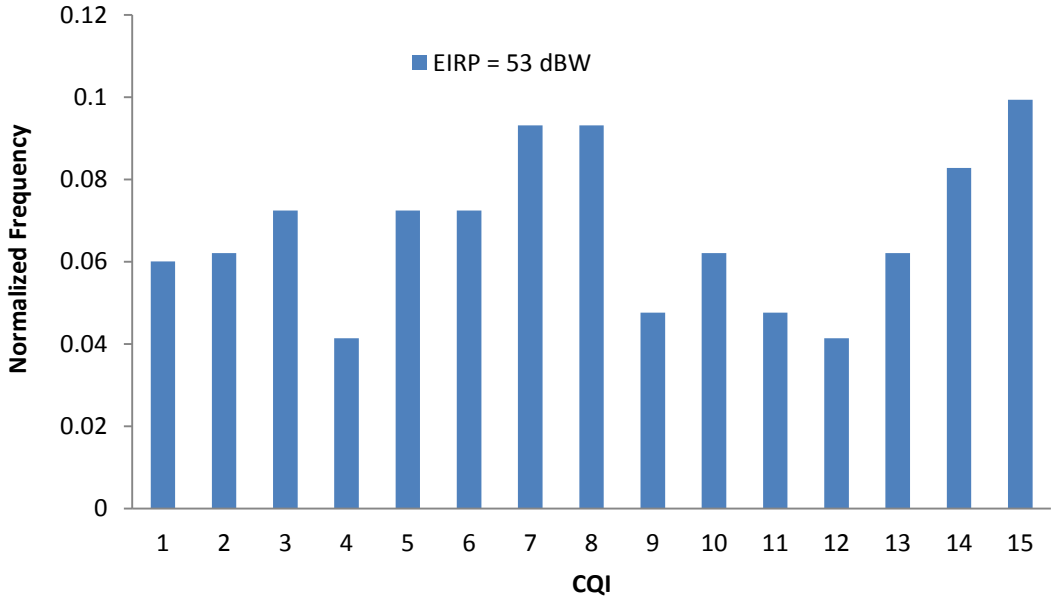

Figure 2-6: The CQI distribution for a subchannel of a UE for EIRP = 53 dBW

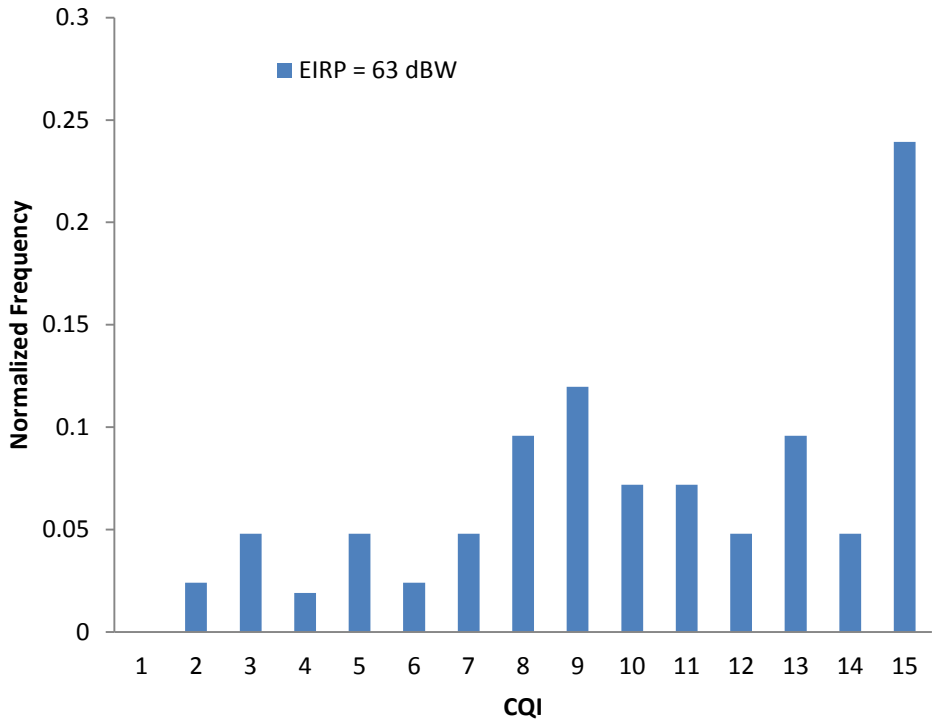

Figure 2-7: The CQI distribution for a subchannel of a UE for EIRP = 63 dBW

The CQI distribution in Fig. 2-7 produces a higher frequency of CQI value of 15 than the CQI distribution in Fig. 2-6 that uses EIRP of 53 dBW. This is due to the fact that, at EIRP value of 63 dBW, a high SNIR is produced; hence, higher CQI values are obtained than when the EIRP value is 53 dBW, which produces more relatively lower CQI values.

2.3.3 Traffic Model

Different traffic types have been considered in this study, including conversational video as an exemplar of GBR traffic and Web traffic as an exemplar of non-GBR traffic.

The video traffic is modeled on the basis of a video trace file as used in several studies on LTE networks [52],[53], which is made available in [54]. The obtained video sequence of 25 frames per second has been compressed, using the H.264 standard, at an average coding rate of 128, 242 or 440 kbps. Hence, the mean bit-rate generated by a video source can either be 128, 242 or 440 kbps.

A deadline of 160 ms is considered for each video packet. If a video packet cannot be transmitted within this delay, we consider that it is cleared from the transmission queue (packet loss).

The web traffic model adopted in this study is that defined by the European Telecommunications Standard Institute (ETSI) and Mobile Wireless Internet Forum (MWIF), and generally used for simulation in 3G and beyond networks as stated in [55]. The web traffic oscillates between an ON (packet call) state and OFF (reading time) state. During the packet call state, the web source produces a number of objects (messages) that are geometrically distributed, with a mean value of 300 and the inter-arrival time is also geometrically distributed, with a mean value of 0.5 s. The OFF time during which no traffic is generated is also geometrically distributed, with a mean value of 2 s. The object length is l_{w_bytes} which is obtained as the floor function of a random variable x with the following truncated Pareto pdf [56, 57]:

$$g(x) = \frac{\zeta . l_{w\_min}^{\zeta}}{x^{\zeta+1}} . \left[u\left(x - l_{w\_min}\right) - u(x - l_{w\_max})\right] + \left(\frac{l_{w\_min}}{l_{w\_max}}\right)^{\zeta} . \delta\left(x - l_{w\_max}\right) \quad (2.16)$$

Where ζ is 1.1, u(.) is the unitary step function, δ(.) is the Dirac Delta function, l_{w_min} and l_{w_max} are the minimum (81.5 bytes) and maximum (66.4 kbytes) object lengths, respectively.

A deadline of 300 ms is considered for each web packet for the purpose of scheduling algorithm computation according to the QoS standards stated in Table 2-3. However, if a web packet cannot be transmitted within this delay, it is not dropped.

2.4 Summary

This chapter discussed the concept of the satellite LTE air interface. A detailed description was provided of the architecture of the satellite LTE network. The MAC Layer, QoS standards and PRB allocation concept in satellite LTE networks were also presented. Furthermore, the system model adopted for the satellite LTE network, under which the MIMO channel model considered for this study falls, was discussed in detail. The link budget analysis, CQI computation, and traffic models for video and web traffic that are considered for this study, were also presented.

Chapter 3

CROSS-LAYER BASED APPROACH SCHEDULING IN SATELLITE LTE NETWORKS

3.1 Introduction

This chapter presents two new, heuristic cross-layer based schedulers, the tagged Channel Based Queue Sensitive (CBQS) and Queue Aware Fair (QAF) schedulers, for Satellite LTE networks that will provide a good trade-off between throughput, degree of fairness and an acceptable QoS, taking current constraints into consideration, in order to improve overall performance. In order to evaluate the performance of the proposed schedulers, a simulation setup is used to compare various schedulers' performance in Satellite LTE networks with the proposed schedulers and the simulation results are presented. The throughput performance, delay performance and the fairness for the schedulers considered are presented. The schedulers considered are Modified Largest Weighted Delay First (M-LWDF), Exponential Proportional Fair (EXP-PF) and the proposed CBQS and QAF schedulers.

The chapter commences with a detailed review of the literature on scheduling. This is followed by the scheduling problem formulation. The chapter goes on to discuss the two proposed schedulers as well as the simulation setup. Finally, the numerical results, including throughput, delay, spectral efficiency and fairness are presented and discussed.

The work presented in this chapter was presented at the Southern Africa Telecommunications Networks and Applications Conference (SATNAC) 2012, George, South Africa and the 9th Institute of Electrical and Electronics Engineers, AFRICON Conference (IEEE AFRICON 2013), Mauritius. Part of it was also presented at the Sixth IFIP International Conference on New Technologies, Mobility & Security (NTMS 2014).

3.2 Related Studies

The ambitious targets of 4G systems in terms of QoS, data rates and fairness can only be achieved with an effective scheduling scheme that is able to achieve an optimal balance of all these requirements. The literature has proposed many schemes, including channel-aware and queue-aware schemes, to address the problem of scheduling and resource allocation in terrestrial LTE networks, as detailed in [58]. However, there is a paucity of research on scheduling schemes suitable for satellite LTE networks. Well-known schedulers such as Proportional Fair's performance is investigated in a satellite LTE network in [51] and M-LWDF and EXP-PF's performance in a satellite LTE network is examined in [59]. However, to the best of our knowledge, very few scheduling schemes have been proposed for a satellite LTE network. Even the on-going, standard work by the International Telecommunication Union - Radio Communication (ITU-R), Satellite-LTE working group only specifies the three 'general' types of schemes that are accommodated in a satellite LTE network, which include dynamic, semi-persistent and fixed schedulers, but does not propose any specific scheduling scheme [60]. Hence, the main aim of this chapter is to propose two new, heuristic scheduling schemes, called Queue Aware Fair (QAF) and Channel Based Queue Sensitive (CBQS) schedulers, respectively that will provide a good trade-off between throughput, QoS and fairness in a satellite LTE scenario and to conduct a performance comparison with other schedulers, for a satellite MU-MIMO LTE air interface. The proposed schedulers are designed using a cross-layer based approach.

Before these two schedulers are presented, existing schedulers in wireless networks are examined in depth. Several schedulers have been proposed or designed for wireless networks. Some schedulers are channel unaware while others are channel aware schemes. Furthermore, some are queue unaware, while others are queue aware. Previous studies have also proposed schedulers that are both channel aware and queue aware. A cross representation of these different types of scheduling schemes is examined below.

3.2.1 First In First Out

The First-In-First-Out (FIFO) scheme is a channel-unaware and queue-unaware scheduler. It is the simplest packet scheduling scheme. This scheduler serves the packets of users in order of request or arrival, just as a FIFO queue operates [61]. This makes the scheduler very easy to implement. The algorithm for this scheme can be expressed as follows;

$$L_k = argmax\left(t - t_{r,k}\right) \quad (3.1)$$

Where t is the present time and $t_{r,k}$ is the time of arrival or request for the head of packet of user *k.*

A major disadvantage of this scheme is that it cannot differentiate between users; therefore all packets of different users, irrespective of their traffic type, experience the same delay, jitter and packet loss. FIFO+ has been proposed to improve the FIFO scheduling scheme [62] in order to reduce the delay and jitter. The main disadvantage of both FIFO based schedulers are that they are unfair schedulers that are not sensitive to the channel condition of users.

3.2.2 Round Robin

The round robin scheduler is also a channel-unaware and queue-unaware scheduler. It is a simple scheduling scheme which serves the packet in each user's queue or class type and moves in a cyclic order to serve packets in the queue of each user that is not empty. While it is fair to all users, it is not able to differentiate between various traffic types. This led to the design of improved round robin schedulers that can provide QoS. These improved versions are called Weighted Round Robin (WRR), Deficit Round Robin (DRR) and Hierarchical Round Robin (HRR). The WRR scheduler allows a user a share of the available resources based on its weight, while the DRR scheduler improves on the WRR by catering for a packet of variable sizes in order to ensure fairness [63]. The HRR scheduler differentiates different traffic class types into levels. High level classes are allocated more bandwidth than lower level classes; hence, it takes less time to service high level classes than low level classes [64],[69]. The major disadvantage of all these RR based schedulers is that, they are only fair in terms of time and not throughput, and they are not sensitive to users' channel conditions.

3.2.3 Weighted Fair Queuing

The Weighted Fair Queuing (WFQ) scheduling scheme is a General Processor Sharing (GPS) [65] based scheme. It was introduced because GPS could not be practically implemented. WFQ, also known as Packetized GPS, adapts the GPS to packets instead of a fluid scenario. The WFQ scheduling scheme selects among all the packets in the queues at every time *t*, the first packet that will complete its service in the corresponding GPS system, assuming that no additional packets arrive in the queue after time *t*. WFQ only uses the time it will take the

packets to finish in the GPS system to make decisions. Worst-case Weighted Fair Queuing (WF^2Q) is another proposed GPS based scheduler. It aims to improve on the WFQ by using not only the finish time of the packet in GPS system as used by WFQ; but both the start and finish time in order to achieve an exact emulation of GPS [66].

3.2.4 Earliest Deadline First

The Earliest Deadline First (EDF) is a channel-unaware but queue-aware scheduling scheme. It is a dynamic priority packet scheduler that allocates resources to mobile users or traffic based on urgency [4]. It schedules the packet that is closest to its set delay deadline. Initially proposed for wired networks [67], this scheme has been used in wireless networks like S-HSDPA networks as noted in [5], [7]. Each traffic type has its own delay deadline and the deadline for each traffic class is based on its delay sensitivity. The EDF algorithm can be expressed as follows;

$$L_k = argmax\left(\frac{1}{T_{deadline} - W_k}\right) \tag{3.2}$$

Where $T_{deadline}$ is the delay deadline and W_k is delay of head of packet of user *k*. While the EDF scheduler is very suitable for real time traffic [68],it is not sensitive to the channel conditions and therefore does not effectively utilize available resources and will starve non-real time traffic in a mixed traffic scenario.

3.2.5 Largest Weighted Delay First

Like the EDF scheduler, the Largest Weighted Delay First (LWDF) [69] scheduler is a channel-unaware and queue-aware packet scheme. It is based on the parameter a_k which represents the acceptable probability that a packet of the *k*-th user is dropped due to deadline expiration. The algorithm is computed as follows;

$$L_k = argmax(a_k.W_k) \tag{3.3}$$

Where

$$a_k = \frac{\delta_k}{T_{deadline,k}} \tag{3.4}$$

and a_k is the QoS differentiation which is the ratio of δ_k to the delay deadline, $T_{deadline,k}$. The a_k allocates to the user with the lowest deadline expiration if two flows experience equal

delays. The major disadvantage is that it does not consider channel conditions and it is suitable to real time traffic only and not mixed traffic scenarios.

3.2.6 Maximum Throughput

The Maximum Throughput (MT) scheduler is a channel-aware and queue-unaware scheduler which aims to maximize the total throughput of the network. This is achieved by allocating resources to the user that achieves the maximum throughput at every interval [70]. This is measured in terms of transmission rate determined using the AMC, from Channel Quality Indicator (CQI) which is a function of the SINR. The algorithm can be computed as;

$$L_k = argmax(R_k) \tag{3.5}$$

Where R_k is the instantaneous transmission rate of user *k.* The major disadvantage of the MT scheduler is that it is an unfair scheduler. Resources are only allocated to users with good channel conditions, while those with low channel conditions will be starved. It also does not consider the status of the queue.

3.2.7 Proportional Fairness

The Proportional Fair (PF) scheduler [71] is also a channel-aware and queue-unaware scheduler. It is said to be an opportunistic scheduling scheme that uses the Relative Channel Quality Indicator (RCQI) to make scheduling decisions. It provides a trade-off between fairness requirements and spectral efficiency by providing equilibrium between maximizing the throughput and ensuring that all users receive a certain level of service. The user with the maximum RCQI is allocated resources. The RCQI is the ratio of the user's maximum supported present transmission rate to the average transmission rate experienced in the past by the user. This can be expressed as;

$$L_k = argmax\left(\frac{R_k}{T_k}\right) \tag{3.6}$$

Where, $$T_k(n) = (1-\alpha)T_k(n-1) + \alpha R_k(n) \tag{3.7}$$

Where T_k is the average transmission rate over the past Transmission Time Interval *n* (TTI) and α is a smoothing parameter used for averaging purposes. The major disadvantage of this scheme is that a good trade-off is only feasible in a single traffic network scenario. This is due to the fact that the scheduler cannot differentiate between different traffic classes and hence cannot provide acceptable QoS for real time traffic [68]. It is also not sensitive to the status of

the queue. Improved versions of the PF scheduler have been proposed in the literature, including Generalized Proportional Fair (GPF) [72] and Adaptive Proportional Fair (APF) [73].

3.2.8 Throughput-to-Average

The Throughput-to-Average (TTA) scheduling scheme is another channel-aware and queue-unaware scheduler. The scheduling algorithm is computed based on user throughput which is a function of the CQI. The TTA scheduler is considered an intermediary scheduler between the MT and PF schedulers [58]. The algorithm is computed as follows [70];

$$L_k = argmax\left(\frac{R_k}{R}\right) \tag{3.8}$$

Where R is the maximum achievable transmission rate of the channel and R_k is the instantaneous transmission rate of user *k*. The TTA scheduler provides high level of fairness on a short term basis, that is, at every TTI. Its major disadvantage is that it only considers the channel and not the status of the queue. It is also not sensitive to users' QoS requirements.

3.2.9 Log Rule

The Log Rule (LR) scheduling scheme is a channel and queue-aware scheduler [58] that considers both channel conditions and status of the queue in its algorithm. It is designed to provide a trade-off between transmission rate, QoS and fairness. The algorithm for the LR scheduling scheme can computed as follows;

$$L_k = argmax\{b_k \log(c + a_k W_k)\, R_k\} \tag{3.9}$$

Where a_k, b_k and c are parameters that can be tuned for best scheduling performance. According to [74], the parameter b_k is best set as 1/E[R_k], E[R_k] is the average transmission rate, c is best set to be equal to 1.1 and a_k is best set to be expressed as 5/$T_{deadline}$. The LR metric increases logarithmically, as the waiting time of the Head of Line packet increases.

3.2.10 Exponential Rule

The Exponential Rule (ER) packet scheduling scheme is also a channel and queue-aware packet scheme that can be used in wireless networks [58]. It considers both channel conditions and the status of the queue. The algorithm that is used to compute the ER scheduling scheme can be expressed as follows;

$$L_k = argmax\left\{ b_k \exp\left(\frac{a_k W_k}{c + \sqrt{\frac{1}{N}\sum_n W_n}} \right) R_k \right\} \quad (3.10)$$

Where N is the number of users; it should be noted that parameters a_k, b_k and c are tunable. These considered parameters to achieve good performance according to [74] can be expressed as follows;

$$\left\{ \begin{matrix} a_k \in \left[\frac{5}{T_{deadline}}, \frac{10}{T_{deadline}} \right] \\ b_k = \frac{1}{E[R_k]} \\ c = 1.1 \end{matrix} \right\} \quad (3.11)$$

The ER metric increases exponentially, as the waiting time of the Head of Line packet increases. The ER metric is said to increase faster than the logarithmic counterpart and it is also said to be more robust.

3.2.11 Modified - Largest Weighted Delay First (M-LWDF)

The M-LWDF scheduler considers both channel conditions and the delay experienced by packets when making scheduling decisions with QoS support. It is based on a probabilistic delay requirement of the following form [75]:

$$Prob.\ (W_k > T_{k,deadline}) \leq \delta_k \quad (3.12)$$

where W_k is the waiting time of the Head of Line (HOL) packet in UE queue *k*, $T_{k,deadline}$ is the deadline for the UE traffic flow *k*, and δ_k is the maximum allowed probability of exceeding the deadline. In the M-LWDF case, the priority index U_k (used to select the UEs on every TTI) is computed as follows [76]:

$$L_k = argmax\left\{ \frac{R_k(-log\delta_k)W_k}{T_k * T_{k,deadline}} \right\} \quad (3.13)$$

Where W_k is the waiting time of the HOL packet in UE queue *k*, R_k is the instantaneous transmission rate of traffic user *k*, T_k is the average transmission rate of user *k* computed before. $T_{k,deadline}$ for conversational video (RT class) is assumed to be 160 ms. The value of δ_k varies on the basis of the service type demanded by the UE. For the purpose of this study, the δ_k for RT traffic is considered to be 0.01 and for NRT traffic it is considered to be 0.1.

3.2.12 Exponential Proportional Fair (EXP/PF)

Exponential Proportional Fairness was proposed to support multimedia applications, considering both RT and NRT traffic types [77]. This algorithm was designed to increase the priority of RT traffic over NRT traffic. As stated in [74], the EXP rule is based on the following priority index:

$$L_k = argmax\left\{\frac{R_k}{T_k} exp\left(\frac{a_k W_k - \overline{aw}}{1+\sqrt{\overline{aW}}}\right)\right\} \quad (3.13)$$

where all parameters are the same as in M-LWDF, except for the term a_k which represents $5/T_{k,deadline}$ as stated in [74] and $\overline{aW}$, which is defined as follows:

$$\overline{aW} = \frac{1}{N}\sum_{k\in N} a_k W_k \quad (3.14)$$

When the HOL packet delays for all UEs do not differ much, the exponential term is close to 1 and the EXP rule performs as the PF algorithm. If the HOL delay becomes very large for one of the UEs, the exponential term overrides the channel state-related term, and the corresponding UE acquires high priority.

3.3 Problem Formulation

The scheduling algorithm reviewed above operates on a channel; however, the satellite LTE network allows scheduling on a subchannel basis since the channel consists of several subchannels. The basic element of all scheduling schemes is the computation of a priority index (or utility function *L*) for all active flows of each UE on a subchannel basis at every TTI. The scheduler decides the UE to allocate PRB resources on a subchannel basis at every TTI; in particular, the UE with the maximum priority index is selected on each subchannel. The priority index for all UEs is computed for the first subchannel and the UE with the maximum priority index is selected for the first subchannel, then the re-computation of priority indices and the selection of the user with the maximum priority index are repeated for all available subchannels.

The resource allocation can be generally stated as an optimization problem as follows:

$$max \sum_{j=1}^{J}\sum_{k=1}^{K} L_{k,j} U_{k,j} \quad (3.15)$$

Subject to

$$\sum_{j=1}^{J} U_{k,j} \leq 1 \qquad \forall\, k \in (1, \ldots, K) \tag{3.16}$$

$$U_{k,j} \in \{0,1\} \tag{3.17}$$

where J is the number of subchannels and K is the number of UEs; $L_{k,j}$ is the utility function that depends on the scheduling algorithm which can be a $f(R_{k,j}, W_k)$; $U_{k,j}$ is the variable that indicates whether user k is assigned to subchannel j or not. $U_{k,j}$ will be 1 if the UE k is assigned to subchannel n; otherwise it will be 0. Constraint (3.16) allows a maximum of one user to be selected and assigned for each subchannel. Hence, only the flow of the UE with the maximum utility function $U_{k,j}$ can be assigned to the corresponding subchannel.

The focus of this chapter is to propose a cross-layer based scheduling scheme (utility function) and examine the different scheduling schemes characterized by different utility functions as detailed below.

3.4 Proposed Heuristic Schemes

The two new heuristic scheduling schemes proposed are QAF and CBQS schedulers. They are designed using a cross-layer based approach. This utilizes cross-layer interactions between different layers when taking scheduling decisions. As shown in Fig. 3-1, the CQI is obtained from the physical layer and QoS and queue information are obtained from higher layers.

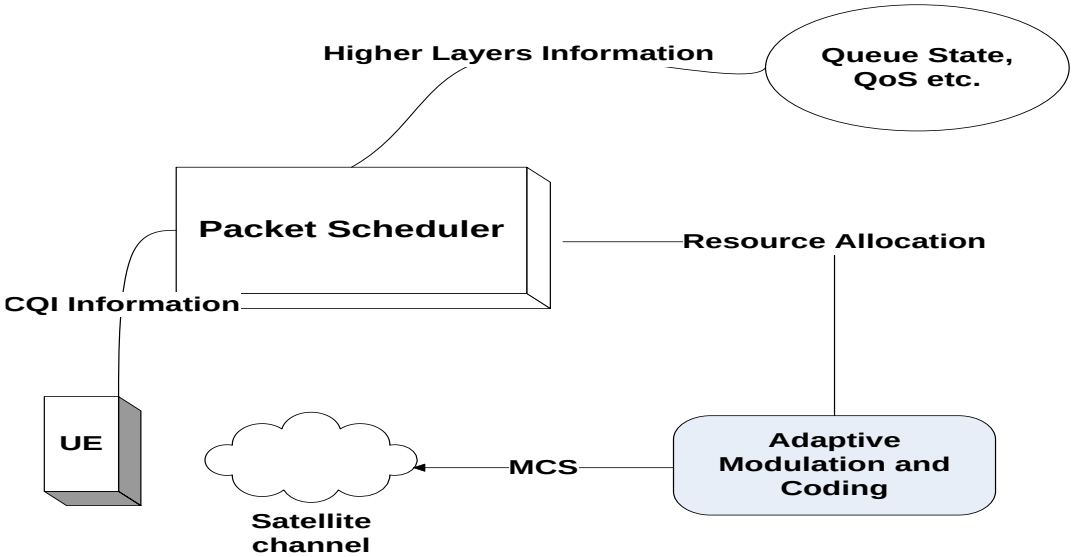

Figure 3-1: The proposed packet scheduling scheme model in a satellite LTE network

3.4.1 Queue Aware Fair (QAF) Scheduler

The QAF scheduler is an extension of the M-LWDF scheduler proposed in [76]. In order to ensure a better level of fairness, the power *c* and *m* are introduced to the M-LWDF scheduling algorithm. The concept of the usage of power *c* and *m* to improve fairness is deduced from the scheduler proposed in [78], which used only Proportional Fairness (PF) in its main algorithm. The proposed scheduler is therefore able to provide a better trade-off between fairness, throughput and QoS. In the proposed scheduler, the product of the QoS differentiator and the waiting time is included rather than just PF. The factor *c* is used as a power for NRT traffic to improve fairness and the factor *m* is used as a power for RT traffic to improve fairness and give priority to RT traffic over NRT traffic when the waiting time approaches the delay deadline. The algorithm is presented below;

$$\begin{cases} if\ NRT \quad L_{k,j} = \ argmax\left(\frac{(R_{k,j})}{T_k(n)}\left(\frac{((-log\delta_k)(W_k(n)))^c}{T_{k,deadline}}\right)\right) \\ if\ RT \quad L_{k,j} = argmax\left(\frac{(R_{k,j})}{T_k(n)}\left(\frac{((-log\delta_k)(W_k(n)))^m}{T_{k,deadline}}\right)\right) \end{cases} \tag{3.18}$$

$$T_k(n) = (1-\alpha)T_k(n-1) + \alpha R_{k,j}(n) \tag{3.19}$$

$R_{k,j}(n)$ is the instantaneous data rate of user *k* over subchannel j, $T_k(n)$ is the average data rate of user *k*, W_k is the waiting time of the Head of Line (HOL) packet in UE queue *k*, $T_{k,deadline}$ is the deadline for the user *k*, and δ_k is the maximum allowed probability of exceeding the deadline. The *c* is determined as follows;

$$c_j = c_j + \Delta c \quad if\left(\frac{R_{k,j}}{T_k(n)} - \frac{1}{N}\sum_{n=1}^{N}\frac{R_{k.,j}}{T_k(n)}\right) < -\varepsilon$$

$$c_j = c_j - \Delta c \quad if\left(\frac{R_{k,j}}{T_k(n)} - \frac{1}{N}\sum_{n=1}^{N}\frac{R_{k.,j}}{T_k(n)}\right) > \ \varepsilon \tag{3.20}$$

The tuning of ε determines what level of fairness is sought. ε = 0 indicates maximum fairness. *N* is the total number of users. The value of Δc is recommended, depending on how fast convergence should occur and the desired level of variation of the values at convergence. The difference between the normalized throughput of the user and the average value normalized throughput of all users determines if the control parameter c_j will be updated or not. It will only be updated if it does not fall within the acceptable value of {-ε, ε}. A value of 0.1 has been

chosen for Δc and a value of 0 has been assumed for ε, for maximum fairness as stated in [78]. Hence, c_j will always be updated since there is no range between {-0, 0}.

In order to meet QoS demands of RT traffic, m is introduced to ensure that priority is given to RT users that are almost approaching the deadline. Hence, this clause is provided:

$$\begin{cases} m_j = 2c & \text{if } T_{k,deadline}\text{-}W_k(n) < \varphi \\ m_j = c & \text{if } T_{k,deadline}\text{-}W_k(n) > \varphi \end{cases} \quad (3.21)$$

For this study, φ is assumed to be 0.002, that is, 2 ms.

3.4.2 Channel Based Queue Sensitive (CBQS) Scheduler

The second new scheduler proposed in this chapter is the Channel Based Queue Sensitive (CBQS) scheme; this is a cross-layer-based scheduler designed to improve throughput performance, without compromising delay and fairness issues. The scheduler uses information from the physical layer (CQI), MAC sub-layer (queue congestion in terms of current delay) and application layer (traffic type and related QoS requirements) to make scheduling decisions, as shown in Fig. 3-1.

The CBQS scheme provides a good trade-off among throughput, fairness and QoS. It is a modification of the exponential term of EXP-PF to take the actual delay deadline into account. Rather than deducting average waiting time from the waiting time as proposed for EXP-PF, a delay deadline is deducted from the instantaneous waiting time of the HOL packet of each user. This is due to the fact that the average waiting time used in EXP-PF is subjective; it depends on the waiting time experienced by all users, compared with a delay deadline that is constant and common to all users with the same traffic type. The corresponding instantaneous waiting time of each user is also used to normalize the difference between the instantaneous waiting time and the delay deadline.

The proposed scheduler is obtained by combining the Proportional Fairness algorithm in order to maximize throughput and an exponential function of a QoS expression. The QoS expression is defined as the ratio of the difference between the delay deadline and the waiting time to the waiting time. The different delay deadline for different traffic types allows a QoS differentiation in the algorithm. The priority index (utility function) of the CBQS scheduling algorithm is defined as follows:

$$U_{k,j} = argmax\left\{\frac{R_{k,j}(n)}{T_k(n)} exp\left(\frac{(W_k(n)-T_{k,deadline})}{W_k(n)}\right)\right\} \quad (3.22)$$

where $W_k(n)$ is the waiting time of the HOL packet in UE queue *k* at TTI *n*, $R_{k,j}(n)$ is the instantaneous transmission rate of traffic user *k* for subchannel *j* at TTI *n*, $T_k(n)$ is the average transmission rate of user *k* computed before the *n*-th TTI. The $T_{k,deadline}$ for conversational video (RT class) is assumed to be 160 ms and for web traffic (NRT class) is assumed to be 300 ms.

For the purpose of this study, the M-LWDF and EXP-PF have been considered for comparison purposes. Hence, both schedulers have been re-formulated on a subchannel basis. In the M-LWDF case, the priority index $L_{k,j}$ (used to select the UEs on a subchannel basis every TTI) is computed as follows [58]:

$$L_{k,j}(n) = argmax\left\{\frac{R_{k,j}(n)(-log\delta_k)W_k(n)}{T_k(n)T_{k,deadline}}\right\} \quad (3.23)$$

where $W_k(n)$ is the waiting time of the HOL packet in UE queue *k* at TTI *n*, $R_{k,j}(n)$ is the instantaneous transmission rate of traffic user *k* for subchannel *j* at TTI *n*, $T_k(n)$ is the average transmission rate of user *k* computed before the *n*-th TTI.

In the EXP-PF case, the priority index $L_{k,j}$ (used to select the UEs on a subchannel basis every TTI) is computed as follows [58]:

$$L_{k,j}(n) = argmax\left\{\frac{R_{k,j}(n)}{T_k(n)} exp\left(\frac{a_k W_k(n)-\overline{aW_n}}{1+\sqrt{aW(n)}}\right)\right\} \quad (3.24)$$

All the parameters used are as stated above.

3.5 Simulation Setup

This section provides the simulation setup that is used to conduct the performance evaluation of the proposed scheduler, in the envisaged MU MIMO GEO satellite system, based on an LTE air interface. A single spotbeam is simulated modeling the inter-beam interference as a contribution to the SINR. UEs are capable of making video streaming and Web surfing uniformly distributed within the spotbeam footprint. The channel and traffic model presented in chapter 2 are adopted for the simulations. Each set of UEs is made of 50% of web browsers and 50% of video streamers. Each UE is assumed to be reporting its channel condition (in terms of CQI) according to fixed intervals to the eNodeB.

The LTE performance is analysed using an open source, discrete event simulator called LTE-Sim [79]–[81]. This is a standalone version of the LTE module in NS-3 that is written in

C++ and was upgraded in [82]. This simulator has been adapted to the GEO satellite scenario. More specifically, the physical layer characteristics, including the channel model and the propagation delay were modified in order to implement the satellite scenario. The new scheduler and the web traffic model have also been included in the simulator.

In this study, it is assumed that CQI is reported by the UE every 100 TTIs; this long interval has been considered in the GEO scenario in order to reduce the frequency of reporting so as to save the UE equipment's power. The details of the simulator parameters are provided in Table 3-1 below.

Table 3-1: Simulation parameters for comparison of schedulers

Parameters	Value
Simulation Time	500 seconds
RTPD	540 ms (GEO satellite)
Channel Model	4 state Markov model
MIMO	2 x 2 (2 antenna ports)
CQI Reporting Interval	100 TTI (= 0.1 s)
TTI	1 ms
Frequency Re-use	7
Mobile user Speed	30 km/h
RLC Mode	AM
Web Traffic Model	ON/OFF M/Pareto
Video Traffic Model	Trace-based @ 440 kbps
Schedulers	M-LWDF, EXP/PF, QAF, CBQS
Bandwidth	15 MHz

3.6 Simulation Results

This section compares the performance of CBQS, QAF, M-LWDF and EXP-PF schedulers in terms of the average delay, throughput, spectral efficiency and fairness index. The average delay for web traffic is shown in Fig. 3-2. The M-LWDF and the two proposed schedulers (QAF and CBQS) achieve better delay performance than EXP-PF, as the number of UEs increases significantly from 30 UEs and above. The M-LWDF scheduler has a small edge over both QAF and CBQS as the number of UEs increases. The delay performance of the EXP-PF scheduler for web traffic can be said to be caused by the fact that too much preference is given to RT traffic through the usage of the exponential function. The QAF scheduler performs in a similar manner to the M-LWDF since these schedulers have much in common except for the

control parameters m and c. These three schedulers have better delay performance due to the fact that they use the delay deadline as a strong reference point in their respective algorithms.

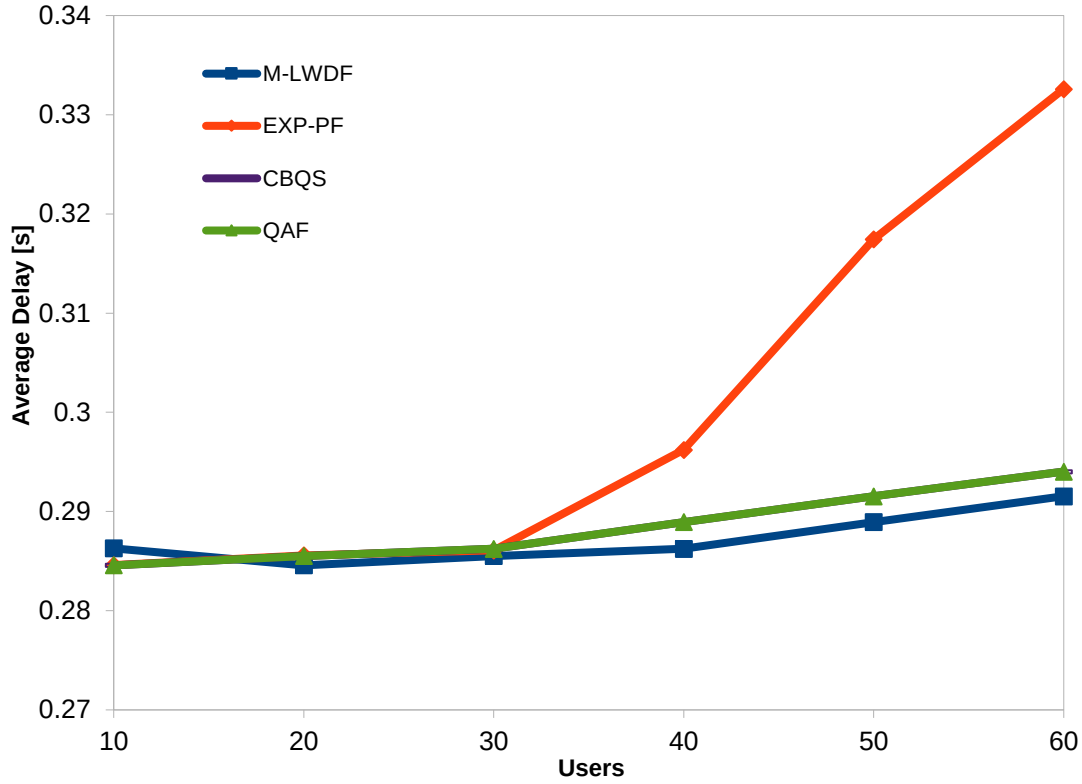

Figure 3-2: Average delay for web users

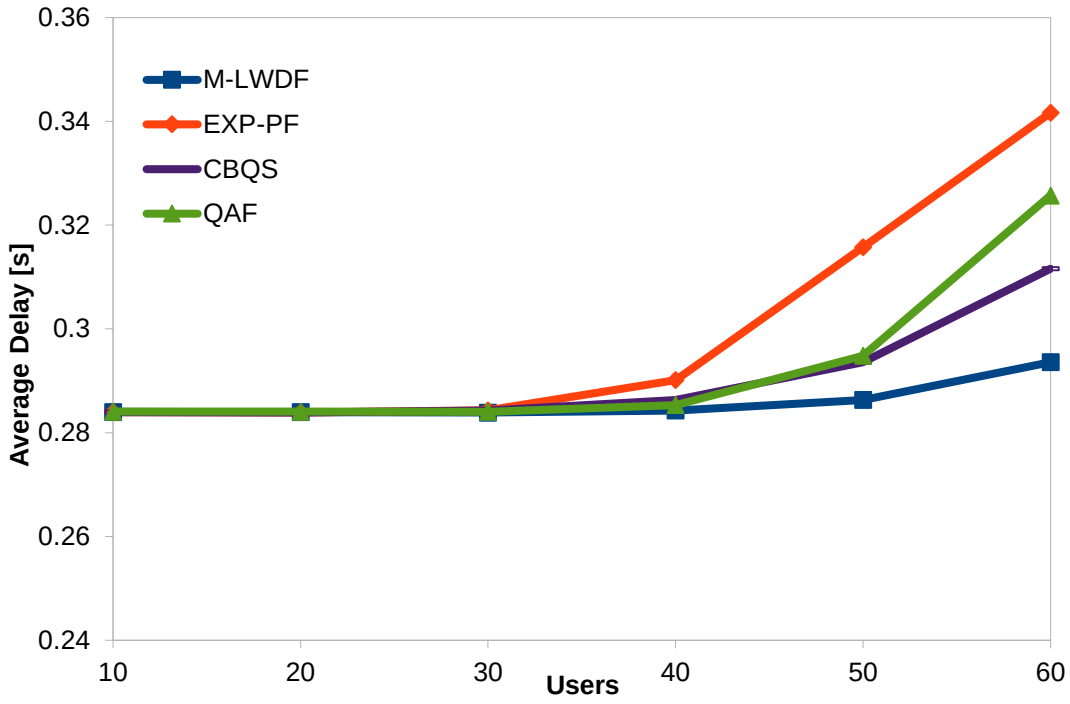

Figure 3-3: Average delay for video users

A similar delay performance is experienced for video (RT) users as shown in Fig. 3-3, with M-LWDF also producing the best delay performance compared with EXP-PF, QAF and CBQS schedulers from 30 UEs and above, while the CBQS and QAF schedulers provide a better delay performance than the EXP-PF scheduler. The direct ratio of the waiting time to the delay deadline used by both M-LWDF and QAF and the difference between the delay deadline and waiting time used by the CBQS scheduler allows these schedulers to schedule users quickly and prevents the delay from reaching the deadline.

This can not be said for the EXP-PF scheduler. The channel delay is 280 ms; hence, the minimum instantaneous delay that can be experienced is 280 ms, assuming no delay is experienced in the queue and since packets that exceed 160 ms are dropped, the maximum instantaneous delay experienced by a user cannot exceed 440 ms. This validates the average delay results that fall within the range of approximately 285 ms to 340 ms.

As for the throughput, it is noted that from Figs. 3-4 and 3-5 that the CBQS scheduler achieves the best performance for both video and web traffic flows in comparison with QAF, M-LWDF and EXP-PF. For video traffic, the M-LWDF, EXP-PF and the proposed QAF schedulers produce similar throughput performance. The CBQS scheduler produces the best performance and this becomes more evident as the number of users increases. For web traffic, the two proposed schedulers produce similar performance with up to 40 users and the CBQS scheduler produces a better delay performance than the QAF scheduler for more than 40 users.

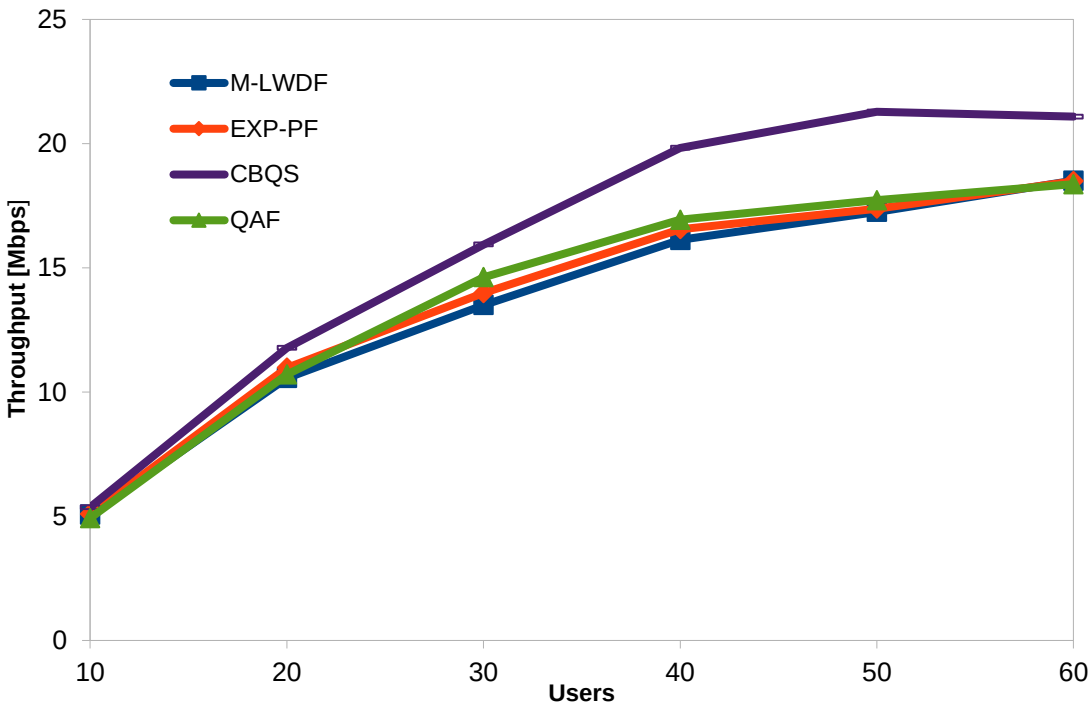

Figure 3-4: Aggregated throughput for video traffic flows

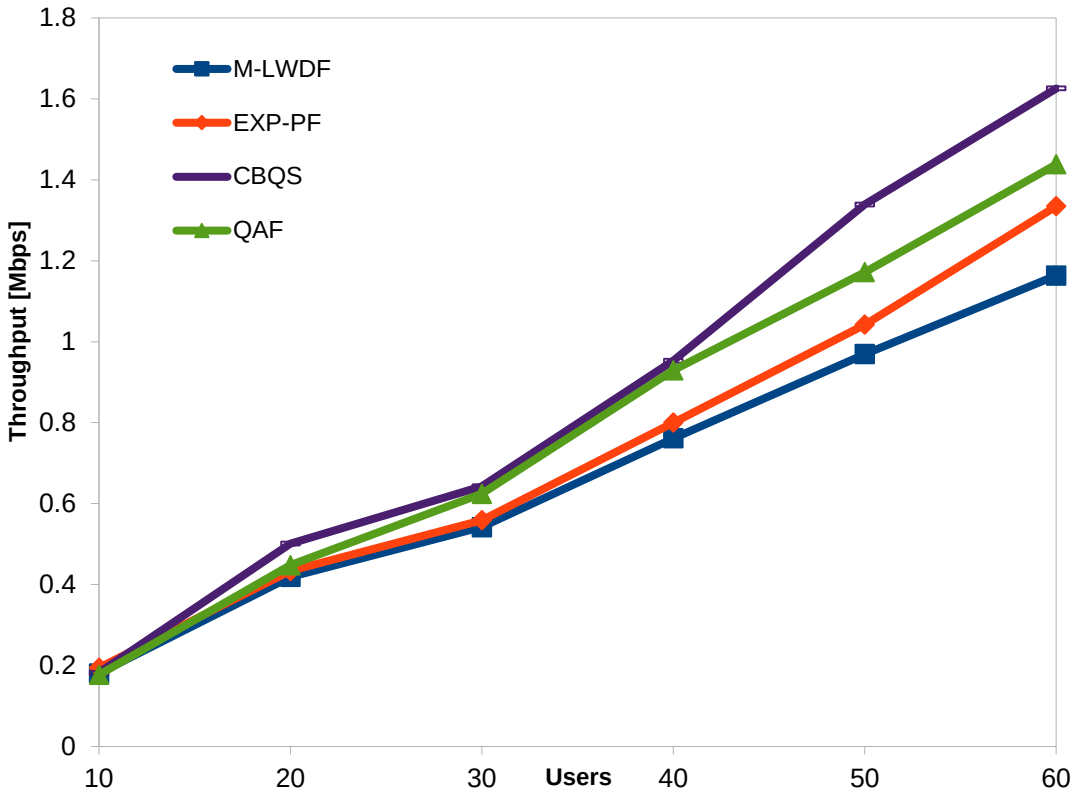

Figure 3-5: Aggregated throughput for web traffic flow.

Both CBQS and QAF produce better throughput performance than the M-LWDF and EXP-PF schedulers. The difference in the throughput performance of CBQS and QAF compared with the other schemes becomes more significant as the number of users increases for web traffic. The QAF scheduler is able to produce better throughput performance than M-LWDF because it uses the power *c* to increase the level of fairness to web (NRT) users rather than only RT users.

Overall, the CBQS scheduler produces the best performance because it considers the relative channel condition in most cases (close to PF performance) and only considers the exponential function of the ratio of the difference between the delay deadline and waiting time, to the waiting time when it is high; this will only happen when the waiting time comes close to the delay deadline. A mean bit rate of 440 kbps for 10 users gives approximately 4.5 Mbps, including MAC, RLC, PDCP, CRC, RTP/IP and PHY overheads. This explains the approximate value of 5Mbps obtained for the throughput results of video traffic for 10 users. It should be noted that the maximum throughput obtained by each scheduler is subject to the scheduler's capability to allocate to users with the best of channels at every TTI. Hence, if users with better channel conditions are selected by a scheduler, the throughput will be higher than if users with poorer channel conditions are selected.

The other performance metric considered is spectral efficiency which is computed as follows as stated in [83] on a subchannel basis;

$$Spectral\ Efficiency = \frac{Throughput\ [bps]}{Bandwith\ [Hz]} \tag{3.24}$$

The above expression for spectral efficiency shows that it is a function of the throughput of the user.

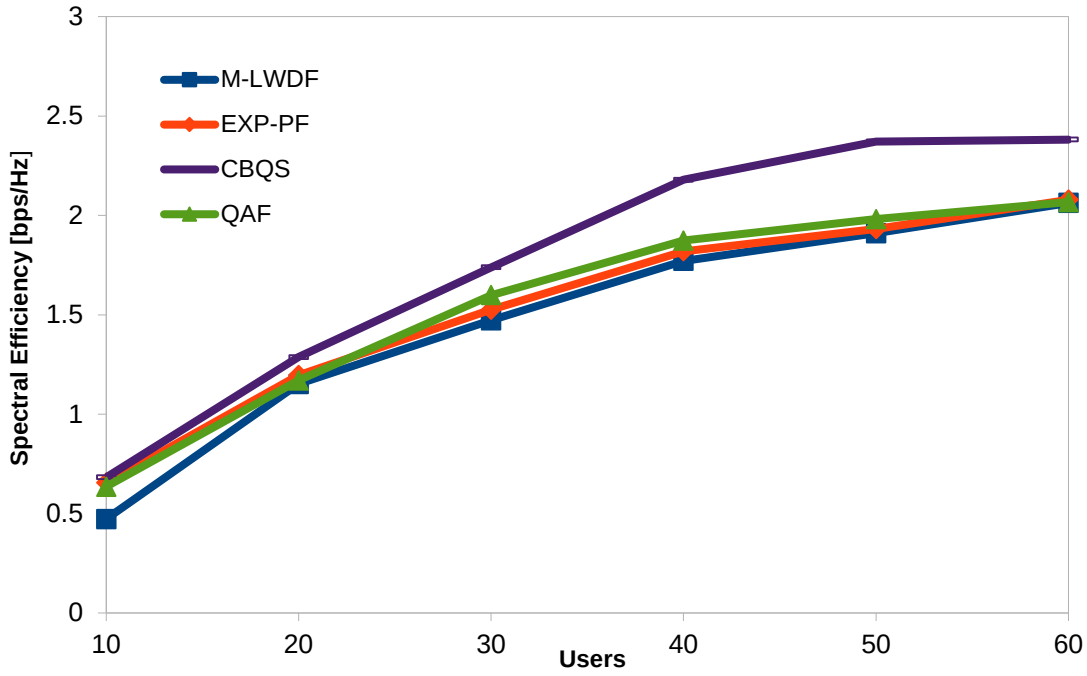

Figure 3-6: Spectral Efficiency

Fig. 3-6 shows that the CBQS scheduler achieves the best spectral efficiency performance in comparison with M-LWDF, QAF and EXP-PF. The difference is more significant as the number of UEs increase. This follows the same trend as throughput performance. This is expected since the spectral efficiency depends on throughput. The figure shows that the proposed scheduler utilizes the spectrum more effectively than the M-LWDF, QAF and EXP-PF schedulers.

The Jain fairness index performance presented in Fig. 3-7 shows that the proposed QAF scheduler has the best fairness index performance when compared with CBQS, M-LWDF and EXP-PF schedulers. The results also show that the M-LWDF and EXP-PF have an edge over the proposed CBQS scheduler at 30 users and above. However, the proposed scheduler still produces a Jain fairness performance of above 0.85 for various numbers of UEs. The usage of *c* and *m* parameters as a tuning parameter to regulate the fairness experienced for NRT and RT

users, respectively, for the QAF scheduler can be said to be responsible for the fairness performance obtained in Fig, 3-7.

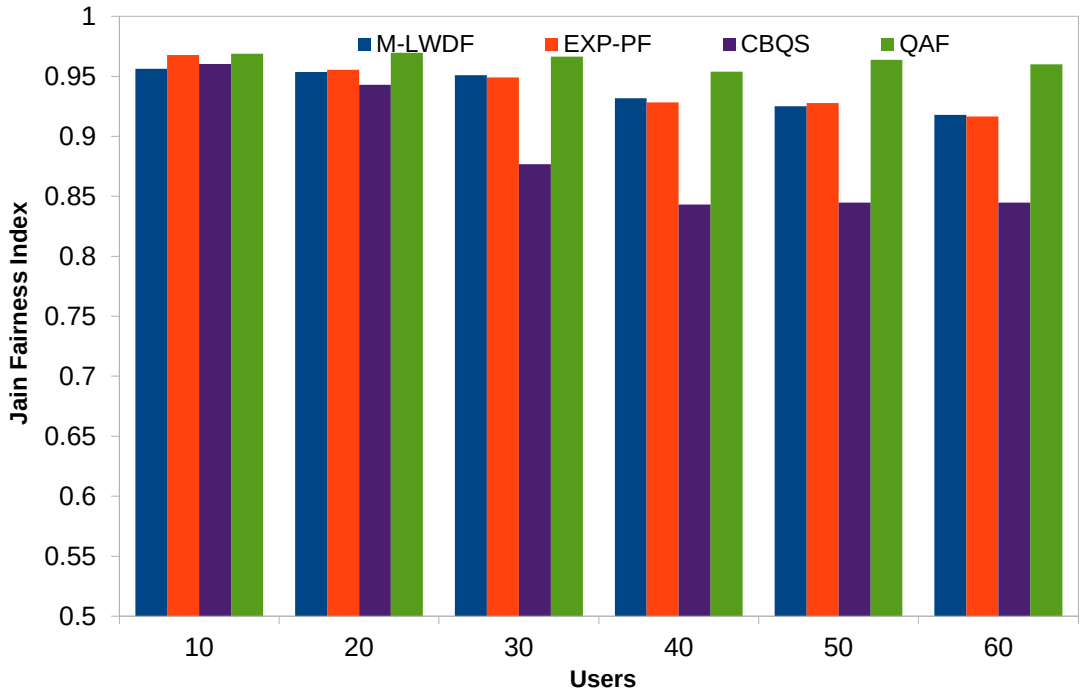

Figure 3-7: Fairness index of all users

Fig. 3-7 above shows that none of the schedulers is able to outperform other schedulers in all of the performance indices considered. This is expected since there is always a trade-off among these major performance indices due to the fact that schedulers consider several factors when making scheduling decisions. This highlights the need for the new scheduling metric that considers all these performance metrics and serves as an overall metric presented in this study. While a throughput to delay ratio has been proposed for this purpose in [131], this proposed metric only considers throughput and delay and does not consider the fairness index. Furthermore, using throughput will suppress the impact of the delay on the overall performance metric due to the fact that if throughput or any other performance index is around 1000, and the other index is around 1, variations of the large performance index will swamp variations of the small performance index. Hence, it is recommended that performance indices of the same range of values are used in the computation of the overall performance index or that the large performance index is normalized. Normalizing the throughput or using spectral efficiency as a substitute for throughput will address this issue. It is on this basis that we propose a new overall performance metric that considers the major performance indices and allows each index to have an almost equal effect on overall performance. This overall performance metric, termed the Scheduling Performance Metric (SPM), can be expressed as follows;

$$SPM = \frac{Spectral\ Efficiency * Fairness\ Index}{Average\ Delay} \tag{3.25}$$

Since spectral efficiency is a function of the throughput, it also represents the throughput in the metric. The average delay is used as a denominator since the objective is to minimize the delay; therefore, the lower the average delay, the higher the *SPM*.

From the SPM results computed and presented in Fig. 3-8, the CBQS has the best SPM performance when compared with other schedulers. However, the QAF scheduler matches the CBQS SPM's performance at 30 – 40 users. This is due to the fact that the high fairness achieved by the QAF is able to compensate for the relatively lower spectral efficiency when compared with the CBQS. The M-LWDF and EXP-PF produce similar SPM performance up to 40 users, but for 40 users and above, the EXP-PF's SPM performance drops as a result of the higher delay experienced as shown in Figs. 3-2 and 3-3.

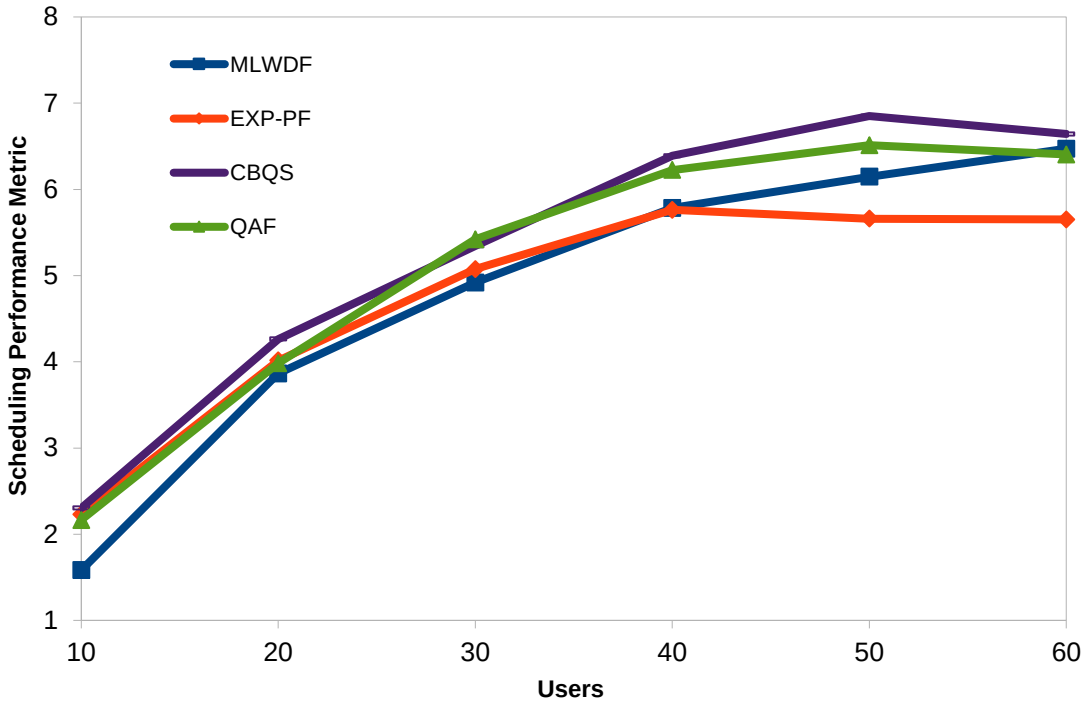

Figure 3-8: Scheduling Performance Metric

3.7 Conclusion

This chapter presented a review of various scheduling schemes. Two new cross-layer based scheduling schemes called Queue Aware Fair (QAF) and Channel Based Queue Sensitive (CBQS) schedulers for satellite LTE networks were presented after formulating a scheduling and

resource allocation problem. The simulation used to conduct the comparison between the proposed schedulers and the two commonly known throughput-optimal schedulers was also presented. Finally, the results of throughput, delay, spectral efficiency and the fairness index from the simulation were presented.

The two proposed schedulers, QAF and CBQS can both support multiple traffic classes (RT and NRT), providing differentiated QoS levels to all of them. The CBQS scheduler provides the best throughput and spectral efficiency performance when compared with the other three schedulers, while the M-LWDF scheduler has an edge over the three schedulers when it comes to delay performance, and both proposed schedulers (QAF and CBQS) have a better delay performance than the EXP-PF scheduler. The proposed QAF scheduler has the best fairness index performance when compared with CBQS, M-LWDF and EXP-PF, while both the M-LWDF and EXP-PF have an edge over the proposed CBQS scheduler.

Furthermore, it can be deduced that the proposed QAF scheduler produces the best fairness index performance without much compromise to throughput and delay performance experienced by the users, while the proposed CBQS scheduler produces the best throughput and spectral efficiency performance without much compromise to delay and fairness perceived by users. Hence both of these schedulers are able to provide a good trade-off between the network throughput, users' QoS demands and perceived fairness. They are also able to support multiple traffic scenarios.

Overall, from the SPM results computed, the CBQS produces the best scheduling performance when compared with other scheduling schemes considered in this chapter. Furthermore, the QAF offers better scheduling performance than the M-LWDF and EXP-PF schedulers.

Chapter 4

LINK ADAPTATION IN SATELLITE LTE NETWORKS

4.1 Introduction

This chapter investigates the impact of the RTPD experienced during CQI reporting in satellite LTE networks. The satellite LTE network's performance is investigated when RTPD is experienced during CQI reporting and when no RTPD is experienced. The proposed Queue Aware Fair (QAF) scheduler presented in chapter 3 is used for this investigation. The comparison between both scenarios is conducted through simulations. The performance metrics considered are throughput, delay and spectral efficiency. The satellite LTE network's performance is also compared with its terrestrial counterparts in order to investigate the impact of RTPD on a satellite LTE network. The performance metrics considered are throughput per area and delay. This investigation is also conducted through simulations. Finally, the impact of varying Effective Isotropic Radiated Power (EIRP) on the performance of a satellite LTE network is investigated through simulations. The performance metric considered is spectral efficiency.

The work presented in this chapter on link adaptation in satellite LTE networks is to be published in Volume 20 Number 2 of Advance Science Letters, 2014 under the title "Impact of propagation delay on the performance of satellite LTE networks".

4.2 Related Studies

Long RTPD and the UE's limited transmission power to send the CQI feedback signal at every TTI has made link adaptation a critical issue in a satellite LTE scenario. The packets of the selected UEs are transmitted using the appropriate Modulation and Coding Scheme (MCS) based on the CQI reported. At the MAC layer, the information is organized in packets

transmitted on the resources of a TTI, whose size is determined by the MCS, according to different possible Transport Block Sizes (TBSs), using the CQI table. However, the long RTPD experienced in a satellite LTE scenario compared with its terrestrial counterparts, causes misalignment between the reported CQI at eNodeB and the current CQI experienced by the UE. This will either cause the eNodeB to transmit at a data rate beyond the MCS level of the UE, leading to a loss of packets, or to transmit at a lower data rate than the MCS level of the UE, leading to underutilization of the resources of the satellite LTE network.

Several studies that considered the design or some aspects of satellite LTE networks have identified the challenge of the long RTPD experienced in the satellite scenario as a major issue in channel (CQI) reporting in a satellite LTE network, but none have investigated the level of the impact of a long RTPD on a satellite LTE network performance. Nor have any studies investigated this impact by comparing a satellite LTE air interface's performance with that of its terrestrial counterparts. While [84],[85] note, respectively, that long RTPD will hinder the exchange of CQI between the eNodeB and UE and the reliability of the obtained CQI, the impact of this delay is not investigated. This is also identified in [86],[87] which state that long RTPD impacts the effectiveness of link adaptation (AMC) and dynamic resource allocation in satellite LTE; however, the RTPD's effect on satellite LTE's performance is not presented. Studies on the architecture of the hybrid satellite and terrestrial network for 4G presented in [88] also raise long RTPD delay as a major issue in the re-use of the terrestrial LTE air interface and satellite LTE air interface, but the two air interfaces are not compared in order to understand the impact of the RTPD on the performance of the satellite air interface.

It is against this background that this chapter investigates the impact of RTPD on a satellite LTE network's performance. The chapter compares the performance of satellite and terrestrial air interfaces, in order to observe the effect of long RTPD experienced in the satellite LTE air interface, compared with the negligible RTPD experienced in the terrestrial LTE air interface. The effect of EIRP on the performance of a satellite LTE network is also investigated.

4.3 Simulation Setup

The impact of a long RTPD is analysed through simulations. An event-driven-based, open source simulator called LTE-Sim [79] which is made available at [89] is used for simulations in this chapter. This is a standalone version of the LTE module in NS-3 [90] and is written in C++. The simulator has been adapted for the satellite scenario by making the necessary changes to both its physical layer and propagation delay. For the purpose of this study, the implementation of the web traffic model presented in the previous chapter is added to this simulation software.

A single spotbeam is considered, with users being capable of video streaming and web surfing, uniformly-distributed within a serving eNodeB footprint. The channel and traffic model presented in the previous chapter are adopted for the simulations.

The Queue-Aware Fair (QAF) scheduler presented in chapter 3 [91] is considered for the purpose of this simulation. Each set of users is made of 60% of web browsers and 40% of video streamers. Each user is assumed to be reporting its channel condition (CQI) at certain intervals to the eNodeB. Two channel reporting scenarios are considered. An RTPD is experienced in one, while no RTPD is assumed in the other scenario. The details of the simulator parameters are provided in Table 4-1 below.

Table 4-1: Simulation parameters for link adaptation

PARAMETERS	VALUE
Simulation Time	500 seconds
RTPD	540 ms
Channel Model	4 state Markov model
TTI	1 ms
Frequency Re-use	7
Mobile user Speed	30 km/h
RLC Mode	AM
Web Traffic Model	On/off Pareto
Video Traffic Model	Trace based @ 440 kb/s
Scheduler	QAF
Bandwidth	15 MHz

4.4 Simulation Results

4.4.1 Impact of RTPD on Channel Reporting

Throughput, average delay and spectral efficiency are the performance metrics considered for this investigation, carried out to observe the impact of CQI reporting on satellite LTE networks.

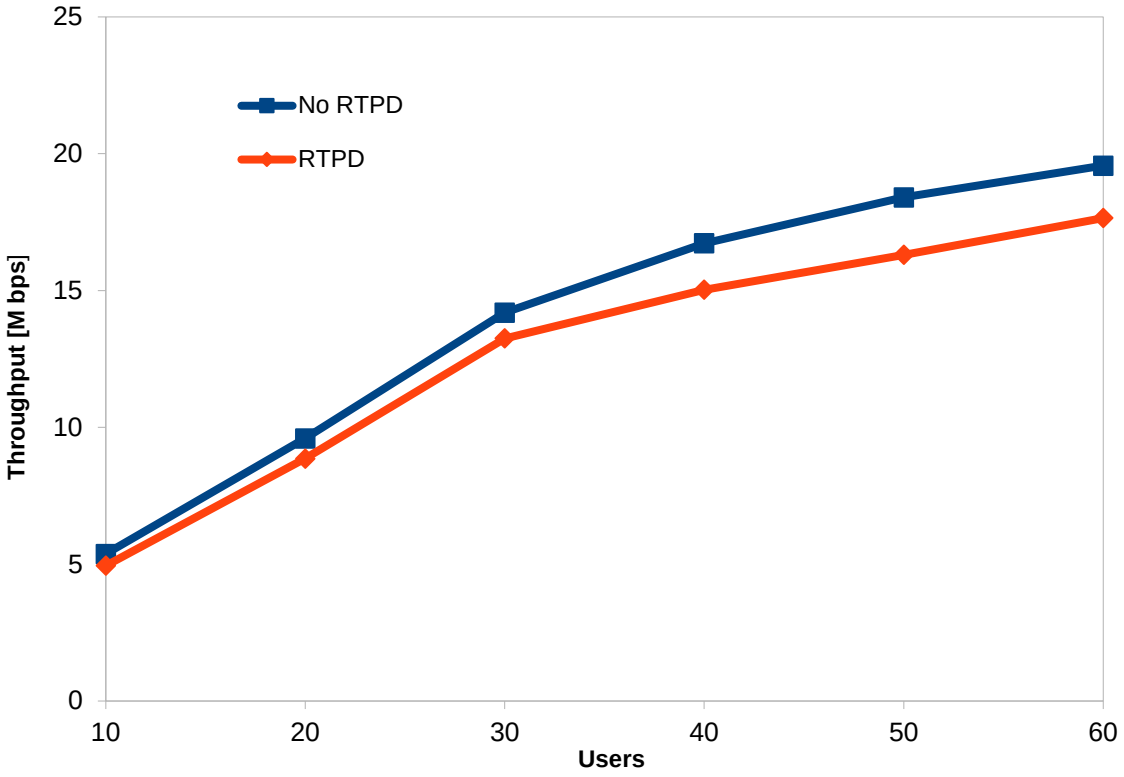

Figure 4-1: The throughput for video users

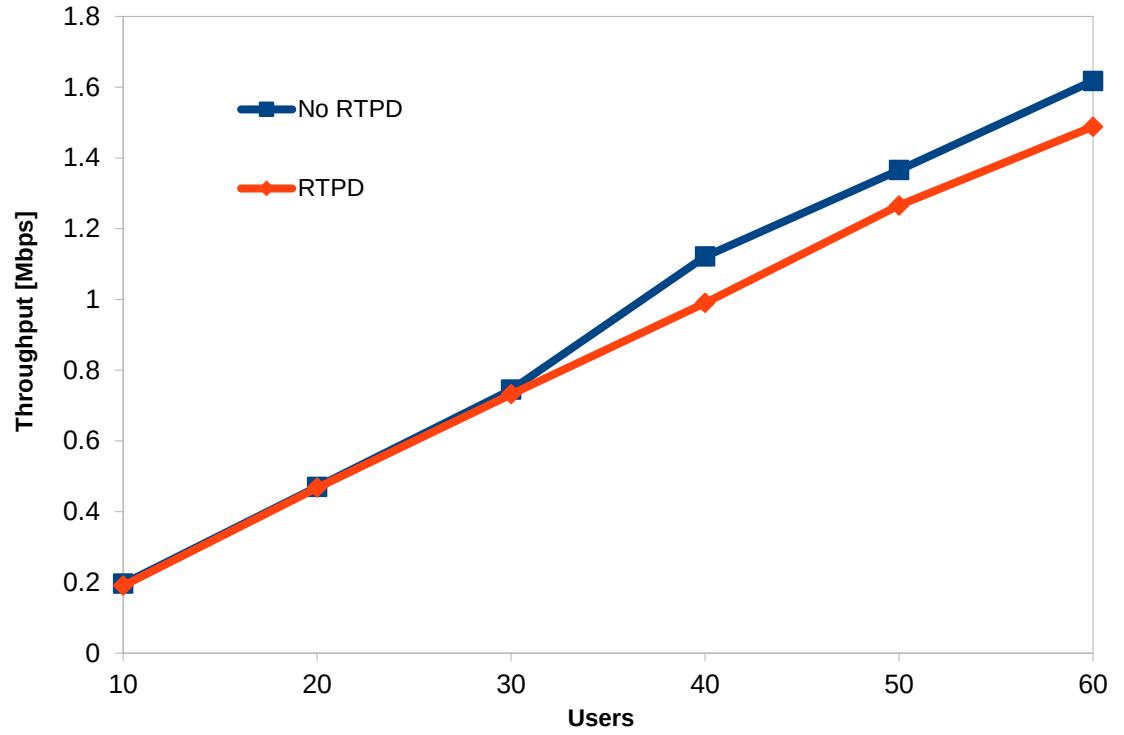

Figure 4-2: The throughput for web users

The results show that there is significant impact as a result of the long propagation delay experienced when the channel condition is reported to eNodeB by the UE. Figs. 4-1 and 4-2 show that the throughput performance when there is no RTPD is better than when RTPD is experienced, for both video and web traffic. The difference becomes more significant as the number of users increases, especially from 30 users and above. This is due to the fact that fewer packets are transmitted as a result of using a lower CQI (transmission rate) compared with the actual CQI experienced by the UE, or due to the loss of packets as a result of using a higher CQI (transmission rate) compared with the actual CQI (transmission rate) the UE is capable of handling.

Delay performance follows the same trend as throughput performance. The delay performance for cases when RTPD is experienced while reporting channel status is worse than cases when there no RTPD is experienced for both video and web traffic, as shown in Figure 4-3. This is due to the fact that since fewer packets are transmitted, there are more packets waiting in the queue. As expected, the delay experienced by web traffic users is higher than that of video traffic users, since the scheduler considers QoS factors when taking scheduling decisions and web traffic has a higher delay deadline than video traffic. It is also worth noting that the difference in delay performance becomes more evident as the number of users increases, most significantly from 30 users and above.

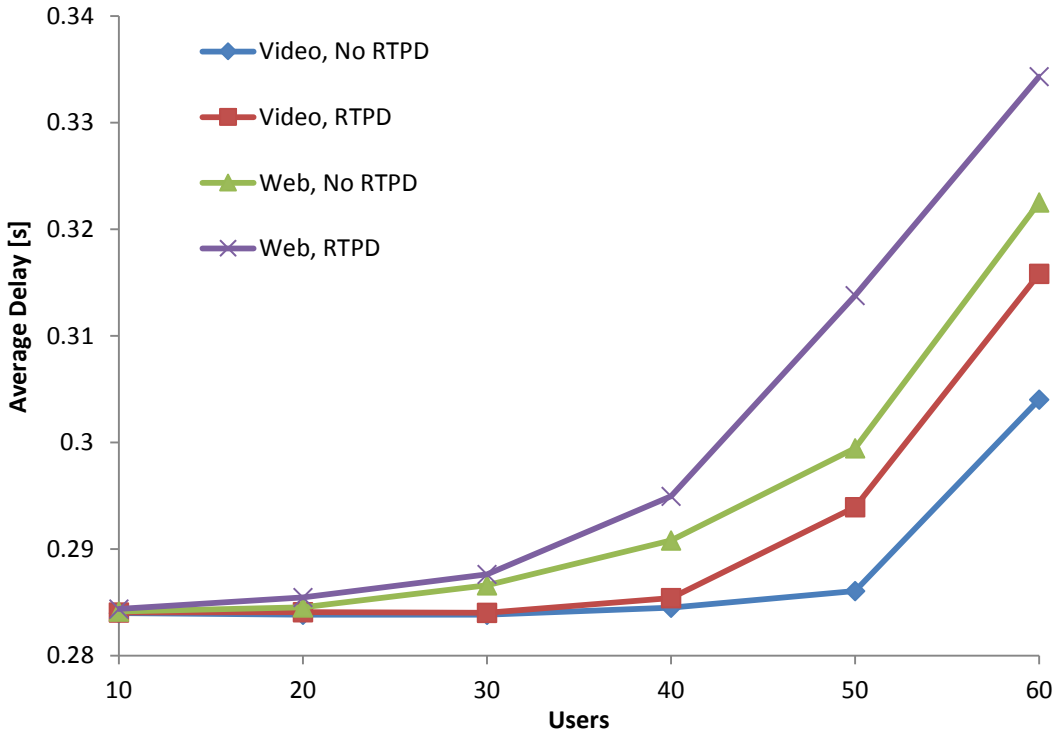

Figure 4-3: The average delay for all users

The spectral efficiency results obtained in Fig. 4-4 depict that when the channel reporting does not experience RTP delay, the spectral efficiency produces better performance than when RTP delay is experienced in channel reporting. The difference in performance is significant at 30 users and above. The spectral efficiency computed is a function of the throughput as presented in chapter 3; hence, the basis for this spectral efficiency result is similar to that of throughput. Since fewer packets are transmitted than the number the UE is capable of receiving, the level at which the spectrum is utilized is reduced, compared with when the eNodeB is using the actual CQI that does not experience any delay.

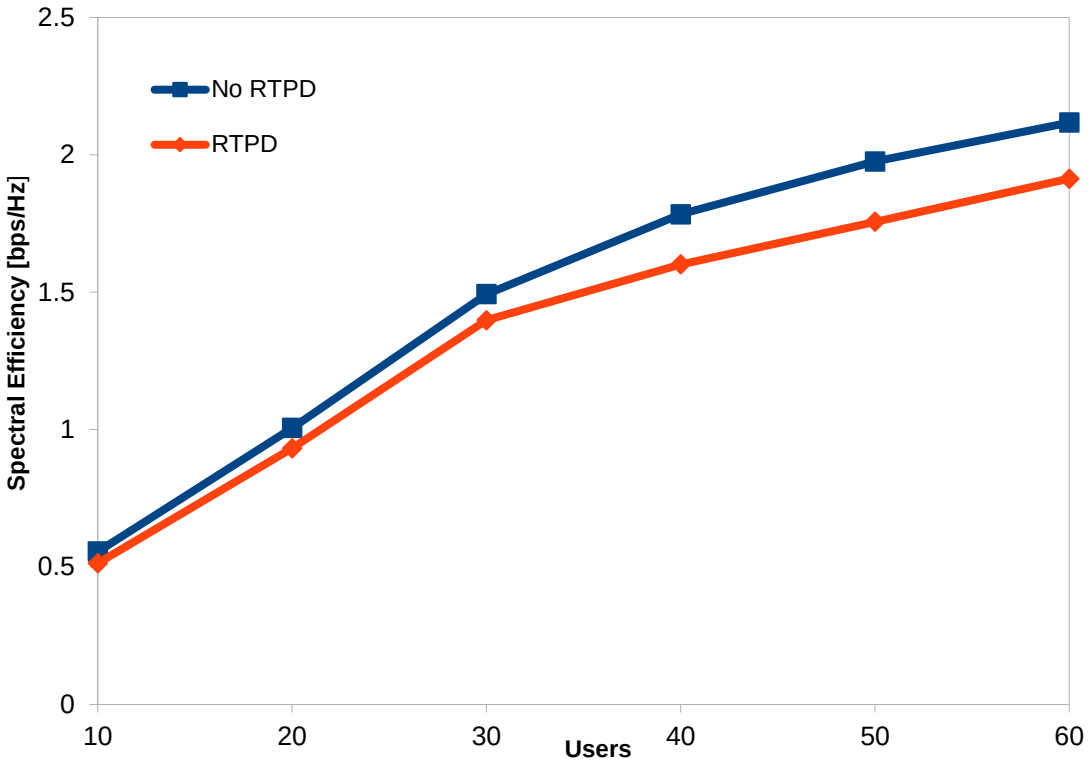

Figure 4-4: The spectral efficiency for all users

4.4.2 Comparison of Satellite and Terrestrial LTE Air Interface

Terrestrial and satellite LTE systems are meant to complement each other in providing LTE services. In this section, we compare the performance of the proposed scheduler in terrestrial and satellite cases, in terms of throughput per cell area, considering the same bandwidth and EIRP of 15 MHz and 43 dBW (these values have been used in order to be consistent with the terrestrial standard values), respectively. Only video (RT) traffic users are considered. The other parameters remain the same as in the previous section.

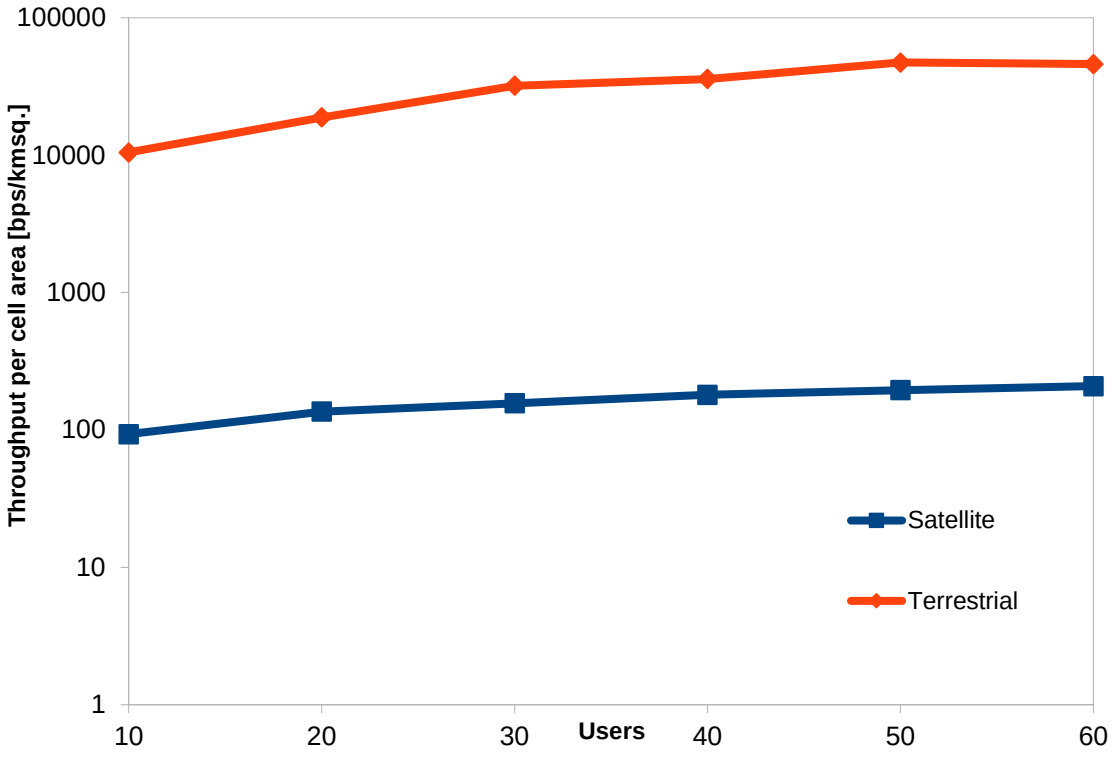

Figure 4-5: Throughput per cell area for video users (RT) for the two air interfaces

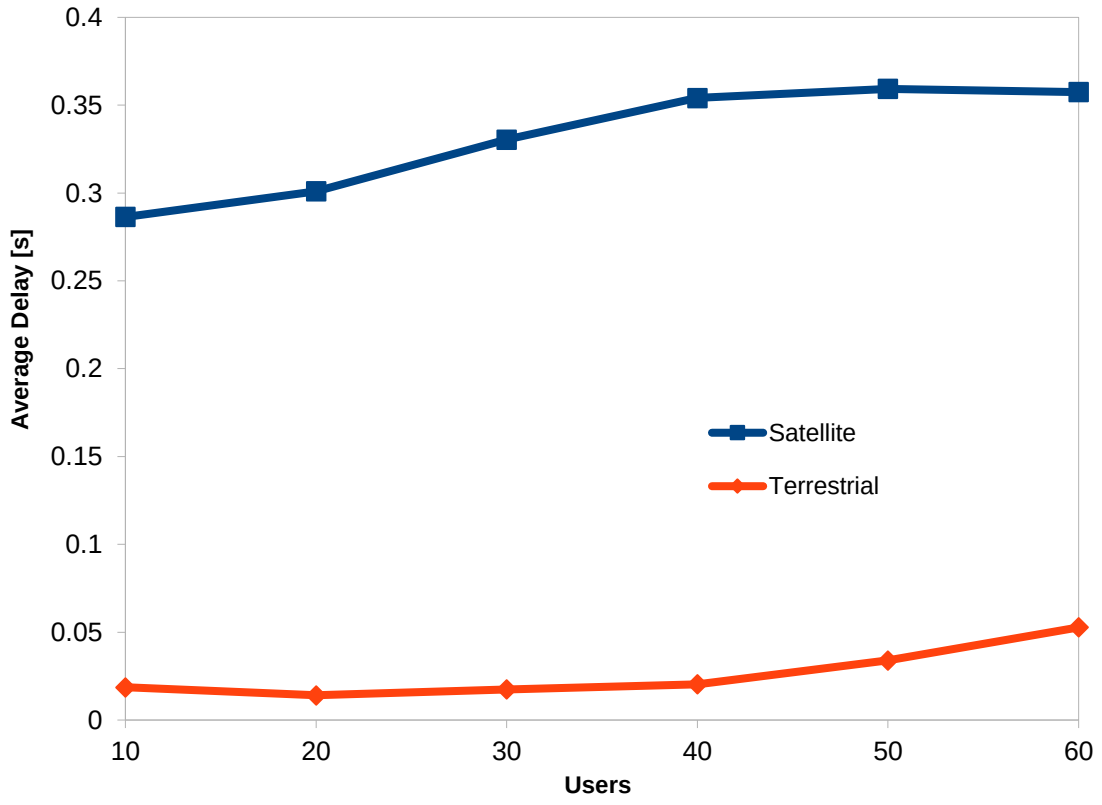

Figure 4-6: Average delay for video users (RT) for the two air interfaces

The results shown in Fig. 4-5, which is in logarithmic scale, show that the throughput per cell area performance for video (RT) users in the terrestrial case is much better than that in the satellite case, under the same conditions. This is due to the RTPD and the fact that the spotbeam area of satellite is bigger than of the terrestrial air interface. The radius of a spotbeam (cell) in a satellite scenario is a minimum of 150 km, compared with a terrestrial scenario of 1 km; hence, the throughput per area in the satellite scenario will be far less than in the terrestrial scenario. The misalignment of the CQI as a result of high RTPD can also reduce throughput performance. This can be addressed by using higher EIRP value in the satellite scenario.

As shown in Fig. 4-6, the average delay experienced in the terrestrial air interface scenario is lower than in the satellite air interface. This is due to the channel delay experienced in the satellite air interface, which is higher than that experienced in the terrestrial air interface. A satellite air interface has a channel delay of approximately 280 ms compared with a 1 ms channel delay in a terrestrial air interface.

4.4.3 Varying EIRP

Recent GEO satellite technologies that could be used to implement satellite LTE can support different EIRP values up to 70 dBW [92]. Therefore, there is a need to investigate the impact of varying EIRP values on system performance, by examining three different EIRP values, such as: 43, 53 and 63 dBW.

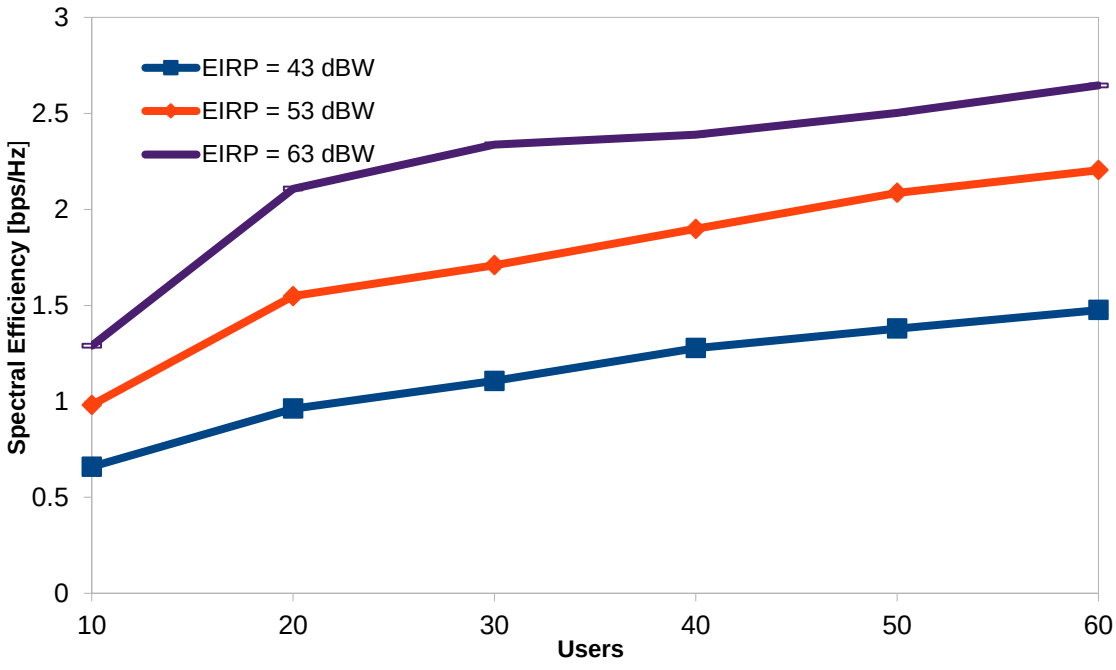

Figure 4-7: The spectral efficiency for all users for varying EIRP

As shown in Fig. 4-7, the highest EIRP of 63 dBW allows us to achieve the highest spectral efficiency followed by 53 dBW and 43 dBW, respectively. These results show that the EIRP value has a significant impact on the performance (capacity) of satellite LTE systems. The basis for this result is that, at EIRP of 63 dBW, an average CQI of approximately 13 is obtained considering the CQI distribution, while at EIRP of 53 dBW, an average CQI of approximately 9 is obtained and a CQI of approximately 7 is obtained at an EIRP of 43 dBW. This explains why a higher spectral efficiency is obtained using EIRP of 63 dBW than with 53 dBW and 43 dBW, since the spectral efficiency depends on the throughput and the throughput depends on the transmission rate (which also depends on the CQI).

4.5 Conclusion

This chapter presented the investigation of the impact of RTPD experienced during CQI reporting from the UE to eNodeB in a satellite LTE network. A comparison between satellite and terrestrial air interfaces, considering the impact of RTPD on their respective performance, was also presented. The scheduler proposed and used for this investigation was presented, as well as the simulation used for the investigation and the results of the investigations.

The RTPD experienced during channel reporting can be said to be of significance to satellite LTE networks' performance. This can be deduced from the performance metrics presented (throughput, delay and spectral efficiency), which show, that the RTPD experienced during CQI reporting reduces the performance of a network compared with when the RTPD is not experienced. This is as a result of the misalignment between the CQI reported at eNodeB and the instantaneous CQI of the UE.

The comparison between the terrestrial and satellite air interface also shows that the terrestrial interface provides better performance than its satellite counterparts and that with the increment of EIRP, improved performance, in terms of capacity, can be obtained from a satellite air interface. This also shows that a satellite LTE air interface can complement a terrestrial air interface.

Chapter 5

NEAR-OPTIMAL SCHEDULING SCHEME IN SATELLITE LTE NETWORKS

5.1 Introduction

This chapter presents a Near-Optimal Scheduling Scheme (NOSS) for satellite LTE networks, which aims to maximize total network throughput, with fairness and delay as possible constraints. This near-optimal scheduler, which is obtained using Karush-Kuhn-Tucker (KKT) multipliers, is expected to further improve the throughput of the satellite LTE network without compromising an acceptable QoS and level of fairness experienced by the user. In order to evaluate the performance of the proposed scheduler, a simulation setup is used to compare various schedulers' performance in satellite LTE networks with the proposed near-optimal scheduler. Throughput performance, delay performance, spectral efficiency and fairness for the three schedulers considered are presented. The schedulers considered are the two most popular throughput-optimal schedulers - Modified Largest Weighted Delay First (M-LWDF) and Exponential Proportional Fair (EXP-PF).

This chapter commences with a review of related literature on optimal scheduling in LTE; this is followed by the scheduling problem formulation. The near-optimal solution to the scheduling problem, using KKT multipliers is then presented. This is followed by a discussion on the other two schedulers considered in this study. The simulation setup is also presented. Finally, the simulation results, including throughput, delay, spectral efficiency and fairness are presented and discussed.

The work in this chapter has been submitted to the Institution of Engineering and Technology (IET) Networks Journal.

5.2 Related Studies

In order to meet the set 4G requirements, the need for an effective scheduling scheme that will ensure optimal performance in throughput, QoS in terms of delay and users' perceived fairness, cannot be over-emphasized. This gave rise to the need to propose an optimal or near-optimal scheduling scheme for satellite LTE networks, which is of concern in this study. Several schemes, including channel-aware and queue-aware schemes, have been proposed to address the problem of scheduling and resource allocation in terrestrial LTE networks, as detailed in [58], using an empirical approach. However, this type of approach does not guarantee optimal performance or near-optimal performance. It is also worth noting that studies have been conducted to design optimal or near-optimal schedulers for an LTE or OFDMA based network. A brief review of some of these optimal or suboptimal scheduling schemes is presented in this section. In [93], a scheduling problem is formulated with the aim of maximizing the total bit rates of all users, with the constraint of mapping only one user to a subchannel. The constraint does not address any QoS or fairness factor and a heuristic algorithm, called genetic algorithm, is used, rather than exact solutions. Furthermore, a sub-optimal scheduler is proposed in [94],[95], with the aim of maximizing the bit rate for both single and multiple users. Although it uses an exact solution to solve the scheduling problem, it only focuses on AMC/MCS as constraints, while [96], which also used an exact solution for the scheduling problem modelled as an Integer Linear Programming (ILP) problem, did not consider QoS constraints. The work in [97] presents a scheduling scheme for both single and multicarrier OFDM MIMO systems, with the aim of maximizing the utility function in terms of data rate, with only power as its constraint. It uses genetic algorithm and Lagrange multipliers. In [98], the formulated scheduling problem aims to maximize the throughput. While it uses KKT multipliers to produce an exact optimal solution, it only considers throughput based QoS constraints and does not consider QoS constraints that relate to delay, which is an important QoS factor in LTE standards. Also of interest in the literature is the work done in [99] which proposed a scheduling solution that aimed to maximize rate distortion and considers delay and AMC as its constraints. However, the delay is not modelled or represented and a heuristic algorithm is used, rather than using exact solutions. Furthermore, the solution is only tested on RT traffic by comparing with M-LWDF and it did not consider a mixed traffic scenario. It is very important to note that all of these schedulers have been proposed for a terrestrial LTE or OFDMA based network, and that, to the best of our knowledge, none has been designed for a satellite LTE network. Hence, the

aim of this chapter is not only to propose a close to optimal scheduling scheme that will maximize the network throughput more than the two common throughput-optimal scheduling schemes, considering delay that is modelled from M/G/1 queuing model and fairness as possible constraints, but one that will also be suitable for a satellite LTE network. The proposed scheduling solution is obtained using an exact solution called KKT multipliers (a special case for Lagrange multipliers). Based on the SPM, the proposed schemes NOSS1 and NOSS3 outperform the M-LWDF and EXP-PF schedulers and also produce better performance than the proposed cross-layer based packet scheduling scheme in chapter 3.

5.3 Scheduling Problem Formulation

A single spotbeam is considered which consists of a base station (eNodeB) where the downlink bandwidth is divided into *J* subchannels. The eNodeB will serve the set of *K* users. The set of subchannels are denoted by $J = \{j | j = 1,2,3, \ldots., J\}$ and the set of users are denoted by $K = \{k | k = 1,2,3, \ldots., K\}$. The objective of this scheduling optimization problem is to use it to derive or obtain an optimal scheduling solution whose aim is to maximize total throughput. The optimal scheduling solution selects a user from a set of users willing to be served with the above objective. Hence, the objective function is to maximize the total throughput of the network, subject to two major constraints, which are fairness among users and experienced waiting time or delay before being served by the network. During each scheduling slot, the eNodeB could allocate *j* subchannels (subchannels are not necessarily contiguous) to user *k*, but each subchannel is assigned to at most one user.

$$max \sum_{j=1}^{J} \sum_{k=1}^{K} R_{k,j} U_{k,j} \tag{5.1}$$

Subject to;

$$\forall_k \frac{R_k}{\alpha_k} - \frac{R_l}{\alpha_l} \leq \delta \tag{5.2}$$

$$\forall_k \overline{W_k} \leq \beta \tag{5.3}$$

Where *J* is the number of subchannels and *K* is the number of users. R_k and R_l are the data rate of user k and l respectively while α_k and α_l are the weight of user k and l respectively and δ is the degree of fairness. $\overline{W_k}$ is the average waiting time or delay experienced by each user k in each queue and β is the delay bound or time deadline that must not be exceeded in the queue.

Constraint (5.2) as similarly expressed in [100] states that the difference between the proportion of data rate that can be experienced between two different users must not be more than δ and constraint (5.3) states that the average waiting time or delay experienced by each user's packet for each subchannel must not exceed β. It is worth noting that α and β vary depending on the type of traffic. In order to simplify the analysis, for the purpose of this study it is assumed that the queuing system can be modelled as M/G/1. The M/G/1 queuing model is assumed for the satellite LTE downlink system since it has a varying service rate (transmission rate) as a result of varying channel conditions. There is need to represent the average waiting time in constraint (5.3) with an expression for the purpose of analysis; hence, the average waiting time expression for the M/G/1 queuing model [101] is used in this optimization problem. The average waiting time $\overline{W_k}$ can be expressed as follows;

$$\overline{W_k} = \frac{A_k(m^2 + {R_k}^2 V_k)}{2R_k(R_k - A_k m^2)} \tag{5.4}$$

R_k is the data rate of user *k*, A_k is the arrival rate of user *k* , V_k is the variance of the service time of user *k*, m is the number of TTI over which the R_k is averaged and *K* is the number of users. The R_k used in the fairness constraint in (5.2) and the waiting time expression in (5.4) can be expressed as;

$$R_k = R'_k + \sum_j R_{k,j} U_{k,j} \tag{5.5}$$

R'_k is the average data rate experienced by user *k* before the present TTI and the expression $\sum_j R_{k,j} U_{k,j}$ represents the sum of the data rate experienced by user *k* over subchannels *j* at the present TTI . $U_{k,j}$ is the variable that indicates whether user *k* is assigned to subchannel *j* or not. $U_{k,j}$ will be 1 if user *k* is assigned to subchannel *j* or else it will be 0. The expression in (5.5) provides a representation of the service experienced by user *k* on an average or long term basis.

From (5.4) and (5.5), the optimization problem can be re-written as;

$$max \sum_{j=1}^{J} \sum_{k=1}^{K} R_{k,j} U_{k,j} \tag{5.6}$$

Subject to;

$$\forall_k \ \frac{R'_l + \sum_j R_{l,j} U_{l,j}}{\alpha_l} - \frac{R'_k + \sum_j R_{k,j} U_{k,j}}{\alpha_k} + \delta \ \geq 0 \tag{5.7}$$

$$\forall_k\ 2\beta_k\left[\left(R'_k+\sum_j R_{k,j}U_{k,j}\right)\left(\left(R'_k+\sum_j R_{k,j}U_{k,j}\right)-A_k m^2\right)\right]-A_k\left[m^2+\left(R'_k+\sum_j R_{k,j}U_{k,j}\right)^2 V_k\right]\geq 0 \quad (5.8)$$

5.4 Derivation of Optimal Scheduling Solution

The problem is solved using Langragian multipliers and since the constraints are inequalities, KKT multipliers λ_1 and λ_2 are considered. C_1 and C_2 are used as slack variables to compensate for the inequalities.

Many practical problems in engineering can be formulated as constrained optimization problems and can be solved using the Lagrange multipliers which KKT multipliers are derived from [102],[103]. The KKT multipliers or conditions allow inequality constraint, while the method of Lagrange multipliers only allows equality constraints. The KKT approach to nonlinear programming generalizes the method of Lagrange multipliers [104]–[106].

Using KKT multipliers, we obtain the following;

$$L=\sum_{j=1}^{J}\sum_{k=1}^{K}R_{k,j}\,U_{k,j}\ +\lambda_1\left[\frac{R'_l+\sum_j R_{l,j}U_{l,j}}{\alpha_l}-\frac{R'_k+\sum_j R_{k,j}U_{k,j}}{\alpha_k}+\delta-C_1^2\right]+\lambda_2\left[2\beta_k\left[\left(R'_k+\sum_j R_{k,j}U_{k,j}\right)\left(\left(R'_k+\sum_j R_{k,j}U_{k,j}\right)-A_k m^2\right)\right]-A_k\left[m^2+\left(R'_k+\sum_j R_{k,j}U_{k,j}\right)^2 V_k\right]-C_2^2\right] \quad (5.9)$$

$$\frac{\partial L}{\partial U_{k,j}}=0;\ \frac{\partial L}{\partial \lambda_1}=0;\ \frac{\partial L}{\partial C_1}=0;\frac{\partial L}{\partial \lambda_2}=0;\frac{\partial L}{\partial C_2}=0 \quad (5.10)$$

Differentiating with respect to a specific instant of $U_{k,j}$; $U_{m,n}$, we have;

$$\frac{\partial L}{\partial U_{m,n}}=R_{m,n}+\lambda_1\left(-\frac{R_{mn}}{\alpha_m}\right)+\lambda_2\left(2\beta_k\left(2R'_m R_{m,n}+2R_{m,n}\sum_j R_{k,j}U_{k,j}-A_k m^2 R_{m,n}\right)-A_k V\left(2R'_m R_{m,n}+2R_{m,n}\sum_j R_{k,j}U_{k,j}\right)\right)=0 \quad (5.11)$$

$$\frac{\partial L}{\partial \lambda_1}=\frac{R'_l+\sum_j R_{l,j}U_{l,j}}{\alpha_l}-\frac{R'_k+\sum_j R_{k,j}U_{k,j}}{\alpha_k}+\delta-C_1^2=0 \quad (5.12)$$

$$\frac{\partial L}{\partial C_1} = -2\lambda_1 C_1 = 0 \tag{5.13}$$

$$\frac{\partial L}{\partial \lambda_2} = 2\beta_k \left[\left(R'_k + \sum_j R_{k,j} U_{k,j} \right) \left(\left(R'_k + \sum_j R_{k,j} U_{k,j} \right) - A_k m^2 \right) \right] - A_k \left[m^2 + \left(R'_k + \sum_j R_{k,j} U_{k,j} \right)^2 V_k \right] - C_2^2 = 0 \tag{5.14}$$

$$\frac{\partial L}{\partial C_2} = -2\lambda_2 C_2 = 0 \tag{5.15}$$

From (5.13) and (5.15), either λ_1 is 0 or C_1 is 0 and either λ_2 is 0 or C_2 is 0. One possible solution is when λ_1 is 0 and C_2 is 0. Assuming $X_k = \sum_j R_{k,j} U_{k,j}$, if we substitute these, from (5.11), we obtain;

$$\lambda_2 = \frac{-1}{2[\beta_k (2R'_m + 2X_k - A_k m^2) - A_k V (R'_m + X_k)]} \tag{5.16}$$

In the solution chosen, λ_1 is 0, so the fairness constraint drops from the solution. In order to compensate for this, an approximate solution of proportional fairness from (3.6) in chapter 3 is chosen as a substitute for $U_{k,j}$. The $U_{k,j}$ in the expression for X_k is then expressed as follows;

$$U_{k,j} = \frac{R_{k,j}}{R'_k} \quad and\ hence, \quad X_k = \sum_j \frac{{R_{k,j}}^2}{R'_k} \tag{5.17}$$

This allows some level of fairness in the solution that will be obtained. The ratio of the instantaneous data rate to the previous data rate is considered for $U_{k,j}$. A user with more allocation in previous TTI will have a higher denominator than a user with lower allocation in previous TTI. Hence, users with more allocation at previous TTI will tend to have lower $U_{k,j}$ than users with lower allocation. This brings a certain level of fairness by enabling users with lower allocation in previous TTI to have higher chances of selection. It is important to note that this fluid approximation of $U_{k,j}$ is only used to obtain the X_k in the KKT multiplier λ_2 presented in (5.16) and it is different from the $U_{k,j}$ used in subsequent equations where $U_{k,j}$ is either a 0 or 1.

Substituting λ_2 in (5.16), we have;

$$L = \sum_{j=1}^{J} \sum_{k=1}^{K} R_{k,j}\, U_{k,j} - \frac{[2\beta_k (R'_m + X_k)^2 - A_k (2\beta_k m^2 (R'_m + X_k) + m^2 + (R'_m + X_k)^2 V_k]}{2[2\beta_k (R'_m + X_k) - A_k (\beta_k m^2 + (R'_m + X_k) V_k)]} \tag{5.18}$$

Since, from (5.5), A_k can be expressed as follows;

$$A_k = \frac{2\overline{W_k}(R'_m + X_k)^2}{m^2 + (R'_m + X_k)^2 V_k + 2\overline{W_k} m^2 (R'_m + X_k)} \tag{5.19}$$

Substituting (5.19) in (5.18), we have;

$$L = \sum_{j=1}^{J}\sum_{k=1}^{K} R_{k,j}\, U_{k,j} - \frac{(R'_m + X_k)[(\beta_k - \overline{W_k})(m^2 + (R'_m + X_k)^2 V_k) - \overline{W_k}\beta_k m^2 (R'_m + X_k)]}{2\left[\beta_k m^2\left(1 + (R'_m + X_k)\right) + (R'_m + X_k)^2 V_k (\beta_k - \overline{W_k})\right]} \tag{5.20}$$

Assuming, $\Delta = (\beta_k - \overline{W_k})$, $\gamma = (R'_m + X_k)^2 V_k$, and $R_k = R'_m + X_k$, then (5.20) can be re-written as;

$$L = \sum_{j=1}^{J}\sum_{k=1}^{K} R_{k,j}\, U_{k,j} \; - \frac{R_k[\Delta(m^2 + \gamma) - \overline{W_k}\beta_k m^2 R_k]}{2[\beta_k m^2 (1 + R_k \overline{W_k}) + \gamma\Delta]} \tag{5.21}$$

(5.21) can be re-written as;

$$L = \sum_{j=1}^{J}\sum_{k=1}^{K} R_{k,j}\, U_{k,j} \; + \frac{R_k[\overline{W_k}\beta_k m^2 R_k - \Delta(m^2 + \gamma)]}{2[\beta_k m^2 (1 + R_k \overline{W_k}) + \gamma\Delta]} \tag{5.22}$$

From the solution obtained in (5.22), the following algorithm is used in deciding the user to be selected on a subchannel basis;

$$L_{k,j} = argmax \left\{ R_{k,j}\, U_{k,j} \; + \frac{R_k[W_k\beta_k m^2 R_k - \Delta(m^2 + \gamma)]}{2[\beta_k m^2 (1 + R_k W_k) + \gamma\Delta]} \right\} \tag{5.23}$$

If the objective function in (5.1) is normalized with the average data rate, the following algorithm can be obtained;

$$L_{k,j} = argmax \left\{ \frac{R_{k,j} U_{k,j}}{R'_k} + \frac{R_k[W_k\beta_k m^2 R_k - \Delta(m^2 + \gamma)]}{2[\beta_k m^2 (1 + R_k W_k) + \gamma\Delta]} \right\} \tag{5.24}$$

For practical implementation and simulation purposes, heuristic solutions similar to the expression of EXP-PF, which are obtained from the derived solutions, are also considered. The main purpose is to observe the performance of these heuristic solutions compared with EXP-PF. The heuristic solutions for the above derived solutions (5.23) and (5.24) can be expressed as follows;

$$L_{k,j} = argmax\left\{ R_{k,j}\, U_{k,j}\ exp\left(\frac{R_k[W_k\beta_k m^2 R_k - \Delta(m^2+\gamma)]}{2[\beta_k m^2(1+R_k W_k)+\gamma\Delta]}\right)\right\} \quad (5.25)$$

$$L_{k,j} = argmax\left\{\frac{R_{k,j}\, U_{k,j}}{R'_k}\ exp\left(\frac{R_k[W_k\beta_k m^2 R_k - \Delta(m^2+\gamma)]}{2[\beta_k m^2(1+R_k W_k)+\gamma\Delta]}\right)\right\} \quad (5.26)$$

It is worth noting that W_k is used from (5.23) to (5.26) instead of $\overline{W_k}$ because the waiting time of the user's HOL packet is used for the purpose of simulation for simplicity and easy computation.

5.5 Other Scheduling Schemes

The proposed scheduler is compared with two well-known throughput optimal scheduling schemes, Modified Largest Weighted Delay First (M-LWDF) and Exponential Proportional Fair (EXP/PF). These two scheduling algorithms can be expressed as follows in (5.27) and (5.28) respectively;

$$L_{k,j} = argmax\left\{\frac{R_{k,j}(n)(-log\delta_k)W_k(n)}{T_k(n)T_{k,deadline}}\right\} \quad (5.27)$$

$$L_{k,j} = argmax\left\{\frac{R_{k,j}(n)}{T_k(n)}exp\left(\frac{a_k W_k(n)-\overline{aW_n}}{1+\sqrt{\overline{aW(n)}}}\right)\right\} \quad (5.28)$$

Details of the parameter are the same as provided in chapter 3.

5.6 Simulation Setup

This section provides the details of the simulation platform that is used to evaluate the performance of the proposed near-optimal scheduling scheme in the satellite LTE air interface. A single spotbeam has been simulated, modeling the inter-beam interference as a contribution to the SINR. UEs are capable of rendering video streaming and web surfing uniformly-distributed within the spotbeam footprint. The channel and traffic model presented in chapter 2 are adopted for the simulations. Two scenarios have been considered for this chapter. The first consists of only RT traffic (video streamers) and the second is made of 50% of NRT traffic

(web browsers) and 50% of RT traffic (video streamers). Each UE is assumed to be reporting its channel condition (in terms of CQI), according to fixed intervals, to the eNodeB.

The LTE performance is analysed, using an open source discrete event simulator called LTE-Sim [79]-[81]; this is a standalone version of the LTE module in NS-3 and is written in C++ and was upgraded in [82]. This simulator has been adapted to the GEO satellite scenario. In particular, the physical layer characteristics, including the channel model and the propagation delay, were modified in order to implement the satellite scenario. Furthermore, the new scheduler and the web traffic model have been included in the simulator.

It is assumed that CQI is reported by the UE every 100 TTIs; this long interval has been considered in the GEO scenario in order to reduce the frequency of reporting so as to save UE equipment's power. The details of the simulator parameters are provided in Table 5-1 below.

Table 5-1: Simulation parameters for comparison of schedulers

Parameters	Value
Simulation Time	500 seconds
RTPD	540 ms (GEO satellite)
Channel Model	4 state Markov model
MIMO	2 x 2 (2 antenna ports)
CQI Reporting Interval	100 TTI (= 0.1 s)
TTI	1 ms
Frequency Re-use	7
Mobile user Speed	30 km/h
RLC Mode	AM
Web Traffic Model	ON/OFF M/Pareto
Video Traffic Model	Trace-based @ 440 kbps
Schedulers	M-LWDF, EXP/PF, NOSS1, NOSS2, NOSS3 & NOSS4
Bandwidth	15 MHz

5.7 Simulation Results

5.7.1 Real Time Traffic Only

A single spotbeam has been considered with only video streaming users uniformly distributed within a serving eNodeB footprint. The channel and traffic model presented in the previous chapter are adopted for the simulations. Each user is assumed to be reporting its channel condition at certain intervals to the eNodeB.

It should be noted that, in the results presented below, the scheduling algorithm presented in (5.23) represents Near Optimal Scheduling Scheme 1 (NOSS1), (5.24) represents NOSS2, (5.25) represents NOSS3 and (5.26) represents NOSS4.

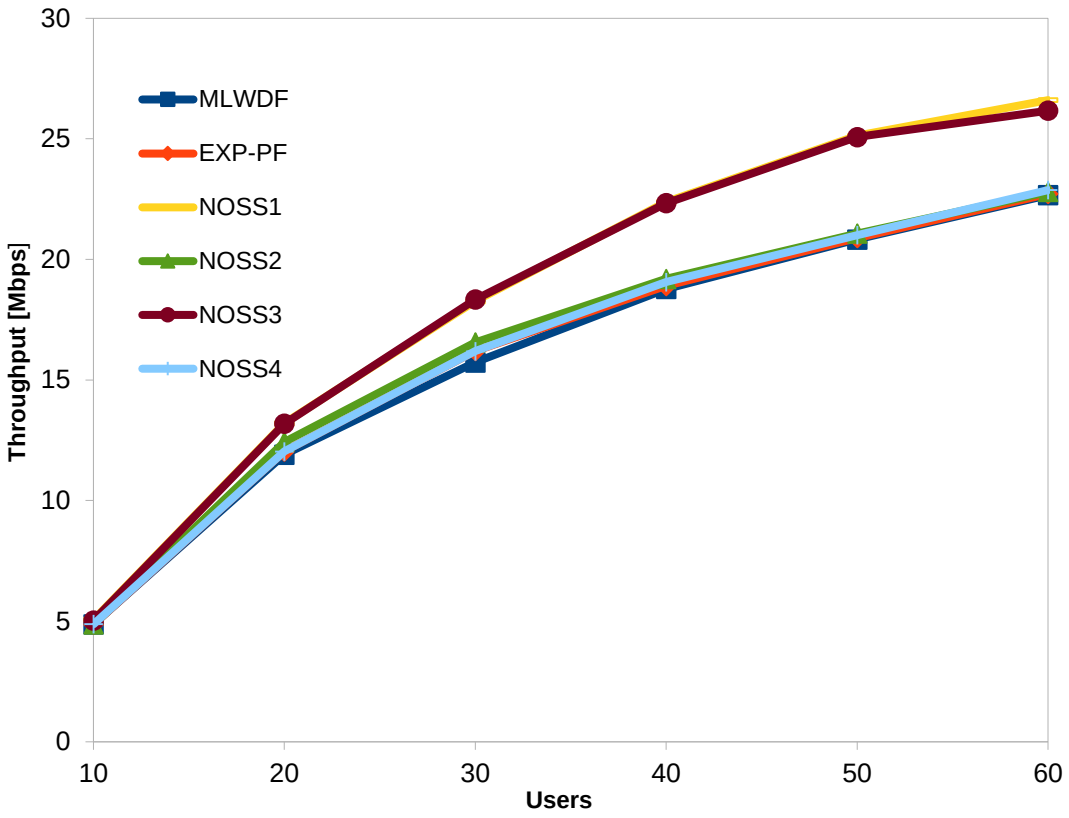

Figure 5-1: Throughput of video traffic users

The throughput performance of the proposed near optimal scheduling scheme (NOSS1 and NOSS3) is better than the other schedulers, as shown in Fig. 5-1 and this is more evident as the number of users increases. NOSS2 and NOSS4 produce very similar performance to the EXP-PF and MLWDF schedulers. While both NOSS2 and NOSS4 have an edge over MLWDF and EXP-PF schedulers in terms of throughput, this is very minimal and explains why it is so close, as shown in Fig. 5-1. This is due to the fact that NOSS1 and NOSS3 use the intantaneous data rate as the main objective function, while NOSS2 and NOSS4 use a data rate based on proportional fairness as used by MLWDF and EXP-PF in their respective algorithms.

As shown in Fig. 5-2, all the proposed near optimal scheduling schemes from NOSS1 to NOSS4 produce very similar delay performance; this is due to the fact they all use the same delay function in their respective algorithms. All the schedulers produce similar delay performance from users 10 to 40; however, from 40 users and above, the MLWDF and all the

NOSS schedulers produce better average delay performance than EXP-PF. This can be deduced from Fig. 5-2, as the EXP-PF delay performance linearly increases at a bigger slope. The MLWDF scheduler has a small edge over all the NOSS in terms of delay performance from 40 users and above. This is due to the fact that the M-LWDF and all the NOSS schedulers directly relate the waiting time to delay deadline in their respective algorithms either by finding the difference between the two for the case of all the NOSS schedulers or by dividing for the case of the MLWDF scheduler.

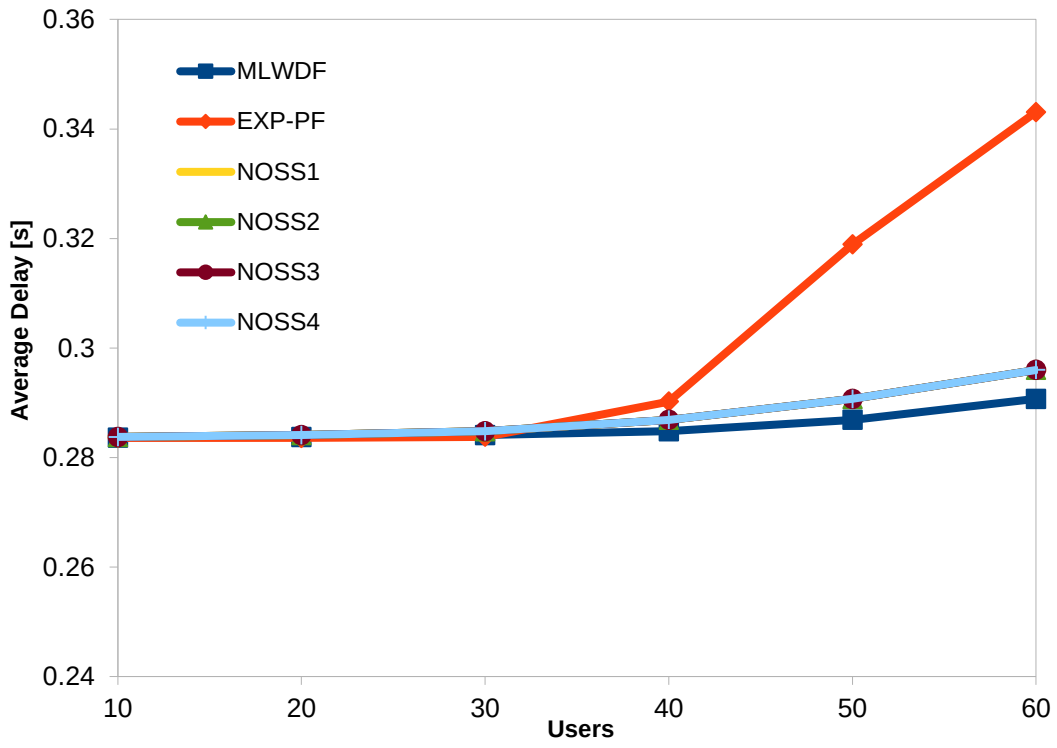

Figure 5-2: Average Delay of video traffic users

Jain fairness index is used to measure the fairness index and as shown in Fig. 5-3, the fairness index performance of all the schedulers is almost equal at users 10 and 20. However, as the number of users increases, the differences in fairness performance becomes evident. The fairness index of the MLWDF, EXP-PF and proposed NOSS schedulers (NOSS2 and NOSS4) is better than the other two proposed schedulers (NOSS1 and NOSS3). This is due to the fact that the four schedulers, MLWDF, EXP-PF, NOSS2 and NOSS4, use proportional fair function for their respective algorithms, while NOSS1 and NOSS3 uses the instantaneous data rate. It is worth noting that NOSS3 produces a better fairness index than NOSS1. This is due to the fact that the exponential function in NOSS3 helps reduce the effect of the instantenous data rate.

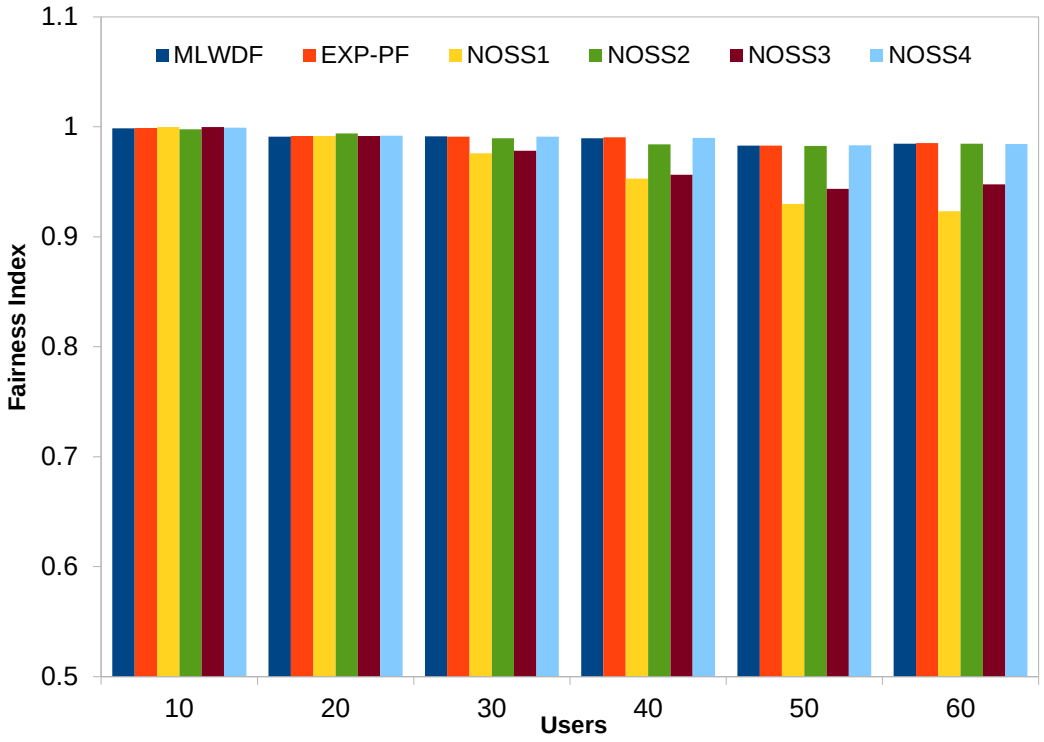

Figure 5-3: Fairness of video traffic users

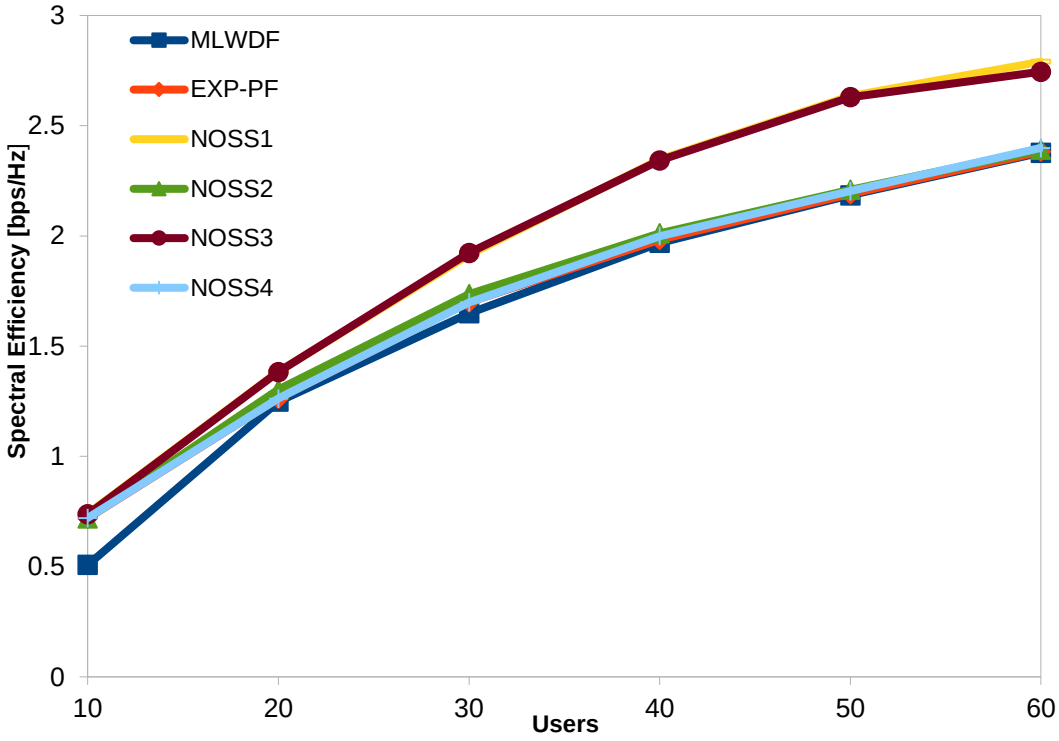

Figure 5-4: Spectral Efficiency

The spectral efficiency performance of the proposed schedulers NOSS1 and NOSS3 for RT only is better than the other schedulers and as shown in Fig. 5-4, the difference becomes more obvious as the number of users increases. This conforms with the trend in throughput performance. The NOSS2 and NOSS4 also produce similar spectral efficiency performance when compared with MLWDF and EXP-PF schedulers.

As presented in chapter 3, the SPM is also presented in this section in order to determine which of the schedulers has the best overall performance. The results of the SPM in Fig. 5-5 show that, overall, NOSS1 and NOSS3 outperform other scheduling schemes over all the number of users considered. This is due to the higher spectrall effficiency, lower delay and reasonable fairness perrformance of these two schedulers. Furthernore, the results show that the NOSS2 and NOSS4 scheduling schemes have a similar performance to M-LWDF with all users, while the EXP-PF scheduler's performance drops at a higher number of users (40 - 60). This drop in performance can be said to be due to the higher delay of the EXP-PF shown in Fig.5-2.

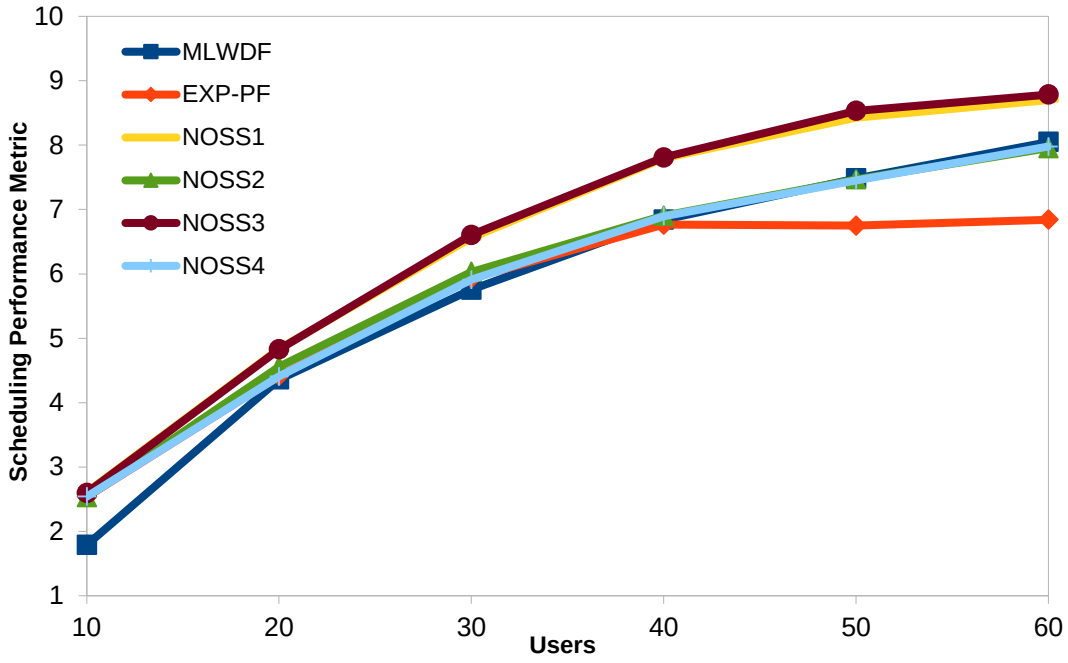

Figure 5-5: Scheduling Performance Metric

5.7.2 Mixed Traffic

A single spotbeam has been considered with users capable of video streaming and web surfing, uniformly distributed, within a serving eNodeB footprint. The channel and traffic models presented in the previous section are adopted for the simulations. Each set of users is made up

of 50% of web browsers and 50% of video streamers. Each user is assumed to be reporting its channel condition at certain intervals to the eNodeB.

As shown in Figs. 5-6 and 5-7, the throughput performance of two of the proposed schedulers, NOSS1 and NOSS3, is better than the other schedulers, for both RT (video streamers) and NRT (web browsers). This difference in performance becomes more evident as the number of users increases.At 60 users, both NOSS1 and NOSS3 exceed the other two schedulers by approximately 4 Mbps and 0.3 Mbps for RT and NRT traffic, respectively. This is as a result of the fact that both schedulers use the instantaneous data rate as the data rate or throughput function in their respective algorithms or solutions, compared with the other four scheduling alorithms which use proportional fairness.

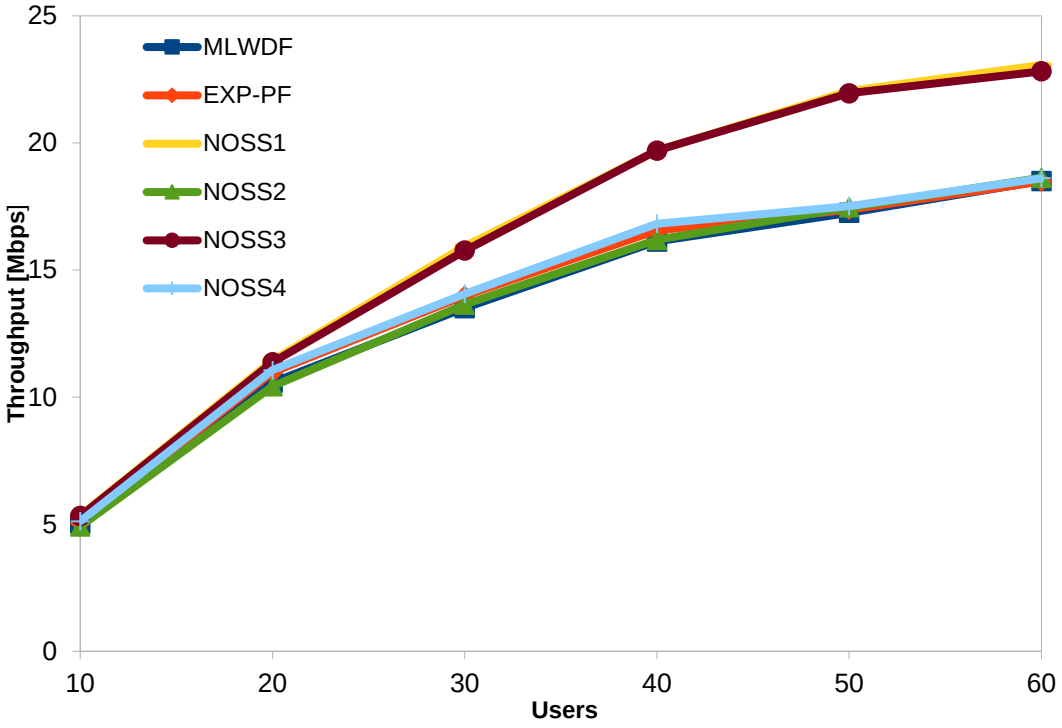

Figure 5-6: Throughput of video traffic users

Fig. 5.6 shows that NOSS2 and NOSS4 produce very similar performance to MLWDF and EXP-PF for RT traffic, since all four schedulers use proportional fairness representation in their algorithms. However, for NRT traffic, as shown in Fig. 5-7, NOSS2 and NOSS4 perform very similarly to the EXP-PF scheduler and these three schedulers perform better than the MLWDF schedulers, especially from 40 users and above. This is based on the fact that the delay function of the three schedulers' mainly exponential function gives more consideration to NRT traffic than the MLWDF scheduler. The maximum throughput achieved by the different schedulers varies depending on the channel condition or the instantaneous data rate of the user that is

selected at every TTI. If users with better channel conditions are selected, the throughput is higher than when users with poorer channel conditions are selected. This explains why NOSS1 and NOSS3 achieve superior throughput; it is due to the influence of the instantaneous data rate in their respective algorithms.

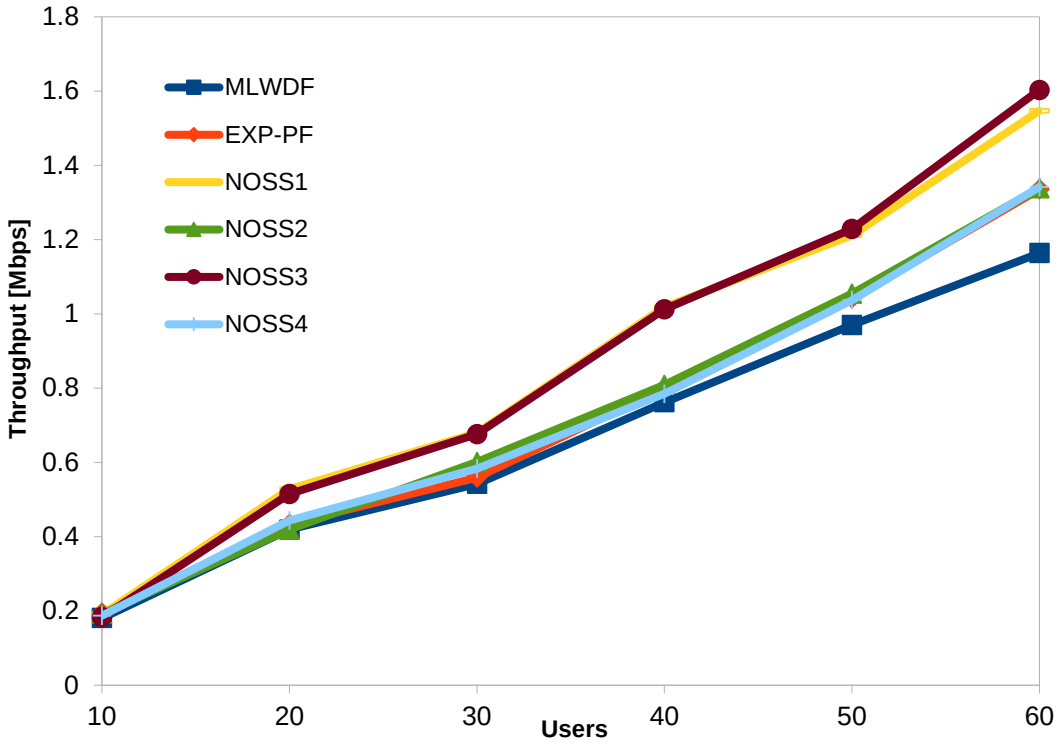

Figure 5-7: Throughput of web traffic users

The average delay performances shown in Figs. 5-8 and 5-9 reveal that both the proposed schedulers, NOSS1 to NOSS4 and M-LWDF schedulers produce better delay performance than the EXP-PF scheduler, for the RT traffic. The NOSS1 to NOSS4 schedulers show similar performance to the MLWDF scheduler. All of these schedulers, except for EXP-PF, are able to keep delay as low as possible even as the number of users increases. As explained above, these results show that the average delay performance for NOSS and M-LWDF schedulers are superior as a result of the fact that they not only consider the waiting time of HOL packets, but also directly relate it to the delay deadline in their respective algorithms.

All the proposed schedulers have very similar delay performance; this is because they all use the same delay or waiting time function in their respective algorithms. As shown in Fig 5-9, a similar trend is observed for the delay performnce of NRT traffic.

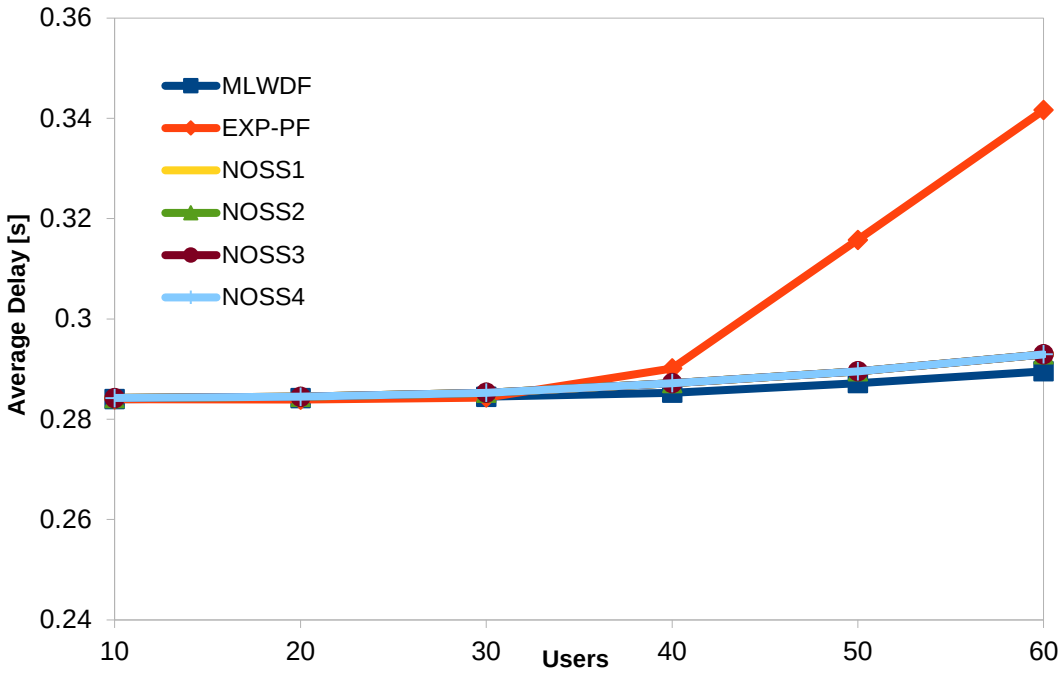

Figure 5-8: Average Delay of video traffic users

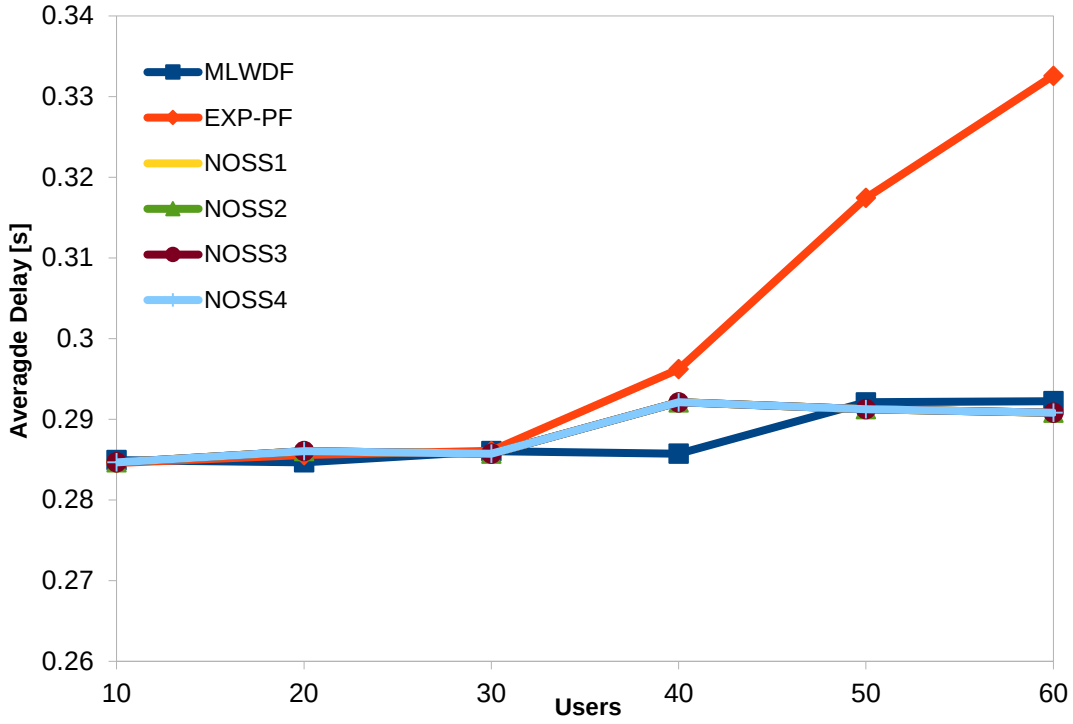

Figure 5-9: Average Delay of web traffic users

As shown in Fig. 5-10, two of the proposed schedulers (NOSS2 and NOSS4), M-LWDF and EXP-PF schedulers produce a better fairness index performances across all the different numbers of users than NOSS1 and NOSS3. The fairness index performances of NOSS2, NOSS4, MLWDF and EXP-PF are similar,with EXP-PF having a small edge at 10-30 users. It

is worth noting that the superior performance of these four schedulers is due to the fact that they use proportional fairness in their respective algorithms, while NOSS1 and NOSS3 only use the instantaneous data rate.

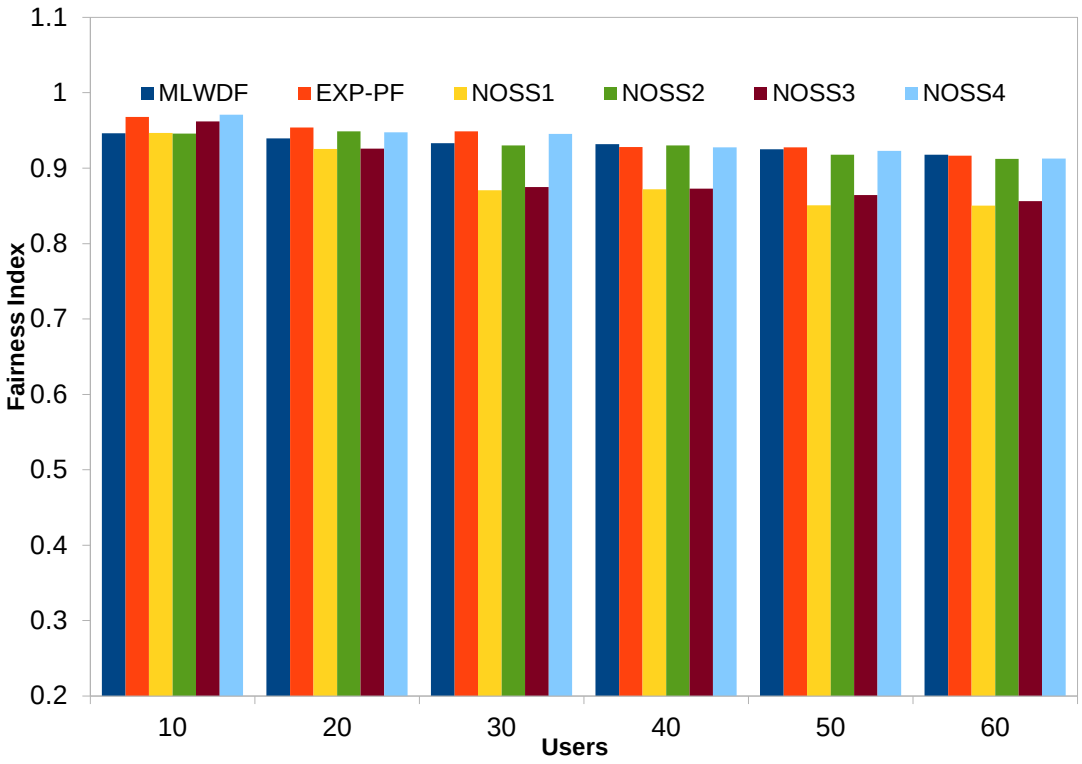

Figure 5-10: Fairness of all users

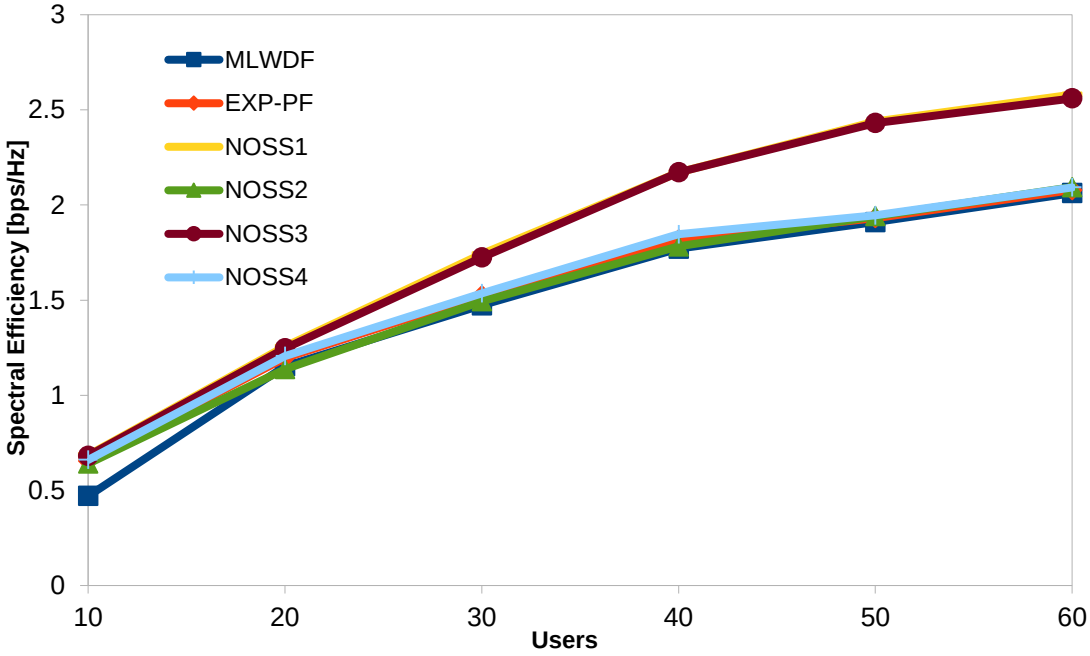

Figure 5-11: Spectral Efficiency of all users

Fig. 5-11 shows that the spectral efficiency performance of the proposed schedulers, NOSS1 and NOSS3, is better than that of the NOSS2, NOSS4, M-LWDF and EXP-PF schedulers. As the number of users increases, the difference in the spectral efficiency performance of NOSS1 and NOSS3, compared with the other four schedulers becomes more significant. Throughput performance follows the same trend. This shows that NOSS1 and NOSS3 utilize the spectrum better than the other four schedulers since they both use the instantaneous data rate.

The SPM results for the mixed traffic scenario are also computed and presented in order to determine the scheduling scheme with the best overall performance in a mixed traffic scenario. The NOSS1 and NOSS3 schedulers also produced the best overall performance. This becomes more evident as the number of users increases. The NOSS2, NOSS4 and MLWDF schedulers show similar SPM performance, with NOSS4 having a small edge. The EXP-PF's performance drops at a high number of users (40 – 60); the higher delays shown in Figs. 5-8 and 5-9 can be said to be responsible.

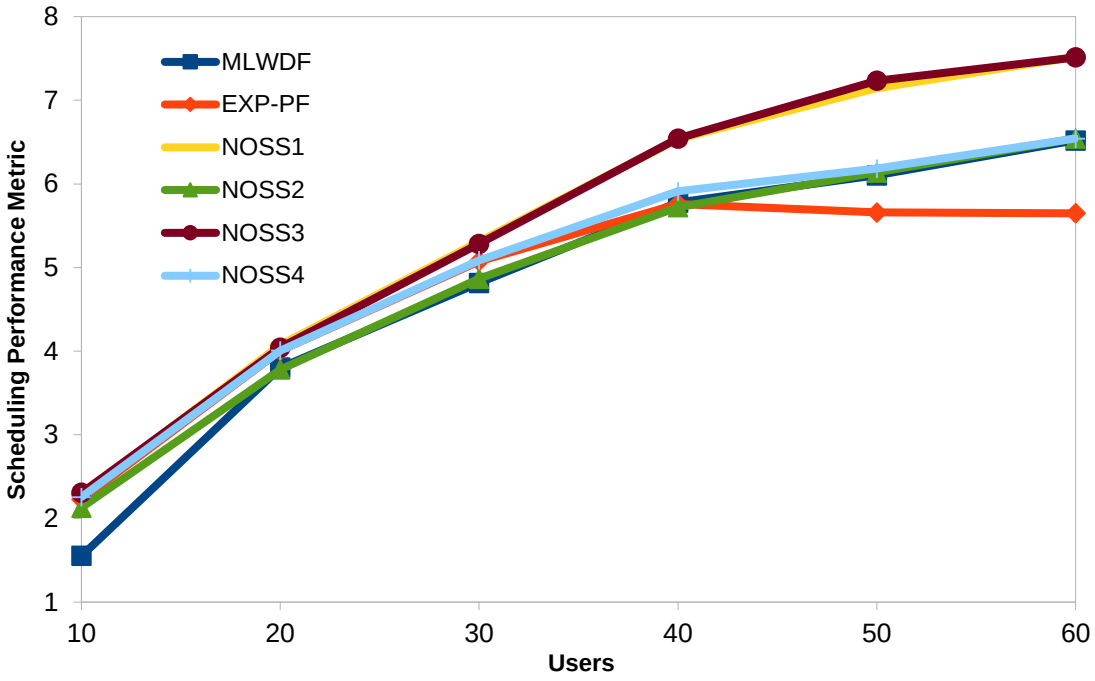

Figure 5-12: Scheduling Performance Metric

5.8 Conclusion

This chapter briefly reviewed related studies on scheduling schemes and presented a scheduling optimization problem. A near-optimal solution, using KKT multipliers, leading to proposed new scheduling schemes, called Near Optimal Scheduling Schemes (NOSS) for satellite LTE

networks was then presented. The simulation used to compare the proposed schedulers and two commonly-known throughput-optimal schedulers was also presented. Finally, the results obtained in terms of throughput, delay, spectral efficiency and the fairness index for RT only and mixed traffic scenarios from the simulation were presented.

The results show that the proposed schedulers, NOSS1 and NOSS3, provide the best throughput and spectral efficiency performance when compared with the other two throughput-optimal schedulers (MLWDF and EXP-PF) and both NOSS1 and NOSS3 have good delay performance that is similar to that of the M-LWDF scheduler and better than that of the EXP-PF scheduler. The M-LWDF and EXP-PF's fairness index performance is better than that of the proposed schedulers, NOSS1 and NOSS3. On the other hand, both NOSS2 and NOSS4 produce better delay performance than EXP-PF for all traffic and better throughput performance than MLWDF for NRT traffic. Furthermore, NOSS2 and NOSS4 produce similar performance to M-LWDF and EXP-PF in terms of throughput for RT traffic and fairness among users.

It should be noted that the proposed schedulers, NOSS1 and NOSS3, produce the best throughput and spectral efficiency performance, without significantly compromising the delay and fairness experienced by users; hence, these schedulers are able to provide an almost optimal network throughput, despite delay and fairness constraints. NOSS2 and NOSS4 therefore provide a good trade-off among throughput, QoS in terms of delay and fairness among users. It should also be noted that the proposed schedulers are able to handle both single and mixed traffic scenarios.

Overall, based on the SPM results computed and presented, NOSS1 and NOSS3 produce the best scheduling performance when compared with other schedulers (M-LWDF and EXP-PF) for both single and mixed traffic scenarios for all the numbers of users considered.

Chapter 6

STABILITY ANALYSIS OF SCHEDULING SCHEMES IN SATELLITE LTE NETWORKS

6.1 Introduction

This chapter presents an analysis of the stability of the proposed scheduler in a satellite LTE network. A review of stability analysis of wireless networks schedulers is presented. The analysis of the proposed scheduler is conducted using fluid limit technique by considering both the weak and strong fluid limit representations. The scheduler considered for the analysis is the proposed near-optimal scheduler in chapter 5. Finally, of interest in this chapter, is the characterization of maximum stability condition, not only for rate stability, but also for stochastic stability and the statement of such stability conditions. Thereafter, proof is presented of the conclusion that the proposed scheduling policy is stable under the maximum stability conditions.

6.2 Stability Analysis

Stability in networks ensures that the number of flows, or users, as the case may be, and their respective delays remain finite at flow-level. Although stability in practical systems is ascertained by the implementation of admission control, it remains a crucial indicator of how robust a scheduling scheme is, especially in networks whose load conditions are not predictable. Moreover, despite the fact that stability in practical systems is catered for, a network's instability can still lead to poor performance such as long delays [107].

Previous studies have been conducted on stability analysis for different schedulers. Some of these scheduling schemes are only channel-aware, while others are channel and queue-aware. The following section provides a brief review of some of these stability analyses.

6.2.1 M-LWDF

The stability analysis conducted for the M-LWDF scheduling scheme is similar to the stability results obtained for MaxWeight-type scheduling schemes in queuing networks. The main reason for this stability analysis is the fact that it minimizes the drift of Lyapunov function [108]. The stability analysis conducted for M-LWDF considers waiting time rather than queue length that is mainly considered in previous studies on MaxWeight-type scheduling schemes [109],[110] except for [111], where stability results considering waiting time or delay are derived. A fluid limit technique is used to analyse the stability of the M-LWDF scheduling scheme. It shows that M-LWDF keeps the queue stable provided that the vector of arrival rates is not in the system's maximum stability region, considering a variable channel.

A Static Service Split (SSS) scheduling rule has been considered as a much simplified version of M-LWDF which is parameterized by the matrix ϕ. When the server is in state *m*, the SSS rule chooses for user *k* with probability ϕ_{ki}. The stability conditions that are necessary and sufficient for any scheduling policy or rule to be stable are stated as follows [108];

$$A \leq R(\phi) \qquad \text{for some stochastic matrix } \phi \tag{6.1}$$

$$A < R(\phi) \qquad \text{for some stochastic matrix } \phi \tag{6.2}$$

The condition (6.1) is necessary while (6.2) is sufficient. Where $R(\phi)$ is the service rate and A is the arrival rate. Considering the M-LWDF scheduling rule to be expressed in a general form as;

$$L_k = argmax\left\{\frac{R_k^m(-log\delta_k)(W_k(t))^\beta}{T_k * T_{k,deadline}}\right\} \tag{6.3}$$

Where R_k^m is the service rate for user *k* at state *m*, $W_k(t)$ is the waiting time or delay of the HOL packet of user *k* at time *t*, β *and* δ_k are constants. The stability of the M-LWDF scheduling rule above is based on the following theorem [108];

Theorem 6.2.1.1: Let an arbitrary set of positive constants $\gamma_1, \gamma_2 \ldots \gamma_N$ and $\beta > 0$ be fixed. Then, the scheduling rules, M-LWDF is throughput optimal; namely, they make the system stable as long as condition (6.2) holds.

The theorem is proved using the fluid limit technique because it allows it to derive its stability from the stability of M-LWWF which is a MaxWeight-type scheduling rule since it uses queue length. The proof is simplified by assuming β is 1 and by replacing the Lyapunov function used for M-LWWF with a power law function. The details of the proof for this theorem, which confirms that the scheduling rule is still stable despite replacing the queue length with the waiting time, are presented in [108].

6.2.2 Exponential Rule

The stability analysis of the exponential rule (ER) scheduling policy follows the same approach as that of the M-LWDF scheduling policy. It considers ER-W (waiting time) and ER-Q (queue length). An assumption that only scheduling rule *H* such that Markov chain S, which is a discrete time countable Markov chain, is aperiodic and irreducible is made in this stability analysis. A scheduling rule *H* is defined to be universally stable if it makes a system stable, provided the stability of the system is feasible at all by any other scheduling rule [112]. The ER-W and ER-Q are stated as;

$$L_k = argmax\left\{\frac{R_k^m}{T_k} exp\left(\frac{a_k W_k(t) - \overline{aW(t)}}{\beta + \overline{W(t)}^{\eta}}\right)\right\} \tag{6.4}$$

$$L_k = argmax\left\{\frac{R_k^m}{T_k} exp\left(\frac{a_k Q_k(t) - \overline{aQ(t)}}{\beta + \overline{Q(t)}^{\eta}}\right)\right\} \tag{6.5}$$

Where R_k^m is the service rate for user *k* at state *m*, $W_k(t)$ is the waiting time or delay of user *k* at time *t*, β *and* a_k are positive constants and $\eta \in (0,1)$. The ER-Q is expressed in a similar form as shown in (6.5). The main theorem for the basis of the stability of the ER scheduling policy is stated as follows [112];

Theorem 6.2.2.1: An ER scheduling policy (either ER-W or ER-Q) with any fixed parameters of $\beta, \eta \in (0,1)$ and $a_k,\ k \in N$ is throughput optimal or stable.

The stability necessary and sufficient conditions are identical to those used for M-LWDF stability analysis. The fluid limit technique is also used for the proof and the detailed proof for the ER-Q is presented in [112] but that of ER-W is not presented.

6.2.3 Frequency Domain Scheduling Policy

There are very few previous studies on stability analysis of scheduling schemes. One of the few is the stability analysis for the not so popular Frequency Domain Scheduling Policy (FDSP)-based scheduler tagged Local Rule (L-R) scheduler, that is presented in [113]. The scheduler uses a local ratio technique which is quite different from M-LWDF and EXP-PF presented in sections 6.2.1 and 6.2.2, respectively but it also considers channel information and queue length. A Lyapunov drift method is used for stability analysis as used in [114]. The network considered is the LTE uplink network scenario. This assumes network stability and the sufficient conditions for stability as presented in [109],[110] and stated as follows;

A system is stable if, for the queue length process *y,* we have;

$$P(\tau_y < \infty) = 1 \qquad \forall\ y \in T \tag{6.6}$$

Where τ_y is the recurrent time, *T* belongs to all states that do not belong to any closed set of communicating states and all states $y \in \cup_{k=1}^{\infty} R_k$ are positive recurrent. The theorem below is stated as the sufficient conditions for stability [113];

Theorem 6.2.3.1: Consider a Markov Chain *M (t)* with a subspace $\mathcal{M}$, where *M (t)* represents the Markov state of server (that will serve the user) at time *t*. If there exists a lower bounded real function $V: \mathcal{M} \rightarrow \mathbb{R}$, $\emptyset > 0$ and a finite subset $\mathcal{M}_0$ of $\mathcal{M}$, such that;

$$E\left[V(\mathcal{M}(t+1)) - V(\mathcal{M}(t))|\mathcal{M}(t) = y\right] \leq -\emptyset \qquad \text{If } y \notin \mathcal{M}_0 \tag{6.7}$$

$$E[V(\mathcal{M}(t+1)))|\mathcal{M}(t) = y] \leq \infty \qquad \text{If } y \in \mathcal{M}_0 \tag{6.8}$$

Then the above definition applies for stability under this condition. The theorem to prove the stability of the L-R scheduler is proven using the drift Lyapunov analysis. On the assumption that the service rates,R_k, queue sizes of each user *k* and the arrival process, *A*, are bounded, the following theorem must hold [113];

Theorem 6.2.3.2: The L-R scheduling policy is stable for any (ω_0, ϵ_0)-admissible LTE uplink system as long as $\forall k$, the user rate $R_k(t)$ cannot be zero for arbitrarily long periods.

The ω_0 and ϵ_0 are parameters that are determined in the analysis. The details of the proof for the above theorem are provided in [113].

6.2.4 Priority Based Scheduling Policy

The stability analysis of channel-aware priority based schedulers is conducted in [115]. Both priority based schedulers and priority based schedulers with tie breaking rule are considered. A cellular downlink system with a base station that has different flow sizes which are independent and identically distributed has been considered for the analysis. Different scheduling policies that are priority based and utility based, which include PF and Potential Delay Minimization (PDM) schedulers, are presented. The necessary condition for stability as presented in [107] for all these channel-aware schedulers is stated as follows;

$$\rho = \frac{A^*}{R} \leq 1 \tag{6.9}$$

Where $$\frac{A^*}{R} = \left(\frac{A}{R}\right)^*_1 + \left(\frac{A}{R}\right)^*_2 + \cdots \left(\frac{A}{R}\right)^*_K \tag{6.10}$$

Where, ρ is the traffic load, A is the arrival rate, R is the service rate and K is the number of users. This condition has also been proven to be sufficient for utility based schedulers like the PF scheduler [116]. This set of scheduling policies is said to be stable based on the following theorems [115];

Theorem 6.2.4.1: Consider a rate-based priority scheduling policy, π. If $\left(\frac{A}{R}\right)^*_K > \left(\frac{A}{R}\right)^{**}_l$ for all k≠ l, then policy π is stable under condition (6.9).

Theorem 6.2.4.2: Consider a rate-based priority scheduling policy π that break ties within any priority class at random. If $\left(\frac{A}{R}\right)^*_K > \left(\frac{A}{R}\right)^{**}_l$ for all $k \neq l$, then policy π is stable under condition (6.9).

Based on the above theorem 1, these four deductions are made [115];

Corollary 1: Any proportional rate priority policy (including Proportionally Best) is stable under condition (6.9).

Corollary 2: Any Cumulative Distribution Function (CDF) based priority policy (including CDF Scheduler) is stable under condition (6.9).

Corollary 3: If $R^*_K = R_J$ for all user classes *k*, then any absolute rate priority policy (including Maximum Rate) is stable under condition (6.9).

Corollary 4: If $R^*_K/R'_k > R^{**}_l/R'_l$ for all $k \neq l$, then any relative rate priority policy (including Rate Based) is stable under condition (6.9).

Where, R is the possible service or channel rate and R' is the average service rate. The proof

and explanation behind these theorems is provided in [115].

6.2.5 Reservation Based Scheduling Policy

The Reservation Based Distributed Scheduling (RBDS) policy is designed for mesh wireless networks and is therefore quite different from M-LWDF and EXP-PF scheduling policies. It has not been presented in any previous chapters but is one of the few previous studies on stability analysis of scheduling policy in wireless networks. The analysis to test for stability of Reservation Based Distributed Scheduling (RBDS) policy is presented in [117]. This scheduling policy is based on negotiating with the neighbouring nodes in order to secure or reserve time slots for transmission purposes. An RBDS network is assumed for the purpose of this analysis which follows the 2-hop interference model also adopted by the IEEE 802.16 mesh mode standard. Each link is assumed to have an input queue and output queue. The input queue is the number of packets in the queue, while the output queue is the number of scheduled packets in the queue. The RBDS wireless network *G* is represented by a Markovian system S^G. The arrival rate, *A,* and the departure rate, *D,* which correspond to the input queue and output queue are expressed as follows [117];

$$A'^{(i,j)}(m) \triangleq \begin{cases} \sum_{l=0}^{m_{ds}-1} A^{(i,j)}(k_m - l) & m = multiple\ of\ m_{cs} \\ 0 & otherwise \end{cases} \tag{6.11}$$

$$D'(m) \triangleq \begin{cases} 1 & m = multiple\ of\ m_{cs} \\ 0 & otherwise \end{cases} \tag{6.12}$$

$A'^{(i,j)}(m)$ and $D'(m)$ are the arrival rate at time slot *m* for link (*i, j*) and the departure rate at time slot *m* respectively. k_m is the last time slot of a sub-frame. The m_{ds} and m_{cs} are the number of data timeslots and control timeslots, respectively. The following definitions form the basis on which the theorem used for the stability analysis for the scheduler is conducted.

Definition 6.2.5.1: Wireless network *G* is stable if the queue process *Q* in S^G is positive recurrent.

Definition 6.2.5.2: An RBDS wireless network is stationary if the random processes $N_{\mu_1}^{j}$,$\left|H^j(n)\right|$, $\left|G^{(i,j)}(n)\right|$ are stationary for all *j* in *N* and all (i,j) in *L*.

Where $H^j(n)$ is the set of data-subframes covered by the grants that node *j* listens to between its *n th* and (*n*+1) *th* scheduling-packet transmissions, $\left|H^j(n)\right|$ is the number of frames covered by $H^j(n)$, $N_{\mu_1}^j$ is the number of events between node *j*'s *n th* and (*n*+1) *th* scheduling packet transmissions and μ_1 is the event that the subframe starts. The theorem on which the stability test for the RBDS scheduler is based can be stated as follows [117];

Theorem 6.2.5.1: The output-queues in a stationary RBDS wireless network are stable if (6.13) holds, and the input-queues are stable if (6.14) holds. Therefore, an RBDS wireless network is stable if both (6.13) and (6.14) hold.

$$\max_{j \in N} \left(\overline{H^J} - \overline{N_{\mu_1}^J} \right) < 0 \qquad (6.13)$$

$$\max_{j \in N} \left(\overline{N_{\mu_1}^J} \sum_{i \in S^j} A^{(i,j)} - \sum_{i \in S^j} \overline{\left| G^{(i,j)} \right|} \right) < 0 \qquad (6.14)$$

Where, $A^{(i,j)}$ is the arrival rate of link (i,j) and S^j is the 1-hop neighbour of node *j*. The proof of the theorem is based on the proof presented in [118] and the details of the proof of this theorem are presented in [117]. The conditions (6.13) and (6.14) help guarantee stability since they ensure that all the queues decrease their lengths at a rate lower than they increase their lengths.

The stability analysis of the proposed scheduler in chapter 5 is presented in the following sections in the current chapter.

6.3 Model description

The stability analysis of the proposed scheduler which closely follows the work in [119] commences by describing the network considered for the analysis. A time-slotted system that serves one user in each time slot for each subchannel in a satellite LTE network is considered. There are *k* users and for each time slot, the arrival rate A_k of the number of *k* users follows an independent and identically distributed (i.i.d) sequence of random variables in the system Q_k. Where, Q_k is the arrival process system for which user *k* is waiting to be served. Hence,

$$\boldsymbol{E}(Q_k) = A_k \qquad (6.15)$$

$$E\left(Q_k^2\right) < \infty \qquad (6.16)$$

The departure probability for each user varies with time, depending on the channel quality (CQI) at every time slot. The channel quality for a user is also modelled as an i.i.d sequence of random variables which falls within a finite set of values $C_k := \{1,2, \ldots\ldots, c_k\}$. For example, for the satellite LTE network scenario, c_k is 15 (possible number of channel states according to LTE standard). Hence, the channel condition of user *k* is assumed to be independent of other users and of its previous channel conditions.

At each time slot, it is assumed that $P_{k,c}$ represents the probability that a user *k* is in channel state $c \in C_k$ and the corresponding departure probability of channel state c is $\mu_{k,c}(R_{k,c})$ which is a function of $R_{k,c}$, where $R_{k,c}$ is the data rate of user *k* at channel state *c*. It is also assumed that the channel conditions for user *k* are arranged in an order such that

$$0 \leq \mu_{k,1}(R_{k,1}) \leq \mu_{k,2}(R_{k,2}), \leq \cdots . \leq \mu_{k,C_k}(R_{k,C_k}) \leq 1 \qquad (6.17)$$

And that

$$P_{k,C_k}\mu_{k,C_k}(R_{k,C_k}) \neq 0 \quad \forall\, k \qquad (6.18)$$

In each time slot *t*, the proposed scheduling policy,L_k, makes decisions on which user should be served. Due to the Markov property of the system, the scheduler decides on the basis of the number of users present, their present channel conditions and the waiting time (W_k) of the user, which is a function of the arrival rate A_k.

For every time slot *t* and considering the proposed scheduling policy, L_k, let $X_k^{L_k}(t)$ represents the *K* users waiting to be scheduled by scheduling policy L_k at time slot *t* and $X^{L_k}(t) = \left[X_1^{L_k}(t), \ldots\ldots\ldots\ldots X_k^{L_k}(t)\right]$. Since the channel conditions are i.i.d and independent of the process $X^{L_k}(.)$, the process X^{L_k} is Markov. Based on this, it is sufficient to concentrate on the Markovian description in terms of the number of users in each class $X^{L_k}(t)$ instead of the number of users in each channel level. Also, let $|x|$ represent the *l* norm of a vector *x* and the notation $x \leq y$ is considered as element-wise ordering;

$$x_i \leq y_{i,} \; \forall\, i \qquad (6.19)$$

And that uniform convergence on compact sets is represented by u.o.c.

Definition 6.3.1: A scheduling policy L_k is stable if the process X^{L_k} is positive recurrent [117], [119].

Due to the fact that the channel condition varies, the system is not work-conserving; hence, the network mainly depends on the scheduling policy to determine if the system is stable.

Maximum stability conditions can be defined as conditions on the traffic inputs, in which a scheduling policy that can make the system stable exists and maximum stable policy is a scheduling policy that ensures stability under the maximum stability conditions.

Remark 1: For the purpose of modelling, it is assumed that the channel state variation is independent across different users for subsequent fluid limit analysis.

Remark 2: A time-slotted system that serves one user in each time slot for each subchannel and a channel state that varies (using AMC) for different users are considered. This simple model takes care of the major characteristics of the satellite LTE network.

6.4 Scheduling Policy

The proposed scheduling policy uses the concept of Priority Index (PI) by serving the user with the highest PI; this is a utility based scheduling policy. The PI is computed at every time slot (*t*) based on channel quality, R_{k,C_k}, and waiting time, W_k, which is a function of A_k, both of which are assumed to be i.i.d. It is worth noting that the PI based scheduling policy is grouped into the class of policies known as Best Rate (BR) as stated in [119]. The scheduling policy can be expressed as follows;

$$L_k = argmax \left\{ R_{k,C_k} + \frac{R_k\left[W_k\beta_k m^2 R_{k,C_k} - \Delta(m^2+\gamma)\right]}{2\left[\beta_k m^2\left(1+R_{k,C_k}W_k\right)+\gamma\Delta\right]} \right\} \qquad (6.20)$$

Where R_k is the average data rate for user *k* and β_k is the delay deadline for user *k*.

6.5 Fluid Limit Technique

The fluid technique stability method, which is one of the important methods in determining the stability of a network, as described in [120], has been adopted for this study. In order to determine the stability results, the limits of the fluid-scaled process need to be characterized. This includes the weak and strong fluid limits. Of interest to us is the fluid-scaled process, which is expressed as;

$$Y_k^{L_k,r}(t) = \frac{X_k^{L_k,r}(\lfloor rt \rfloor)}{r} \quad t \geq 0; \quad k = 1, \ldots\ldots\ldots K; \quad Y^r(0) = x(0) \quad (6.21)$$

$$Y_k^{L_k,r}(t) = x_k(0) + \frac{1}{r}\sum_{s=1}^{\lfloor rt \rfloor} Q_k(s) - \frac{1}{r}\sum_{c=1}^{C_k} S_{k,c}\left(T_{k,c}^{L_k,r}(rt)\right) \qquad (6.22)$$

Where $T_{k,c}^{L_k,r}(t)$ is the time spent on serving user *k* at channel state *c* during [0, t] interval under a scheduling policy, L_k, *r* is the sequence of the systems and $S_{k,c}$ is the total number of *K* users that have completed transmission in channel state *c*.

6.5.1 Convergence towards weak fluid limits

The following result is obtained from (6.22), which explains the default characterization of weak fluid limits for a given policy L_k. This proposition will allow the maximum stable policy to be determined.

Proposition 6.5.1.1: For almost all sample paths ω and any sequence r_{k_l} such that for all $k = 1,2,3,\ldots\ldots,K, c = 1,2,3,\ldots\ldots\ldots,C_k$ and $t \geq 0$.

$$\lim_{l\to\infty} Y_k^{L_k,r_{k_l}}(t) = y_k^{L_k}(t), \qquad \text{u.o.c.}$$

$$\lim_{l\to\infty} \frac{T_{k,c}^{L_k,r_{k_l}}(t)}{r_{k_l}} = \tau_{k,c}^{L_k}(t), \qquad \text{u.o.c.} \qquad (6.23)$$

with $(y_k^{L_k}(.), \tau_{k,c}^{L_k}(.))$ as continuous function. So, we have;

$$y_k^{L_k}(t) = x_k(0) + A_k t - \sum_{c=1}^{C_k} \mu_{k,c}(R_{k,c})\, \tau_{k,c}^{L_k}(t) \qquad (6.24)$$

$y_k^{L_k}(t) \geq 0, \tau_{k,c}^{L_k}(t) = 0, \sum_{k,c} \tau_{k,c}^{L_k}(t) \leq t,$ and $\tau_{k,c}^{L_k}(.)$ are non-decreasing and Lipschitz functions.

Proof: Using the law of large numbers, the following is almost surely obtained;

$$\lim_{r\to\infty} \frac{1}{r}\sum_{s=1}^{\lfloor rt \rfloor} Q_k(s) = A_k t, \qquad \lim_{r\to\infty} \frac{1}{r} S_{k,c}(rt) = \mu_{k,c}(R_{k,c})t \qquad (6.25)$$

Substituting (6.25) in (6.22), one can deduce that $\lim_{l\to\infty} Y_k^{L_k,r_{k_l}}(t) = y_k^{L_k}(t)$, as presented in (6.24). This confirms proposition 6.5.1.1. Details of this proof are provided in [119].

Definition 6.5.1.1: The processes $y^{L_k}(t)$ and $\tau^{L_k}(t)$ are the weak fluid limits for policyL_k.

The expressions in (6.23) to (6.25) are used in the stability proof presented later in this chapter.

6.5.2 Convergence towards strong fluid limit

The derivation of the strong limit provides an avenue to determine the exact stability conditions. In order to obtain an accurate fluid limit characterization, averaged drifts need to be used in the description of the fluid limit. This is important as a user may reach its stationary point while other users have yet to do so. Hence, it is necessary to average the drift of all users. Details of the drift functions; drift vector fields and average drift vector are provided in [119].

The description of the strong fluid limit is stated below;

For a given policy *L* inducing a partially increasing drift vector field with uniform limits,

$$\lim_{r\to\infty} P\left(\sup_{0\le s\le t} |Y^{L_k,r}(s) - y^{L_k}(s)| \ge \epsilon\right) = 0 \qquad \text{for all } \epsilon > 0 \qquad (6.26)$$

Hence, the process $y^{L_k}(t)$ as obtained above is the strong fluid limit for the scheduling policy L_k. Details of the proof for the above, strong fluid limit description are in [119], since it is not of much relevance to this analysis.

6.6 Stability Tests

The weak fluid limit presented above provided the premise to prove and make conclusions on the stability of the proposed scheduling policy.

In the following theorem, the maximum stability condition is stated and proof that the scheduling policy achieves maximum stability under this condition is presented. The proof presented is based on the weak fluid limit characterization.

As generally recognized in [115],[119],[121], the maximum stability condition is stated as follows;

$$\sum_{k=1}^{K} \frac{A_k}{\mu_{k,C_k}(R_{k,c})} < 1 \qquad (6.27)$$

In order to prove that the proposed scheduling policy, which falls under BR or PI, or utility based policy as described in [119], is maximum stable, (6.27) is a necessary condition that must be fulfilled. In order to achieve this proof, the following have to be proven;

- That under the proposed policy or any other BR related policy, the set of sample paths, where a user that is not certainly in its best state is served, is asymptotically empty.

- That the fluid limit will be equal to zero, almost certainly for time *T*, large enough under necessary stability conditions.

Throughout the following proof, it is assumed that condition (6.27) holds. Let T , which is the time spent before the system is emptied, be the ratio of the total work in the system, at time 0 to 1 minus the workload, be defined as follows;

$$T = \frac{\sum_{k=1}^{K} \frac{y_k^U(0)}{\mu_{k,C_k}}}{\left(1 - \sum_{k=1}^{K} \frac{A_k}{\mu_{k,C_k}}\right)} < \infty \qquad (6.28)$$

And the random variable $T_\epsilon^r = inf\left\{t: \sum_{k=1}^{K} \frac{y_k^{L_k}(t)}{\mu_{k,C_k}} \leq \epsilon\right\}$ for $0 < \epsilon < 1$ (6.29)

Let $\overline{T_\epsilon^r} = min\{T_\epsilon^r, T\}$ and considering event E_r which occurs if at least one user has been served while not in its best PI or utility or channel state between the time interval of $\left[0, \lfloor r\overline{T_\epsilon^r} \rfloor\right]$.

Since the proposed scheduling policy will only serve the user with best PI or utility, it follows that;

$$P(E_r) = 1 - \prod_{s=0}^{\lfloor r\overline{T_\epsilon^r} \rfloor} \left[1 - \prod_{k=1}^{K} \left(1 - p_{k,C_k}\right)^{rY_k\left(\frac{s}{r}\right)}\right] \qquad (6.30)$$

Since, $\overline{T_\epsilon^r} \leq T$ and using basic algebra, one can test that there exists a constant $\xi \in [0,1]$ such that;

$$P(E_r) \leq 1 - (1 - \xi)\hat{}rT =: g(r) \qquad (6.31)$$

Then, the next step is to show that;

$$P\left(\bigcap_{r=1}^{\infty} \bigcup_{\tilde{r}=r}^{\infty} E_{\tilde{r}}\right) = 0 \qquad (6.32)$$

Since $\log(1 + x) = x + o(x)$ when x is close to 0, then $(1 - \xi)^{rT} = e^{-rT\xi^r + o(r\xi^r)}$ is obtained for all large values of r. Using Taylor's expansions and the fact that $\sum_{r=1}^{\infty} r\xi^r < \infty$, it follows that;

$$\sum_{r=1}^{\infty} g(r) = \sum_{r=1}^{\infty} (1 - (1 - \xi)^{rT}) = \sum_{r=1}^{\infty} (1 - e^{-rT\xi^r + o(r\xi^r)}) < \infty \qquad (6.33)$$

Hence, using Borel-Cantelli's proposition in [122], (6.32) is obtained.

To prove the next point that the weak fluid limit is almost surely equal to zero at time *T*. From (6.32), an event E_r^c almost surely occurs when *r* is large enough. Hence, only users with the best priority index or utility or channel state are served within the time interval $\left[0, r\overline{T_\epsilon^r}\right]$ when *r* is large enough i.e. $T_{k,c}^{L_k,r}(t) = 0$, for $c \neq C_k$ and $t \leq r\overline{T_\epsilon^r}$, for *r* is large enough.

Hence, for almost all sample paths ω, it holds that; $\sum_{k=1}^{K} \tau_{k,C_k}^{L_k}(t) = t$ and $\tau_{k,c}^{L_k}(t) = 0$ for all $c \neq C_k$, $t \leq \lim inf_{r\to\infty} \overline{T_\epsilon^r}$ in the weak fluid limit representation in proposition 6.5.1.1.

Thus, for $t \leq \lim inf_{r\to\infty} \overline{T_\epsilon^r}$, any weak fluid limit $y^{L_k}(.)$ satisfies the following;

$$\sum_{k=1}^{K} \frac{y_k^{L_k}(t)}{\mu_{k,C_k}(R_{k,C_k})} = \sum_{k=1}^{K} \frac{x_k(0)}{\mu_{k,C_k}(R_{k,C_k})} + \sum_{k=1}^{K} \frac{A_k}{\mu_{k,C_k}(R_{k,C_k})} t - \sum_{k=1}^{K} \tau_{k,C_k}^{L_k}(t) \quad (6.34)$$

Since, $\sum_{k=1}^{K} \tau_{k,C_k}^{L_k}(t) = t$, substituting this in (6.34)

$$\sum_{k=1}^{K} \frac{y_k^{L_k}(t)}{\mu_{k,C_k}(R_{k,C_k})} = \sum_{k=1}^{K} \frac{x_k(0)}{\mu_{k,C_k}(R_{k,C_k})} + \sum_{k=1}^{K} \frac{A_k}{\mu_{k,C_k}(R_{k,C_k})} t - t \quad (6.35)$$

$$\sum_{k=1}^{K} \frac{y_k^{L_k}(t)}{\mu_{k,C_k}(R_{k,C_k})} = \sum_{k=1}^{K} \frac{x_k(0)}{\mu_{k,C_k}(R_{k,C_k})} - \left(1 - \sum_{k=1}^{K} \frac{A_k}{\mu_{k,C_k}(R_{k,C_k})}\right) t \quad (6.36)$$

Let $T_\epsilon < \infty$ represents the moment at which $\sum_{k=1}^{K} \frac{y_k^{L_k}(t)}{\mu_{k,C_k}} = \epsilon$ and let r_k be the subsequence corresponding to $\lim inf_{r\to\infty} \overline{T_\epsilon^r}$ for a particular sample path ω.

Using the proposition 6.5.1.1, it is known that there exists a subsequence r_{k_l} of r_k such that;

$$\left| \sum_k \frac{y^{L_k}\left(\overline{T}_\epsilon^{r_{k_l}}\right)}{\mu_{k,C_k}(R_{k,C_k})} - \sum_k \frac{y^{L_k,r_{k_l}}\left(\overline{T}_\epsilon^{r_{k_l}}\right)}{\mu_{k,C_k}(R_{k,C_k})} \right| \leq \epsilon' \quad \text{for } \epsilon' > 0 \text{ and } l \text{ large enough.} \quad (6.37)$$

Hence, if $\overline{T}_\epsilon^{r_{k_l}} \leq T_\epsilon$, then;

$$T_\epsilon - \overline{T}_\epsilon^{r_{k_l}} \leq \frac{\epsilon'}{\sum \frac{A_k}{\mu_{k,C_k}(R_{k,C_k})}}$$

$$\overline{T}_\epsilon^{r_{k_l}} \geq T_\epsilon - \frac{\epsilon'}{\sum \frac{A_k}{\mu_{k,C_k}(R_{k,C_k})}} \quad (6.38)$$

And since $lim_{\epsilon' \downarrow 0} \liminf_{r \to \infty} \overline{T_\epsilon^r} \geq T_\epsilon$, then (6.36) holds for all $t \leq T_\epsilon$. Let $\epsilon \to 0$ and $T_\epsilon \to T$, hence (6.36) holds for all $t \leq T$ and in specific $|y^{L_k}(T)| = 0$. Therefore, it can be concluded that for almost all sample paths, any weak fluid limit converges to 0 at time *T*. Hence, it can also be concluded that almost surely $\lim_{r \to \infty} Y_m^{L_k,r}(T) = y_m^{L_k}(T) = 0$.

6.7 Conclusion

This chapter presented a review of the stability analysis of different groups of scheduling policies. This was followed by the system under which the proposed scheduling policy is analysed for stability and the definitions and theorems that form the basis of the stability test. The scheduling policy was presented, as well as the stability test of the proposed scheduler and its proof.

From the stability analysis conducted using fluid limit technique, it is shown that the proposed scheduler, called NOSS, that has the capability to support both single and multiple traffic classes (RT and NRT) scenarios, is stable under the maximum stability conditions.

Chapter 7

SUBCHANNEL ALLOCATION SCHEME IN SATELLITE LTE NETWORKS

7.1 Introduction

This chapter presents a cross-layer based subchannel allocation scheme for Satellite LTE networks, with the aim of maximizing total network utility without compromising users' QoS demands and the fairness experienced by users. In some scenarios in both satellite and terrestrial LTE networks, the scheduler performs user scheduling without mapping it to a specific subchannel. In a scenario of this nature, which is quite different from the scenarios presented in previous chapters, there is a need for an effective subchannel allocation or mapping scheme that will allocate or map the scheduled users to the available subchannels. It is on this basis that a new subchannel allocation scheme is proposed that is used to map the users selected by the scheduling scheme to the available subchannels, in order to further improve the throughput of the satellite LTE network without compromising an acceptable QoS and the level of fairness experienced by the user. In order to evaluate the performance of the proposed subchannel allocation scheme, a simulation setup that compares the default scheme in Satellite LTE networks with the proposed subchannel allocation scheme and the simulation results are presented. The throughput performance, spectral efficiency and the fairness for the two schemes considered are also presented.

The chapter commences with a review of previous studies on subchannel allocation/assignment schemes; this is followed by the assignment/allocation problem formulation. A heuristic solution to the subchannel assignment/allocation problem is then presented. The other subchannel allocation scheme considered in this work is presented, as well as the simulation

setup. Finally, the simulation results, including throughput, spectral efficiency and fairness are presented and discussed.

7.2 Related Studies

The subchannel allocation scheme is an important element not only of the satellite LTE network, but every LTE network as a whole. In order to achieve the high throughput targets set for the 4G standard, it is crucial to be able to effectively assign the users selected by the scheduling scheme to the available subchannels, with the aim of improving the network throughput. Hence, the subchannel allocation scheme is designed to complement the scheduling scheme in the network in order to achieve high network throughput. It is also important that this is achieved without compromising the set QoS targets and fairness perceived by users. In order to design an effective subchannel allocation scheme, several previous studies have modelled the problem of assigning users to available subchannels or allocating subchannels to users as an assignment problem and proposed different exact or heuristic solutions as a subchannel allocation or assignment scheme for the network. Several schemes have been proposed for terrestrial LTE or OFDMA based or MIMO based networks in the literature. In [123], an optimal solution called Hungarian method is used as an assignment problem solution; however, the major issue is that this solution is limited to a scenario where the number of users is equal to the number of channels. In [124], an exact solution called the Kuhn-Munkres algorithm is proposed, and near-optimal solutions called Max Loss Delete (MLD), Max Deviation Delete (MDD) and Max Difference Top Two (MDTT) are proposed, respectively, in [125]–[127]. However, the major challenge for all these solutions is also that the solutions are limited to scenarios where the number of users is equal to the number of channels or antennas. While [128],[129] proposed a heuristic solution based on the auction algorithm which is applicable to the network considered, only data rate is used and other QoS factors are not considered. It is worth noting that exact solutions are only applicable to scenarios where the number of users is equal to the number of subchannels and antenna; hence, for the network considered, where the number of subchannels may not be equal to the number of selected users and the number of subchannels can sometimes be more than the selected number of users, only heuristic solutions are applicable. It is also worth noting that these solutions have been proposed for terrestrial networks; to the best of our knowledge, no solutions have been proposed for satellite LTE networks. It is against this background that this chapter proposes a new subchannel allocation scheme that is derived using heuristic solutions with the aim of maximizing the utility of the satellite LTE network.

7.3 Problem Formulation

The subchannel allocation problem has been formulated as an assignment problem, a constraint optimization problem with the aim of maximizing the total utility function. The assignment problem solution is to map a user from a group of users that has been selected by a scheduling scheme to a particular subchannel from the available sub-channels with the above objective (i.e. to maximize the utility that will be achieved in transmitting data of user *n* over subchannel *j* in the network). Hence, the objective function is to maximize the total utility function of the network, subject to two major constraints.

A single spotbeam is considered which consists of a base station (eNodeB) where the downlink bandwidth is divided into *J* subchannels. It is assumed that in this scenario the scheduler only schedules users, without assigning them to specific subchannels. A set of *N* users with the best priority index or utility function or metrics selected by the scheduler from *K* users is considered for the purpose of subchannel allocation or mapping. The set of subchannels are denoted by $J = \{j|j = 1,2,3, \dots, J\}$ and the set of users are denoted by $N = \{n|n = 1,2,3, \dots, N\}$. $U_{n,j}$ denotes whether user *n* is mapped or assigned to subchannel *j* or not; if assigned, it will have a value of 1 or else it will be 0. $L_{n,j}$ represents the utility achieved to transmit the data of user n over subchannel j.

The assignment problem, which aims to maximize the total utility function of the network, can then be expressed as follows;

$$max \sum_{j=1}^{J} \sum_{n=1}^{N} L_{n,j} U_{n,j} \tag{7.1}$$

Subject to;

$$\sum_{j=1}^{J} U_{n,j} \leq J \qquad \forall\, n \in (1, \dots, N) \tag{7.2}$$

$$\sum_{n=1}^{N} U_{n,j} \leq 1 \qquad \forall\, j \in (1, \dots, J) \tag{7.3}$$

$$U_{n,j} \in \{0,1\} \tag{7.4}$$

where constraint (7.2) states that a user can be assigned to as many subchannels as possible depending on the number of subchannels available. It has also been shown according to [130] that this constraint does not produce a significant reduction in the total utility of the network, and constraint (7.3) states that a maximum of one user can be assigned to a subchannel. Hence, a subchannel can only accommodate one user at a time (or each timeslot).

7.4 Proposed Scheme

The respective data rate $R_{n,j}$ and priority index $L_{n,j}$ for each flow or user *n* over subchannel *j* is known. The bidding function $\Delta_n(j)$ is computed for each user, which is the difference between the priority index or utility of the best subchannel and that of the second best subchannel of a particular user *n*. The user with the maximum or best bidding function is allocated the subchannel. The $\Delta_n(j)$ is assumed to be the maximum willingness to pay for subchannel *j* of user *i*. This process is repeated until all subchannels have been assigned. The algorithm is presented as follows;

Utility Auction Based (UAB) Subchannel Allocation Algorithm

---

1. Initialize S = {1,2,3, … … … … … … … … . . N_s} and

   $S_n = \phi$ for all selected user *n*

2. While $S \neq \emptyset$
3. For user *n* = 1 to N
4. $\Delta_n(j) = \max_j\{L_{n,j}\} - \max_{i \neq j}\{L_{n,i}\}$

   end

5. $j_n = arg\max_n \Delta_n(j)$
6. $R_{n*} = R_{n*} + R_{n,j}$
7. $S = S - j_{n*}$
8. $S_n = S_n + j_{n*}$

   end

---

where S is the set of all subchannels and S_n is the set of subchannels allocated to user n. This algorithm will run for S iterations. This means that the number of iterations depends on the number of available subchannels.

7.5 Other Subchannel Allocation Scheme

The commonly used, default subchannel allocation scheme is actualized by computing the priority index of all users on a subchannel basis and the user with the best priority index is allocated the subchannel. This is repeated for each subchannel or PRB. Hence, the computation of the priority index or utility function is repeated for every subchannel.

Maximum Utility per Subchannel (MUS) Subchannel Allocation Algorithm

---

1. For subchannel j = 1 to J
2. $j_k = arg\max_k \{ L_{k,j} \}$
3. $R_{k*} = R_{k*} + R_{k,j}$

end

J is the total number of subchannels and K is the total number of users waiting to be served. It should be noted that K is greater than N that is used in the proposed subchannel allocation algorithm. N is a group of users selected by the scheduler from the total number of users K.

7.6 Simulation Setup

A single spotbeam has been considered for this simulation in order to evaluate the performance of the proposed subchannel allocation scheme. The UEs are capable of rendering video streaming and web surfing uniformly distributed within the spotbeam footprint. The channel and traffic model presented in chapter 2 are adopted for the simulations. Each set of UEs is made up of 50% of web browsers and 50% of video streamers. Each UE is assumed to be reporting its channel condition (in terms of CQI) according to fixed intervals to the eNodeB.

LTE performance is analysed using an open source discrete event simulator called LTE-Sim [79]-[81]; this is a standalone version of the LTE module in NS-3 and is written in C++ and was

upgraded in [82].This simulator has been adapted to the GEO satellite scenario. In particular, the physical layer characteristics, including the channel model and the propagation delay, were modified in order to implement the satellite scenario. Furthermore the new scheduler and the web traffic model have been included in the simulator.

It is assumed that CQI is reported by the UE every 100 TTIs; this long interval has been considered in the GEO scenario in order to reduce the frequency of reporting, so as to save UE equipment's power. Two set of simulations have been carried out for bandwidth of 5 and 15 MHz. The purpose is to determine the behaviour and performance of the subchannel allocation schemes when the numbers of PRBs are relatively low (5 MHz) and high (15 MHz). The details of the simulator parameters are provided in Table 7-1 below.

Table 7-1: Simulation parameters for comparison of subchannel allocation schemes

Parameters	Value
Simulation Time	500 seconds
RTPD	540 ms (GEO satellite)
Channel Model	4 state Markov model
MIMO	2 x 2 (2 antenna ports)
CQI Reporting Interval	100 TTI
TTI	1 ms
Frequency Re-use	7
Mobile user Speed	30 km/h
RLC Mode	AM
Web Traffic Model	ON/OFF M/Pareto
Video Traffic Model	Trace-based @ 440 kbps
Scheduler	CBQS
Subchannel Allocation	UAB & MUS
Bandwidths	5 & 15 MHz

7.7 Simulation Results

The total throughput of both video and web traffic results for 5 and 15 MHz are presented in Figs.7-1 and 7-2, respectively. Fig. 7-1 shows that, for bandwidth of 5MHz, the proposed UAB subchannel allocation scheme produces a better throughput performance than the MUS subchannel allocation scheme from 10 to 30 UEs, but as the number of UEs increases from 30, the gap between the two subchannel allocation schemes decreases. This is due to the fact that as the number of UEs increases, the limited available resources or subchannels have to be used; hence, the two subchannel allocation schemes approach the limit.

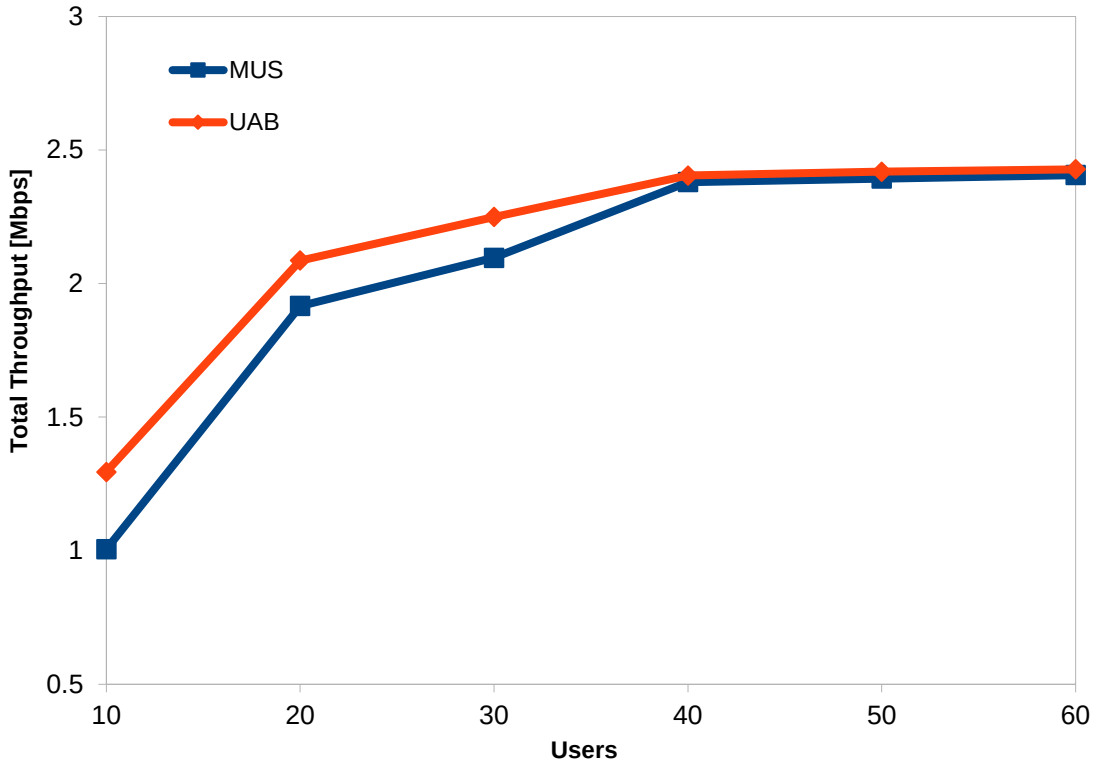

Figure 7-1: Total Throughput of all users @ 5MHz

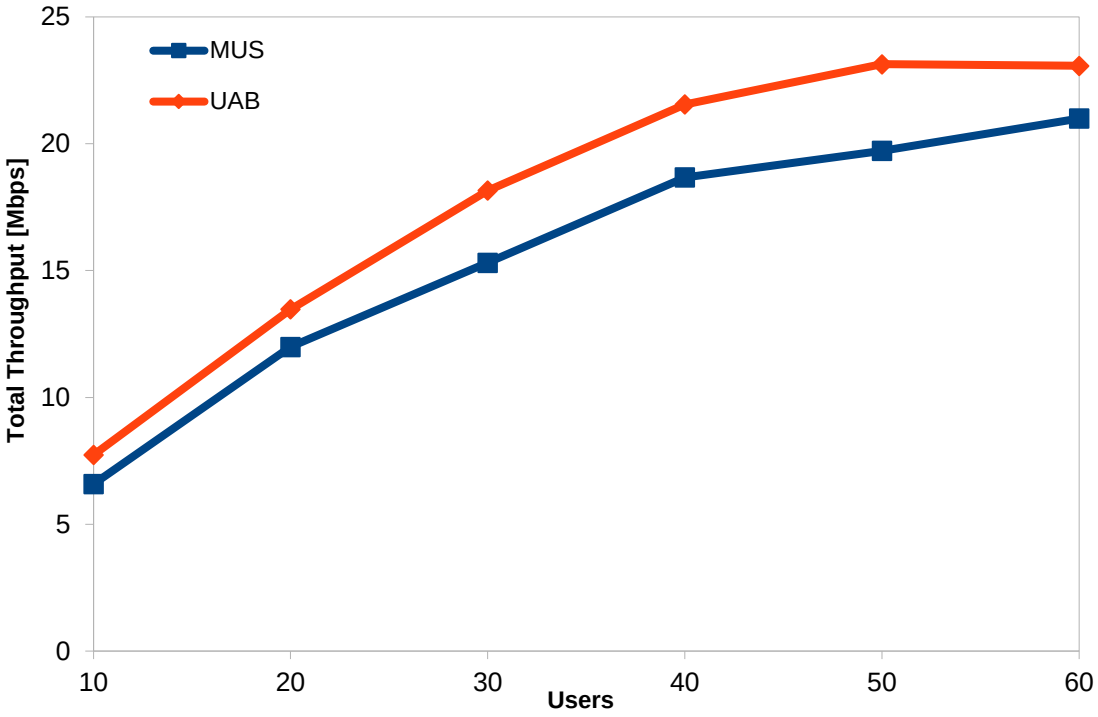

Figure 7-2: Total Throughput of all users @ 15MHz

When the number of subchannels is increased by considering a bandwidth of 15 MHz, the proposed UAB subchannel allocation scheme produces better throughput performance for all the UEs considered. As the

number of UEs increases, the difference in throughput performance become more evident, as shown in Fig. 7-2.

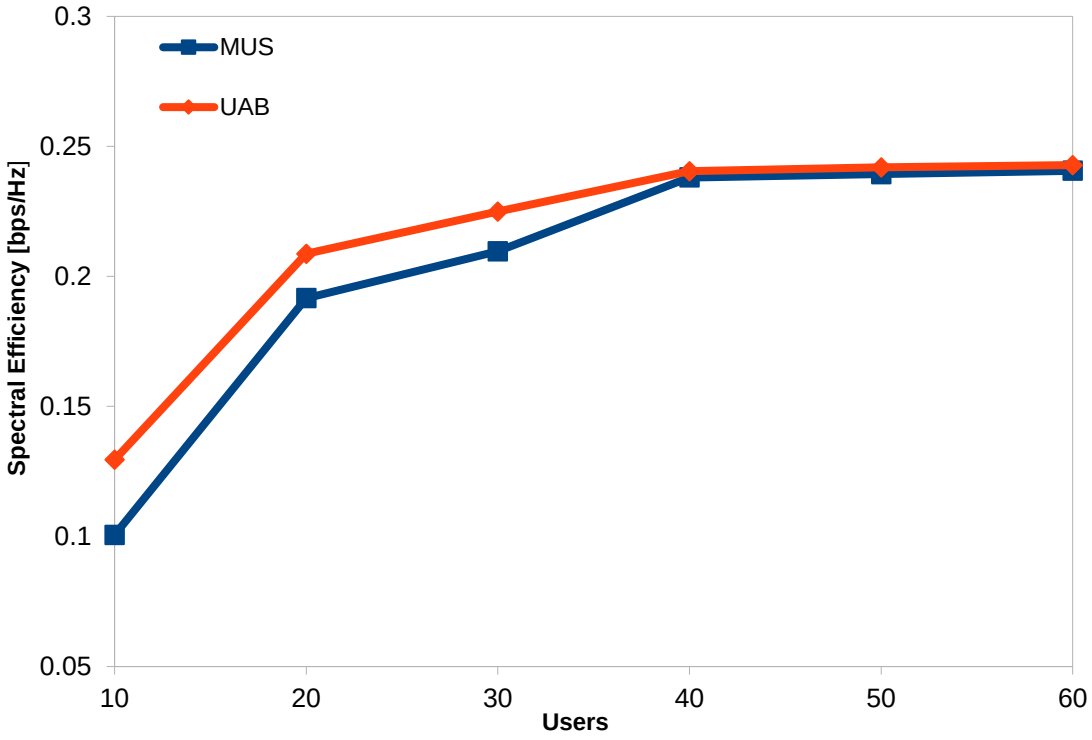

Figure 7-3: Spectral Efficiency @ 5MHz

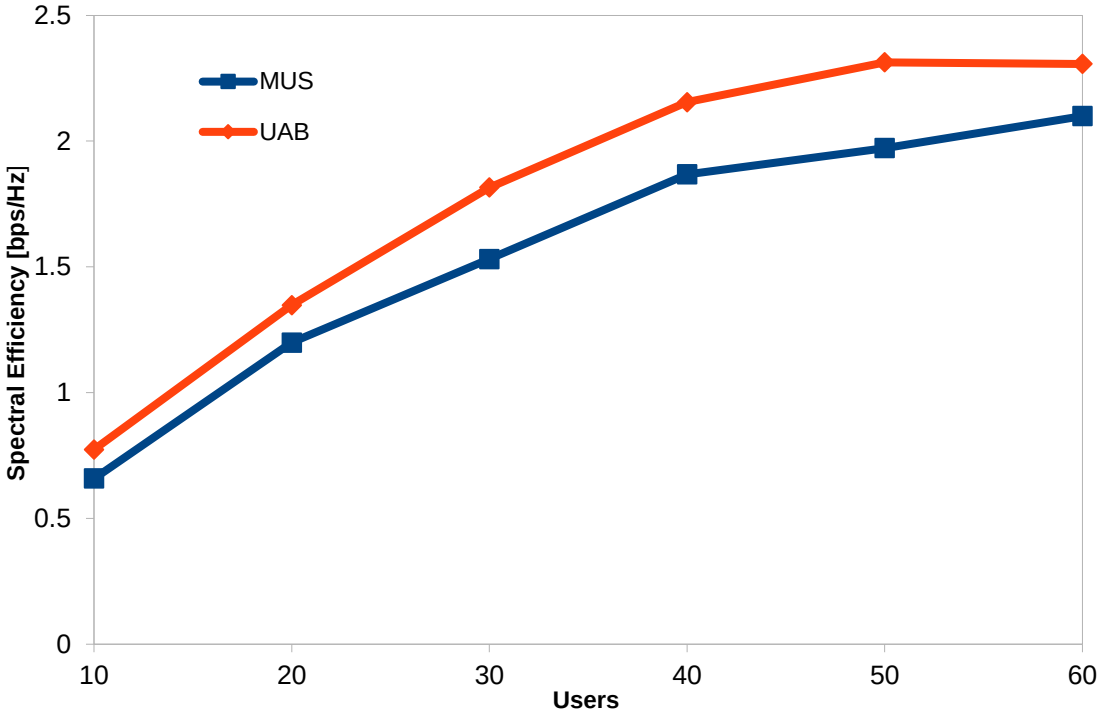

Figure 7-4: Spectral Efficiency @ 15MHz

The spectral efficiency performance for 5 MHz and 15 MHz is shown in Figs. 7-3 and 7-4, respectively. Spectral efficiency performance follows the same trend as the throughput performance. The proposed UAB subchannel allocation scheme utitlizes the spectrum more effectively than the MUS subchannel allocation scheme, especially from 10 to 30 UEs, but, from 40 to 60 UEs, the spectral efficiency performance is similar, with the proposed UAB scheme having a small edge. This performance trend changes when a bandwidth of 15 MHz is considered. The proposed UAB scheme utilizes the spectrum more effectively than the MUS subchannel allocation scheme for all the considered UEs. As the number of UEs increases, the difference in the spectral efficiency performance of both schemes becomes more significant.

The fairness index performance for 5 MHz and 15 MHz is presented in Figs. 7-5 and 7-6, respectively. Fig 7-5 shows that, for 5 MHz, the two subchannel allocation schemes have a similar fairness index performance. The UAB subchannel allocation scheme has an edge over MUS for 10 and 20 UEs. However, at high UEs of 50 and 60, the MUS has an edge over the proposed UAB subchannel allocation scheme.

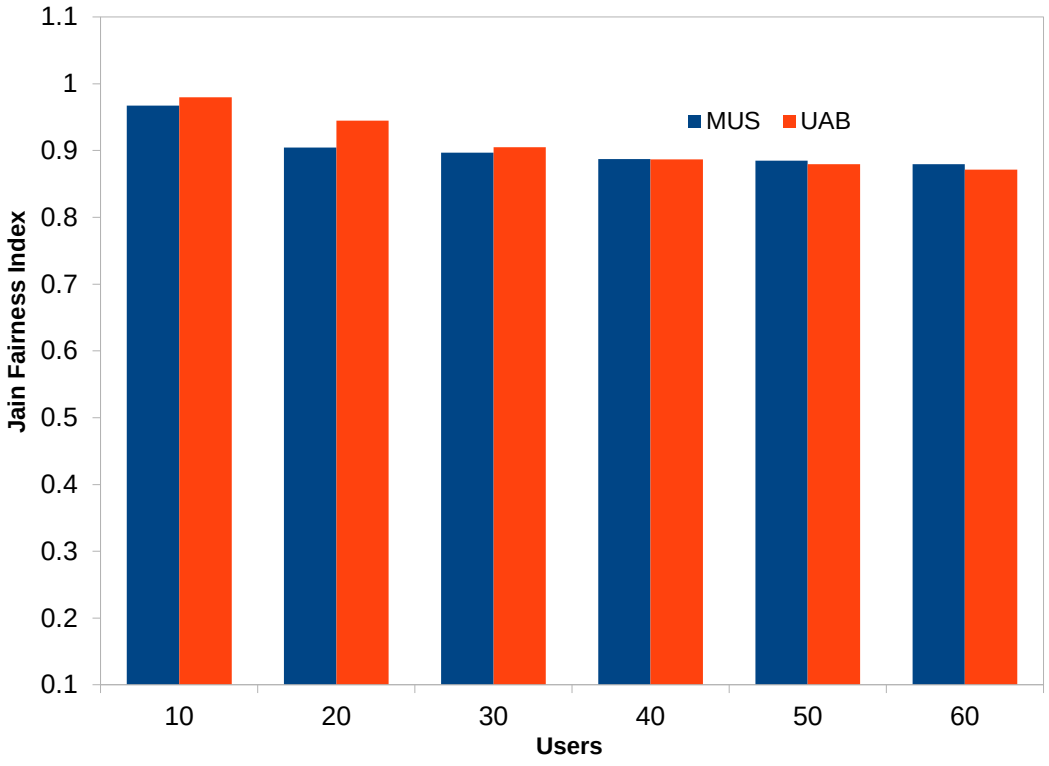

Figure 7-5: Fairness Index of all users @ 5MHz

Fig. 7-6 shows that, when 15 MHz is considered, the MUS subchannel allocation scheme has an edge from 20 UEs to 60 UEs, while both schemes exhibit the same performance at 10 UEs. This

shows that when the bandwidth, i.e., the number of subchannels, is increased, the MUS has a small edge over the proposed UAB. This is due to the fact that the MUS assigns subchannel to UEs on a subchannel basis; hence, the probability of more UEs being assigned subchannels is higher than in the UAB subchannel allocation scheme.

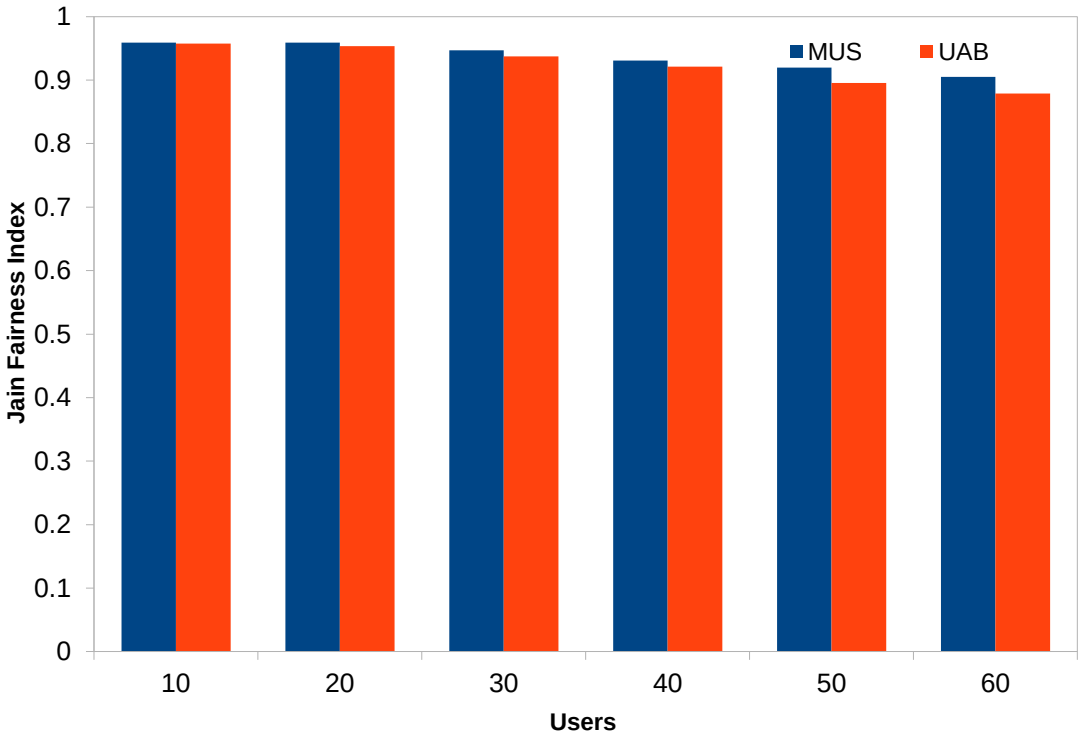

Figure 7-6: Fairness Index of all users @ 15MHz

7.8 Conclusion

This chapter reviewed the literature on subchannel allocation schemes and presented a subchannel assignment optimization problem. A heuristic solution, called Utility Auction Based (UAB) was also presented to solve the subchannel assignment problem for satellite LTE networks. The simulation used to conduct the comparison between the proposed subchannel allocation scheme and the Maximum Utility per Subchannel (MUS) was presented. Finally, the results obtained in terms of throughput, spectral efficiency and the fairness index from the simulations were presented.

The results show that, the proposed UAB subchannel allocation scheme provides better throughput and spectral efficiency performance than the MUS subchannel allocation scheme without seriously compromising fairness. The proposed scheme was able to improve throughput and spectral efficiency performance in addition to the previous performance produced by the

user/packet scheduling scheme. Furthermore, the proposed heuristic solution is relatively easier to implement than the exact solution, which is not a feasible solution to assignment problems of this nature.

Chapter 8

CONCLUSIONS & FURTHER RESEARCH

In an attempt to achieve the set 4G targets for throughput and QoS and to ensure the same level of service to every mobile user, anytime and anywhere, satellite LTE networks remain a vital component in achieving Next Generation Networks (NGN). Satellite LTE networks' ability to provide higher data rates will be actualized with reliable link adaptation and an effective scheduling and resource allocation scheme. This chapter presents a summary of the study and suggestions for further research.

8.1 Conclusions

The introductory chapter provided an overview of the evolution of satellite mobile communications, including third and fourth generation networks. It included an overview of the three different satellite types and mobile satellite communication systems. A brief discussion followed of MIMO technology which is adopted in this study. The motivation for the research study and the structure of the thesis were outlined. Finally, the original contributions and publications from this research were stated.

Chapter 2 presented a description of the satellite LTE air interface and the architecture of the satellite LTE network, as well as the details of the system model adopted for the satellite LTE network in this study, including the network, channel and traffic models.

Chapter 3 reviewed the literature on scheduling schemes and presented the formulated problem. It presented the proposed cross-layer based schedulers tagged Queue Aware Fair (QAF) and Channel Based Queue Sensitive (CBQS) scheduling schemes as well as a comparison of the

proposed schedulers and other schemes through simulations, the simulation setup and the evaluation of these schemes' performance. An overall scheduling performance index termed Scheduling Performance Metric (SPM) that provides the basis to measure the overall performance of a scheduler was derived and presented. The results showed that the proposed schedulers, QAF and CBQS, can support multiple traffic classes (RT and NRT), providing differentiated QoS levels to all of them. The QAF scheduler provides the best fairness index performance while CBQS offers the best throughput and spectral efficiency performance, compared with the other two (M-LWDF and EXP-PF) schedulers. Furthermore, the M-LWDF scheduler has an edge in delay performance over the proposed schedulers, with the three schedulers showing better delay performance than the EXP-PF scheduler. Based on the SPM, the two proposed schedulers, QAF and CBQS, provide better performance than the M-LWDF and EXP-PF schedulers.

This CBQS' performance is due to the fact that the scheduler combines the proportional fair and exponential form of delay, which is referenced to the delay deadline of each traffic type, while QAF performance is a result of the usage of parameters *m* and *c* to improve the level of fairness among users. Hence, it can be stated that the proposed CBQS scheduler produces the best throughput performance without significantly compromising delay and fairness perceived by users. This scheduler is therefore able to provide a good trade-off between the network throughput, users' QoS demands and perceived fairness.

Chapter 4 presented the investigation of the effect of RTPD experienced between UE and eNodeB during CQI reporting on satellite LTE networks' performance. The effect of the RTPD of both terrestrial and satellite air interfaces on their respective performance, and the impact of EIRP on satellite LTE networks' performance, was also investigated. After conducting this investigation through simulation, the long RTPD experienced during channel reporting in a satellite LTE network can be said to be of significance. This can be deduced from the results obtained. These results stem from the misalignment between the reported CQI at eNodeB and the current CQI at the UE. Furthermore, the results obtained in this chapter reveal that the terrestrial LTE air interface produces better performance than the satellite LTE air interface, as a result of the long RTPD experienced and the bigger size of the spotbeam (cell) in the satellite air interface. The results also show that by increasing the EIRP, as accommodated in the satellite LTE air interface, the performance of the satellite air interface improves.

Chapter 5 reviewed the literature on optimal and near-optimal scheduling schemes. The formulated problem, which aimed to maximize the throughput, with delay (modelled after M/G/1 queuing model) and fairness as major constraints, was presented. The derivation of the near-optimal solution, using KKT multipliers, was also presented. The proposed schedulers and

other throughput-optimal schedulers were compared by conducting simulations. The simulation setup and numerical results obtained from simulations were then presented. It can be concluded from the results that two of the proposed schedulers (NOSS1 and NOSS3) have the best throughput and spectral efficiency performance when compared with the other two throughput-optimal schedulers, while the M-LWDF scheduler has a small edge in delay performance over the proposed schedulers, with all the proposed schedulers offering better delay performance than the EXP-PF scheduler.

Although the fairness index performance of both M-LWDF and EXP-PF has an edge over two of the proposed schedulers, overall, the proposed NOSS1 and NOSS3 schedulers provide near-optimal throughput performance, without significantly compromising delay and the fairness experienced by users. The other two proposed schedulers, NOSS2 and NOSS4, provide a good trade-off among throughput, QoS and fairness. Based on the SPM results, the proposed NOSS1 and NOSS3 outperform both M-LWDF and EXP-PF schedulers. It is important to note that the proposed schedulers (NOSS1 and NOSS3) produce a better throughput, spectral efficiency and SPM performance than the cross-layer based schedulers (QAF and CBQS) proposed in chapter 3.

Chapter 6 reviewed previous studies on stability analysis and described the model adopted for stability analysis. The scheduling policy and the fluid limit technique adopted, which consists of both weak fluid and hard fluid limits were presented. The stability test was then conducted. Based on the stability test, it can be concluded that the proposed scheduling scheme is stable under maximum stability conditions based on the stability analysis conducted using fluid limit technique.

Chapter 7 reviewed the literature on subchannel allocation or assignment schemes and presented the formulated assignment problem, which aimed to maximize the utility function. The heuristic solution for the assignment problem was then presented. The comparison with the other subchannel allocation scheme was conducted through simulations. The simulation setup and the results were presented. It can be concluded that the proposed UAB subchannel allocation scheme provides better throughput and spectral efficiency performance, without seriously compromising the fairness index. The proposed scheme further improved the performance of the proposed packet scheduling scheme in the previous chapter.

8.2 Further Research

This study identified the following areas or topics of interest for further investigation.

The long RTPD in satellite LTE networks or satellite networks as a whole remains a challenge as it affects link adaptation and AMC. Since the long RTPD cannot be reduced, it is best to introduce a mechanism to reduce the impact of this long delay. One way is to use a very low BLER which was adopted in this study. However, a more suitable approach would be to be able to predict CQI of the UE at the eNodeB in advance without frequent CQI reporting. CQI prediction in satellite networks is more complex than in terrestrial networks. This is due to the fact that in a satellite air interface, the prediction length is very long; hence, the CQI Prediction in satellite LTE air interface could be the subject of further research.

Chapters 3 and 5 highlight the need to design and implement an effective scheduling scheme that will provide a very good trade-off among high throughput, acceptable QoS and good fairness. The design of an optimal scheduling scheme that is multi-objective, with possibly more constraints would be an interesting research area to explore in order to meet the demands of 4G and beyond networks. Hence, a multi-objective optimal scheduling scheme in a satellite LTE network could also be the subject of further research.

Finally, there is a need to design a joint admission control, scheduling and subchannel allocation scheme that will ensure high throughput, acceptable QoS and good perceived fairness by mobile users. A joint scheme will render all these Radio Resource Management (RRM) functions more effective and make the actualization of 4G and beyond targets more realistic. Hence, a joint admission control, scheduling and resource allocation scheme for satellite LTE networks is worthy of consideration for further research.

REFERENCES

1. **Stojce D., Ilcev.** "*Global Mobile Satellite Communications."* s.l. : Springe, 2005. ISBN 1-4020-7767-X.

2. **Ray, E. Sheriff and Y., Fun Hu.** "*Mobile Satellite Communication Networks."* West Sussex : John Wiley & Sons Ltd, 2001. ISBN 0471 72047 X.

3. **Littman, Marlyn K.** *Building broadband networks.* s.l. : CRC Press, 2002. ISBN 9780849308895.

4. **Giovanni, Giambene (Editor).** "*Resource management in satellite networks: optimization and cross-layer design."* s.l. : Springer, 2007. ISBN 978-0-387-36897-9.

5. **Giovanni Giambene, Samuele Giannetti, Cristina Párraga Niebla, Michal Ries, Aduwati Sali.**"*Traffic management in HSDPA via GEO satellite."* Space Communications, Vol. 21, No. 1, 2007, pp. 51 - 68.

6. **A. Azizan, A.U Quddus, B.G Evans.** "*Satellite High Speed Downlink Packet Access Physical Layer Performance Analysis."* 4th Advanced Satellite Mobile Systems, Bologna, Italy, 2008. pp. 156 - 161. doi: 10.1109/ASMS.2008.34.

7. **G. Giambene, S. Giannetti, C.P. Niebla, M. Ries.** "*Video Traffic Management in HSDPA via GEO Satellite."* International Workshop on Satellite and Space Communications, Madris, Spain, 2006, pp. 188 - 192. doi: 10.1109/IWSSC.2006.256021.

8. **D. Martín-Sacristán, J. F. Monserrat, J. Cabrejas-Peñuelas, D. Calabuig, S. Garigas, N. Cardona.** "*On the Way towards Fourth-Generation Mobile: 3GPP LTE and LTE-Advanced."* EURASIP Journal on Wireless Communications and Networking, 2009, p. 10. doi:10.1155/2009/354089.

9. **J. Duplicy, B. Badic, R. Balraj, et al.** "*MU-MIMO in LTE Systems."* EURASIP Journal on Wireless Communications and Networking, 2011, p. 13. doi:10.1155/2011/496763.

10. **ETSI TR 102 662.** "*Satellite Earth Stations and Systems (SES); Advanced satellite based scenarios and architectures for beyond 3G systems v1.1.1."* ETSI. March 2010. Technical Report.

11. **ESA.** "*Study of Satellite Role in 4G Mobile Networks Final Report."* European Space Agency. May 2009. Technical Report.

12.**Volker Jungnickel, Holger Gaebler, Udo Krueger, Konstantinos Manolakis, Thomas Haustein. "***LTE Trials in the Return Channel Over Satellite."* 6th Advanced Satellite Multimedia Systems Conference (ASMS) and 12th Signal Processing for Space Communications Workshop (SPSC), Sept. 2012, pp. 238 - 245. doi: 10.1109/ASMS-SPSC.2012.6333083.

13. **A. Perez-Neira, C. Ibars, J. Serra, A. del Coso, J. Gomez, M. Caus.** "*MIMO applicability to satellite networks."* 10th International Workshop on Signal Processing for Space Communications, October 2008, pp. 1-9. doi: 10.1109/SPSC.2008.4686701.

14. **R.T. Schwarz, A. Knopp, B. Lankl, D. Ogermann, C.A. Hofmann.** "*Optimum-Capacity MIMO Satellite Broadcast System: Conceptual Design for LOS Channels."* 4th Advanced Satellite Mobile Systems (ASMS), August 2008, pp. 66-71. doi: 10.1109/ASMS.2008.19.

15. **R.T. Schwarz et. al.** "*Optimum-Capacity MIMO Satellite Link for Fixed and Mobile Services."* Workshop on Smart Antennas (WSA) 2008, pp. 209 -216.

16. **A. Knopp, et al.** "*Satellite System Design Examples for Maximum MIMO Spectral Efficiency in LOS Channels."* IEEE Global Telecommunications Conference (IEEE GLOBECOM), November/December 2008., pp. 1 - 6.

17. **P. Arapoglou, K. Liolis, M. Bertinelli, A. Panagopoulos, P. Cottis, R. De Gaudenzi.** "*MIMO over Satellite: A Review."* IEEE Communications Surveys & Tutorials, Vol. 13, No. 1, First Quarter 2011, pp. 27-51. doi: 10.1109/SURV.2011.033110.00072.

18. **European Space Agency** "MIMOSA: Characterization of the MIMO channel for mobile satellite systems." *ESA.* [Online] [Cited: 25 May 2010.] http://telecom.esa.int/.

19. **European Space Agency.** "MIMO HW demonstrator." *ESA.* [Online] [Cited: 25 May 2010.] http://telecom.esa.int/.

20. **V. Dantona, R.T. Schwarz, A. Knopp, B. Lankl.** "*Uniform circular arrays: The key to optimum channel capacity in mobile MIMO satellite links."* 5th Advanced satellite multimedia systems conference (ASMA) and the 11th signal processing for space communications (SPSS), September 2010, pp. 421 - 428. doi: 10.1109/ASMS-SPSC.2010.5586873.

21. **A. Knopp, R.T. Schwarz, B. Lankl.** "*On the Capacity Degradation in Broadband MIMO Satellite Downlinks with Atmospheric Impairments."* IEEE International Conference on Communications (ICC), May 2010, pp. 1 - 6. doi: 10.1109/ICC.2010.

22. **P. R. King and S. Stavrou.** "*Land mobile-satellite MIMO capacity predictions."* Electronics Letters, Vol. 41, No. 13, 2005, pp. 749 - 751.

23. **P. R. King, B. G. Evans, and S. Stavrou.** "*Physical-statistical model for the land mobile-satellite channel applied to satellite/HAP MIMO."* 11th European Wireless Conference. Vol. 1, Nicosia, Cyprus, April 2005, pp. 198 – 204.

24. **P. Horvath, G. K. Karagiannidis, P. R. King, S. Stavrou and I. Frigyes.** "*Investigations into satellite MIMO channel modeling; accent on polarization."* EURASIP Journal on Wireless Communications and Networking, 2007.

25. **A. I. Perez-Neira, C. Ibars, J. Serra, A. del Coso, J. Gomez-Vilardebo, M. Caus, K. P. Liolis.** *"MIMO channel modeling and transmission techniques for multi-satellite and hybrid satellite-terrestrial mobile networks"* Physical Communications, Vol. 4, No. 2, June 2011, pp. 127-139. ISSN 1874-4907, DOI: 10.1016/j.phycom.2011.04.001..

26. **K.P. Liolis, J. Gomez-Vilardebo J, E. Casini, A. Perez-Neira.** "*On the statistical modeling of MIMO land mobile satellite channels: a consolidated approach."* 27th AIAA International Communication Satellite Systems Conference (ICSSC), Edinburgh, June 2009..

27. **K. P. Liolis, A. D. Panagopoulos, and P. G. Cottis.** "*Multi-Satellite MIMO Communications at Ku-Band and Above: Investigations on Spatial Multiplexing for Capacity*

Improvement and Selection Diversity for Interference Mitigation.," EURASIP Journal on Wireless Communications and Networking, 2007.

28. **F. Bastia, C. Bersani, E. A. Candreva, et al.** "*LTE Adaptation for Mobile Broadband Satellite Networks."* EURASIP Journal on Wireless Communications and Networking, 2009,p. 13. doi:10.1155/2009/989062.

29. **S. Parkvall, A. Furuskär, E. Dahlman.** "*Evolution of LTE Toward IMT-Advanced."* IEEE Communications Magazine, Vol. 49, No. 2, February 2011, pp. 84-91. doi: 10.1109/MCOM.2011.5706315.

30. **Li, Qinghua, et al.** "*MIMO techniques in WiMAX and LTE: a feature overview."* IEEE Communications Magazine, Vol. 48, No 5, May 2010, pp. 86-92.

31. **R. Ghaffar, and R. Knopp.** "*Making multiuser MIMO work for LTE."* 21st IEEE International Symposium on Personal Indoor and Mobile Radio Communications (PIMRC), September 2010, pp. 625 - 628. doi: 10.1109/PIMRC.2010.5671753.

32. **3GPP.** "*Technical Specification Group Radio Access Network; E-UTRA Physical layer procedures."* September 2012. 3GPP TS 36.213 V11.0.0.

33. **3GPP.** "*Tech. Specif. Group Radio Access Network; Physical Channel and Modulation."* September 2012. 3GPP TS 36.211.

34. **LTE University.** "LTE Frame Structure." *LTE University.* [Online] [Cited: 25 October 2013.] Web site with URL:http://lteuniversity.com/.

35. **Motorola, Inc.** "*Long Term Evolution (LTE):" Overview of LTE Air-Interface.* 2007. Technical White Paper .

36. **A. Molisch.** "*Wireless Communications."* s.l. : Wiley-IEEE Press, 2011. pp. 665 - 698 . 9781119992806.

37. **W. Ben Hassen, M. Afif, S. Tabbane.** "*A recursive PRB allocation algorithm using AMC for MIMO-OFDMA LTE systems."* 10th International Multi-Conference on Systems, Signals & Devices (SSD) March 2013. doi: 10.1109/SSD.2013.6564021.

38. **3GPP.** *Technical Specification Group Services and System Aspects, Policy and Charging Control Architecture.* 2011. TS 23.203 V11.0.0(release-11).

39. **Sun, Siyue, et al.** "*A configurable dual-mode algorithm on delay-aware low-computation scheduling and resource allocation in LTE downlink."* IEEE Wireless Communications and Networking Conference (WCNC), April 2012, pp. 1444-1449. doi: 10.1109/WCNC.2012.6214008.

40. **Simic, M.B.** "*Feasibility of long term evolution (LTE) as technology for public safety."* 20th Telecommunications Forum (TELFOR)., November 2012., pp. 158 - 161. doi: 10.1109/TELFOR.2012.6419172.

41. **P.R. King, T.W.C. Brown, A. Kyrgiazos, B.G. Evans.** "*Empirical-Stochastic LMS-MIMO Channel Model Implementation and Validation. "* IEEE Transactions on Antennas and Propagation, Vol. 60, No. 2, February 2012, pp. 606-614. doi: 10.1109/TAP.2011.2173448.

42. **K.P. Liolis, J. Gómez-Vilardebó, E. Casini, A. I. Pérez-Neira.** "*Statistical Modeling of Dual-Polarized MIMO Land Mobile Satellite Channels."* IEEE Transactions on Communications, Vol. 58, No. 11, November 2010, pp. 3077-3083. doi:10.1109/TCOMM.2010.09.

43. **P.R. King, S. Stavrou.** "*Low Elevation Wideband Land Mobile Satellite MIMO Channel Characteristics."* IEEE Transactions on Wireless Communications, Vol. 6, No. 7, July 2007, pp. 2712-2720. doi: 10.1109/TWC.2007.051018.

44. **Y. R. Zheng, C. Xiao.** "*Simulation Models with Correct Statistical Properties for Rayleigh Fading Channels."* IEEE Transactions on Communications, Vol. 51, No. 6, June 2003, pp. 920-928. doi: 10.1109/TCOMM.2003.813259.

45. **H.W. Kim, K.S. Kang, B.J. Ku, D. Ahn.** "*Coordinated Multi-point Transmission Combined with Cyclic Delay Diversity in Mobile Satellite Communications."* Proceedings of PSATS 2011. pp. 274-285.

46. **Wei Zheng et. al.** "*Interference Modeling and Analysis for Inclined Projective Multiple Beams of GEO Satellite Communication Systems."* Advanced Materials Research, Vols. 756-759, 2013, pp. 1204 -1209. doi 10.4028/www.scientific.net/AMR.756-759.1204.

47. **C. Mehlfuhrer, M. Wrulich, J.C. Ikuno, D. Bosanska, M. Rupp.** "*Simulating the Long Term Evolution Physical Layer."* European Signal Processing Conference (EUSIPCO), Glasgow, Scotland, August 2009.

48. **H. Song, R. Kwan, J. Zhang.** "*Approximations of EESM Effective SNR Distribution."* IEEE Transactions on Communications, Vol. 59, No. 2, February 2011,pp. 603-612. doi: 10.1109/TCOMM.2011.011811.100056.

49. **H. Song, R. Kwan, J. Zhang.** "*On Statistical Characterization of EESM Effective SNR over Frequency Selective Channels."* IEEE Transactions on Wireless Communications , Vol. 8, No. 8, 2009, pp. 955-3960. DOI:10.1109/TWC.2009.081597 .

50. **Jesus Arnau, Alberto Rico-Alvari and Carlos Mosquera.** "*Adaptive Transmission Techniques for Mobile Satellite Links."* Ottawa, Canada : s.n., September 2012. 30th AIAA International Communications Satellite Systems Conference (ICSSC). pp. 1-14.

51. **Deslandes, C. Morel and V. "***LTE-MARS: an Open Source Tool for Simulating OFDMA Satellite Systems."* 29th AIAA International Communications Satellite Systems Conference (ICSSC-2011), November 2011.

52. G. **Piro, et al.** "*Two-Level Downlink Scheduling for Real-Time Multimedia Services in LTE Networks."* IEEE Transactions on Multimedia, Vol. 13, No. 5, October 2011, pp. 1052-1065.

53. **M. Iturralde, et al.** "*Resource allocation for real time services using cooperative game theory and a virtual token mechanism in LTE networks."* IEEE Consumer Communications and Networking Conference (CCNC), January 2012, pp. 879-883, . doi: 10.1109/CCNC.2012.6181183.

54. **Video trace library**. *Arizona State University*. [Online] http://trace.eas.asu.edu/.

55. **Li, Xi.** Introduction of Simulation Models. "*Radio Access Network Dimensioning for 3G UMTS."* s.l. : Springer, 2011, pp. 77-97.

56.**F. De Angelis, et al. "***Scheduling for differentiated traffic types in HSDPA cellular systems."* IEEE Global Telecommunications Conference, 2005. GLOBECOM '05. Vol. 1, Nov./ Dec. 2005. pp. 36 - 40. doi: 10.1109/GLOCOM.2005.1577349.

57. **G. Giambene and A. Andreadis.** "*Protocols for High-Efficiency Wireless Networks."* s.l. : Springer US, 2002. 978-0-306-47795-9.

58. **F. Capozzi, G. Piro, L. A. Grieco, G. Boggia, P. Camarda.** "*Downlink Packet Scheduling in LTE Cellular Networks: Key Design Issues and a Survey."* IEEE Communications Surveys & Tutorials, Vol. 15, No. 2, Second Quarter 2013, pp. 678-700. doi: 10.1109/SURV.201.

59. **G. Aiyetoro, G. Giambene, F. Takawira.** "*Performance Analysis of M-LWDF and EXP-PF Schedulers for Real-Time Traffic for Satellite LTE Networks."* South Africa Telecommunications Networks and Applications Conference (SATNAC), September 2013.

60. **ITU-R.** "*Technical Specification on LTE-Satellite Radio Interface Specifications; LTE-Satellite; General Description (Release 1)."* 2012. LTE-Satellite-366.002.2(draft)V1.0.0 .

61.**Chao H. Jonathan and Guo. Xiaolei.** "*Quality of service control in high-speed networks."* s.l. : Wiley, 2001. ISBN 978-0-471-00397-7.

62. **M. Markaki, E. Nikolouzou, and I. Venieris.** "*Performance evaluation of scheduling algorithms for the internet."* 8th IFIP on Performance Modelling and Evaluation of ATM & IP Networks, 2000.

63. **M. Shreedhar and G. Varghese.** "*Efficient fair queueing using deficit round robin."* IEEE/ACM Transactions on Networking, Vol. 4, No. 3, June 1996, pp. 375-385.

64. **Hui, Zhang and Srinivasan, Keshav.** "*Comparison of Rate-Based Service Disciplines."* ACM SIGCOMM conference, 1991.

65. **Uitert, Maria Johanna Gerarda van.** "*Generalized Processor Sharing Queues."* s.l. : Ponsen & Looijen BV, 2003. ISBN 90 6464 709 7.

66. **Zhang, Hui.** "*Service Disciplines for Guaranteed Performance Service in Packet-Switching Networks."* Proceedings of the IEEE, Vol. 83, No. 10, October 1995, pp. 1374--1396.

67. **D. Liu and Y.-H. Lee.** "*An efficient scheduling discipline for packet switching networks using Earliest Deadline First Round Robin."* IEEE International Conference on Computer Communications and Networks (ICCCN). Dallas, USA, October 2003.pp. 5 – 10.

68. **Giovanni, Giambene, et al.** "*HSDPA and MBMS transmissions via S-UMTS."* Delft, Netherlands, February, 2006.

69.**A. Stolyar and K. Ramanan.** "*Largest Weighted Delay First Scheduling: Large Deviations and Optimality."* 2001, Annals of Aplied Probability, Vol. 11, pp. 1–48.

70. **P. Kela, et al.** "*Dynamic packet scheduling performance in UTRA Long Term Evolution downlink. "* 3rd International Symposium on Wireless Pervasive Computing (ISWPC), May 2008, pp. 308-313. doi: 10.1109/ISWPC.2008.4556220.

71. **T. Kolding.** "*Link and system performances aspects of proportional fair scheduling in WCDMA/HSDPA."* IEEE Vehicular Technology Conference-Fall, Florida, USA, 2003.

72. **C. Wengerter, J. Ohlhorst, and A. von Elbwart.** "*Fairness and throughput analysis for generalized proportional fair frequency scheduling in OFDMA."* IEEE Vehicular Technology Conference VTC-Spring, Stockholm, Sweden, May 2005, Vol. 3, pp. 1903 – 1907.

73. **M. Proebster, C. Mueller, and H. Bakker.** "*Adaptive fairness control for a proportional fair LTE scheduler."* IEEE Personal Indoor and Mobile Radio Communications(PIMRC), Istanbul, Turkey, September 2010. pp. 1504-1509.

74. **B. Sadiq, R. Madan, A. Sampath.** "*Downlink Scheduling for Multiclass Traffic in LTE.***"** EURASIP Journal on Wireless Communications and Networking, 2009, doi:10.1155/2009/510617.

75.**M. Andrews, K. Kumaran, K. Ramanan, A. Stolyar, R. Vijayakumar, P. Whiting.** "*Providing Quality of Service over a shared wireless link."* IEEE Communications Magazine, Vol. 39, No. 2, February 2001, pp. 150 - 154.

76. **R. Basukala, H. A. Mohd Ramli, K. Sandrasegaran.** "*Performance Analysis of EXP/PF and M-LWDF in Downlink 3GPP-LTE system."* First Asian Himalayas International Conference on Internet (AH-ICI 2009). doi:10.1109/AHICI..

77. **M. Iturralde, T. H. Yahiya, A. Wei, A.-L. Beylot.** "*Performance Study of Multimedia Services Using Virtual Token Mechanism for Resource Allocation in LTE Networks."* IEEE Vehicular Technology Conference, VTC-Fall, 2011.

78. **G. Aniba and S. Aissa.** "*Adaptive scheduling for MIMO wireless networks: cross-layer approach and application to HSDPA,*. IEEE Transactions on Wireless Communications, Vol. 6, No. 1, January 2007, pp. 259-268. doi: 10.1109/TWC.2007.05162.

79. **G. Piro, et al.** "*Simulating LTE Cellular Systems: An Open-Source Framework."* IEEE Transactions on Vehicular Technology, Vol. 60, No. 2, 2011, pp. 498-513. doi: 10.1109/TVT.2010.2091660.

80. **F. Capozzi, G. Piro, L. A. Grieco, G. Boggia, and P. Camarda.** "*A system-level simulation framework for LTE femtocell."* 5th International Conference on Simulation Tools and Techniques SIMUTools. ICST, March 2012.

81. **F. Capozzi, G. Piro, L. Alfredo Grieco, G. Boggia, and P. Camarda.** "*On accurate simulations of lte femtocells using an open source simulator."* EURASIP Journal on Wireless Communications and Networking, 2012.

82. **A. Pellegrini, and G. Piro.** "*Multi-threaded Simulation of 4G Cellular Systems within the LTE-Sim Framework"* 27th International Conference on Advanced Information Networking and Applications Workshops (WAINA), March 2013, pp. 101 - 106. doi: 10.1109/WAINA.2013.202.

83. **A. Alexiou, C. Bouras, V. Kokkinos, A. Papazois, G. Tsichritzis.** "*Spectral efficiency performance of MBSFN-enabled LTE networks."* IEEE 6th International Conference on Wireless and Mobile Computing, Networking and Communications (WiMob), October 2010, pp. 361-367. doi: 10.1109/WIMOB.2010.5645042.

84. **M. Amadeo, G. Araniti, A. Iera, A. Molinaro.** "*A Satellite-LTE Network with Delay-Tolerant Capabilities: Design and Performance Evaluation."* IEEE VehicularTechnology Conference (VTC Fall), Sept. 2011, pp. 1-5. doi: 10.1109/VETECF.2.

85.**M. Papaleo, M. Neri, A. Vanelli-Coralli, G.E. Corazza.** "*Using LTE in 4G satellite communications: Increasing time diversity through forced retransmission."* 10th International Workshop on Signal Processing for Space Communications (SPSC), October 2008. pp. 1-4. doi: 10.1109/SPSC.2008.4686699.

86. **S. Liu, F. Qin, Z. Gao, Y. Zhang, Y. He.** "*LTE-satellite: Chinese proposal for satellite component of IMT-Advanced system."* China Communications, Vol. 10, No. 10, Oct. 2013,pp. 47-64. oi: 10.1109/CC.2013.6650319.

87. **Y. Zheng, S. Ren, X. Xu, Y. Si, M. Dong, J. Wu.** "*A modified ARIMA model for CQI prediction in LTE-based mobile satellite communications."* International Conference on Information Science and Technology (ICIST)., March 2012, pp. 822 - 866. doi: 10.1109/ICIST.2012.6221763.

88. **E. Corbel, I. Buret, J. D. Gayrard, G.E. Corazza, A. Bolea-Alamanac.** "*Hybrid Satellite & Terrestrial Mobile Network for 4G : Candidate Architecture and Space Segment Dimensioning."* 4th Advanced Satellite Mobile Systems., 2008. pp. 162 - 166. doi: 10.1109/ASMS.2008.35.

89. **LTE-Sim**. *LTE-Sim.* [Online] http://telematics.poliba.it/LTE-Sim.

90. **NS-3.** *NS-3.* [Online] http://www.nsnam.org.

91. **G. Aiyetoro, G. Giambene, F. Takawira.** "*A New Packet Scheduling Algorithm in Satellite LTE networks."* Mauritius , September 2013. IEEE AFRICON Conference. pp. 1 - 6.

92. **E. Trachtman.** "*BGAN Its Extension and Evolution."* International Workshop for B3G/4G Satellite Communications, Seoul, November 2006.

93. **Mehmet E. Aydin, Raymond Kwan, Wei Ding and Joyce Wu.** "*A genetic algorithm approach for multiuser scheduling in downlink LTE networks."* Proceedings of the world college of engineering. Vol. II. July 2012.

94. **Kwan, R., Leung, C. and Zhang, Jie.** "*Resource Allocation in an LTE Cellular Communication System"*. IEEE International Conference on Communications (ICC '09), June 2009, pp. 1 - 5.

95. **Raymond Kwan, Cyril Leung and Jie Zhang.** Downlink Resource Scheduling in an LTE System. [book auth.] Salma Ait Fares and Fumiyuki Adachi (Ed.). "*Mobile and Wireless Communications Physical Layer Development and Implementation."* s.l. : InTech, 2010.

96. **Ahmed Ahmedin, Kartik Pandit, Dipak Ghosal and Amitabha Ghosh.** "*Content and buffer aware scheduling for video delivery over LTE."* New York, NY, USA, International

Conference On Emerging Networking Experiments And Technologies, December 2013, pp. 43 - 46. doi:10.1145/2537148.2537158.

97. **R.C. Elliott, and W.A. Krzymien.** "*Downlink Scheduling via Genetic Algorithms for Multiuser Single-Carrier and Multicarrier MIMO Systems With Dirty Paper Coding."* IEEE Transactions on Vehicular Technology, Vol. 58, No. 7, September 2009, pp. 3247 - 3262.

98. **Lee, Neung-Hyung, Choi, Jin-Ghoo and Saewoong Bahk.** "*Opportunistic scheduling for utility maximization under QoS constraints.*" 16th IEEE International Symposium on Personal, Indoor and Mobile Radio Communications (PIMRC 2005), Vol. 3, 2005. pp. 1818 - 1822.

99. **Xiaolin Cheng, and P. Mohapatra.** "*Quality-optimized downlink scheduling for video streaming applications in LTE networks."* IEEE Global Communications Conference (GLOBECOM), December2012, pp. 1914 - 1919. doi: 10.1109/GLOCOM.2012.6503395.

100. **M. Dianati, Xuemin Shen, and K. Naik.** "*Cooperative Fair Scheduling for the Downlink of CDMA Cellular Networks."* IEEE Transactions on Vehicular Technology, Vol. 56, No. 4, July 2007, pp. 1749 - 1760. doi: 10.1109/TVT.2007.897209.

101. **W.C. Chan, T.C. Lu, and R.J. Chen.** "*Pollaczek-Khinchin formula for the M/G/1 queue in discrete time with vacations."* July 1997, IEE Proceedings Computers and Digital Techniques, Vol. 144, No. 4, pp. 222 - 226 . doi: 10.1049/ip-cdt:19971225.

102. **H. Li.** "*Lagrange Multipliers and their Applications."* Department of Electrical Engineering and Computer Science, University of Tennessee, Knoxville, TN 37921, USA., 2008.

103. **R. Courant.** "*Differential and Integral Calculus."* 1st. Edition, Inter-science Publishers, 1937.

104. **D. P. Bertsekas.** "*Nonlinear Programming."* 2nd.Edition, Athena Scientific, 1999.

105. **Stephen Boyd, and Lieven Vandenberghe.** "*Convex Optimization."* s.l. : Cambridge University Press, 2004. p. 244. ISBN 0-521-83378-7.

106. **Ruszczyński, Andrzej.** "*Nonlinear Optimization."* s.l. : Princeton University Press, 2006. ISBN 978-0691119151.

107. **S. Borst and M. Jonckheere.** "*Flow-Level Stability of Channel-Aware Scheduling Algorithms."* 4th International Symposium on Modeling and Optimization in Mobile, Ad Hoc and Wireless Networks, April 2006, pp. 1-6. doi: 10.1109/WIOPT.2006.1666471.

108. **M. Andrews, K. Kumaran, K. Ramanan, S. Stolyar, R. Vijayakumar,and P. Whiting.** "*Scheduling in a queueing system with asynchronously varying service rates."* Probability in the Engineering and Informational Sciences, Vol. 18, No. 2, 2004, pp. 191–217.

109. **L. Tassiulas and A. Ephremides.** "*Stability properties of constrained queueing systems and scheduling policies for maximum throughput in multihop radio networks."* IEEE Transactions on Automatic Control , Vol. 37, 1992, pp. 1936–1948.

110. **L. Tassiulas and A. Ephremides.** "*Dynamic server allocation to parallel queues with randomly varying connectivity."* IEEE Transactions on Information Theory, Vol. 39, 1993, pp. 466– 478.

111. **A. McKeown and N. Mekkittikul.** "*Astarvation free algorithm for achieving 100% throughput in an input-queued switch."* International Conference on Computer Communications and Networks (ICCCN), 1996, pp. 226–231.

112. **S. Shakkottai and A. L. Stolyar.** "*Scheduling for Multiple Flows Sharing a Time-Varying Channel: The Exponential Rule."* American Mathematical Society Translations, Vol. 207, No. 2, 2002, pp. 185-202.

113. **Ren, Fengyuan, et al.** "*Frequency Domain Packet Scheduling with Stability Analysis for 3GPP LTE Uplink."* IEEE Transactions on Mobile Computing, Vol. 12, No. 12, December 2013, pp. 2412 - 2426. doi: 10.1109/TMC.2012.223.

114. **M. Andrews and L. Zhang.** "*Scheduling Algorithms for Multi-Carrier Wireless Data Systems."* ACM MobiCom, 2007.

115. **S. Aalto and P. Lassila.** "*Flow-level stability and performance of channel-aware priority-based schedulers."* Proceedings of 6th EURO-NFNGI., 2010, pp. 1–8.

116. **S. Borst.** "*Flow-level performance and user mobility in wireless data networks."* Philosophical Transactions of the Royal Society, Vol. 366, 2008, pp. 2047–2058.

117. **G. Vejarano, and J. McNair.** "*Stability Analysis of Reservation-Based Scheduling Policies in Wireless Networks.***"** IEEE Transactions on Parallel and Distributed Systems, Vol. 23, No. 4, April 2012, pp. 760 - 767. doi: 10.1109/TPDS.2011.201.

118. **X. Wu, R. Srikant, and J. Perkins.** "*Scheduling Efficiency of Distributed Greedy Scheduling Algorithms in Wireless Networks."* IEEE Transactions of Mobile Computing, Vol. 6, No. 6, June 2007, pp. 595-605.

119. **U. Ayesta, M. Erausquin, M. Jonckheere, I.M. Verloop.** "*Scheduling in a Random Environment: Stability and Asymptotic Optimality."* IEEE/ACM Transactions on Networking, Vol. 21, No. 2, February 2013, pp. 258 - 271. doi: 10.1109/TNET.2012.219976.

120. **S. Foss and T. Konstantopoulos.** "*An overview of some stochastic stability methods."* Journal of Operations Research, Society of Japan, Vol. 47, No. 4, 2004, pp. 275 - 303.

121. **S. C. Borst.** "*User-level performance of channel-aware scheduling algorithms in wireless data networks".* IEEE/ACM Transactions on Networking, Vol. 13, No. 3, June 2005, pp. 636–647.

122. **W. Feller.** "*An Introduction to Probability Theory and Its Application."* New York : Wiley, 1961. Vol. 1.

123. **Choi, Young-June, Kim, Jongtack and Bahk, Saewoong.** "*Downlink scheduling with fairness and optimal antenna assignment for MIMO cellular systems."* IEEE Global Telecommunications Conference (GLOBECOM), 2004, Vol. 5, pp. 3165 - 3169.

124. **Sun, Fanglei, et al.** "*Multiobjective optimized subchannel allocation for wireless OFDM systems."* IEEE 20th International Symposium on Personal, Indoor and Mobile Radio Communications (PIMRC), 2009, pp. 1863 - 1867.

125. **M. Torabzadeh, and Yusheng Ji.** "*Efficient Assignment of Transmit Antennas for Wireless Communications."* 2nd IEEE/IFIP International Conference in Central Asia on Internet, Sepember 2006, pp. 1-5. doi: 10.1109/CANET.2006.279256.

126. **M. Torabzadeh, and Yusheng Ji.** "*A Novel Antenna Assignment Scheme for Packet Scheduling in MIMO Systems."* 10th IEEE Singapore International Conference on Communication systems (ICCS), October 2006, pp. 1 - 5. doi: 10.1109/ICCS.2006.301526.

127. **M. Torabzadeh, and Yusheng Ji.** "*A Near Optimal Antenna Assignment for MIMO Systems with Low Complexity."* 15th IEEE International Conference on Networks (ICON), November 2007. pp. 336 - 341. doi: 10.1109/ICON.2007.4444109.

128. **Sang-wook Han and Youngnam Han.** "*A Competitive Fair Subchannel Allocation for OFDMA System Using an Auction Algorithm."* IEEE 66th Vehicular Technology Conference, 2007 (VTC-2007 Fall), 2007, pp. 1787 - 1791 . doi: 10.1109/VETECF.2007.377.

129. **Jinyoung Oh, Sang-wook Han, and Youngnam Han.** "*Efficient and fair subchannel allocation based on auction algorithm."* IEEE 19th International Symposium on Personal, Indoor and Mobile Radio Communications (PIMRC), September 2008, pp. 1 - 5. doi: 10.1109/PIMRC.2008.4699475.

130. **G. Aniba, and S. Aissa.** "*Cross-layer design for scheduling and antenna sharing in MIMO networks."* IEEE Global Telecommunications Conference (GLOBECOM '05). December 2005. Vol. 6, pp. 3185-3189. doi:10.1109/GLOCOM.2005.1578363.

131. **S. Floyd,** Ed. "*Metrics for the Evaluation of Congestion Control Mechanisms*." RFC 5166, March 2008.